2014

ROLE OF SCAVENGER RECEPTOR CLASS B TYPE I IN THYMOPOIESIS

Zhong Zheng
University of Kentucky, zizzizheng@gmail.com

STUDENT AGREEMENT:

I represent that my thesis or dissertation and abstract are my original work. Proper attribution has been given to all outside sources. I understand that I am solely responsible for obtaining any needed copyright permissions. I have obtained needed written permission statement(s) from the owner(s) of each third-party copyrighted matter to be included in my work, allowing electronic distribution (if such use is not permitted by the fair use doctrine) which will be submitted to UKnowledge as Additional File.

I hereby grant to The University of Kentucky and its agents the irrevocable, non-exclusive, and royalty-free license to archive and make accessible my work in whole or in part in all forms of media, now or hereafter known. I agree that the document mentioned above may be made available immediately for worldwide access unless an embargo applies.

I retain all other ownership rights to the copyright of my work. I also retain the right to use in future works (such as articles or books) all or part of my work. I understand that I am free to register the copyright to my work.

REVIEW, APPROVAL AND ACCEPTANCE

The document mentioned above has been reviewed and accepted by the student's advisor, on behalf of the advisory committee, and by the Director of Graduate Studies (DGS), on behalf of the program; we verify that this is the final, approved version of the student's thesis including all changes required by the advisory committee. The undersigned agree to abide by the statements above.

Zhong Zheng, Student

Dr. Xiang-An Li, Major Professor

Dr. Howard Glauert, Director of Graduate Studies

ROLE OF SCAVENGER RECEPTOR CLASS B TYPE I IN THYMOPOIESIS

DISSERTATION

A dissertation submitted in partial fulfillment of the
requirements for the degree of Doctor of Philosophy in the
College of Medicine
at the University of Kentucky

By
Zhong Zheng
Lexington, Kentucky
Director: Dr. Xiang-An Li, Associated Professor of Pediatrics
Lexington, Kentucky

ABSTRACT OF DISSERTATION

ROLE OF SCAVENGER RECEPTOR CLASS B TYPE I IN THYMOPOIESIS

T cells, which constitute an essential arm in the adaptive immunity, complete their development in the thymus through a process called thymopoiesis. However, thymic involution can be induced by a couple of factors, which impairs T cell functions and is slow to recover. Therefore, understanding how thymopoiesis is regulated may lead effort to accelerate thymic recovery and improve immune functions in thymocyte-depleted patients. In this project, we identified scavenger receptor BI (SR-BI), a high density lipoprotein (HDL) receptor, as a novel modulator in thymopoiesis. In mice, absence of SR-BI causes a significant reduction in thymus size after puberty and a remarkable decrease in thymic output. Consequently, SR-BI-null mice show a narrowed naïve T cell pool in the periphery and blunted T cell responses, indicating that the impaired thymopoiesis due to SR-BI deficiency leads to compromised T cell homeostasis and functions. The impaired thymopoiesis of SR-BI-null mice is featured by a significant reduction in the percentage of earliest T progenitors (ETPs) but unchanged percentages of other thymocyte subtypes, suggesting that SR-BI deficiency causes a reduction in progenitor thymic entry. Further investigations reveal that SR-BI deficiency impairs thymopoiesis through affecting bone marrow progenitor thymic homing without influencing the lymphoid progenitor development in bone marrow. Importantly, SR-BI-null mice exhibit delayed thymic recovery after sublethal irradiation, indicating that SR-BI is also required for thymic regeneration. Using bone marrow transplantation models, we elucidate that it is non-hematopoietic rather than hematopoietic SR-BI deficiency that results in the defects in thymopoiesis. However, SR-BI deficiency-induced hypercholesterolemia is not responsible for the impaired thymopoiesis. Using adrenal transplantation models, we found that absence of adrenal SR-BI is responsible for the impaired thymopoiesis, as shown by that adrenalectomized mice transplanted with SR-BI-null adrenal gland display reduced thymus size, decreased percentage of ETPs and delayed thymic regeneration compared with

those transplanted with wild-type adrenal. Altogether, results from this study elucidate a previously unrecognized role of SR-BI in thymopoiesis. We reveal that SR-BI expressed in adrenal gland is critical in maintaining normal T cell development and enhancing thymic regeneration, providing novel links between adrenal functions and T cell development.

Keywords: T cell development, scavenger receptor class B type I, thymic recovery, progenitor thymic homing, adrenal gland

Zhong Zheng

Student's Signiture

5-5-2014

Date

ROLE OF SCAVENGER RECEPTOR CLASS B TYPE I IN THYMOPOIESIS

By

Zhong Zheng

Xiang-An Li

Director of Dissertation

Howard Glauert

Director of Graduate Studies

5-5-2014

Date

This work is dedicated to my grandmother Xiuyun Zhao, my father Lianjun Zheng, my mother Ruijin Jia, my wife Junting Ai, my daughter Melinda Zheng, and to the memory of my grandfather Hua Zheng (1926-1993).

ACKNOWLEDGMENTS

During my Ph.D. studies, I have had incredible help and support from many individuals. Here, it is my great pleasure to express my appreciation for their assistance in obtaining my degree.

First of all, I would like to gratefully and sincerely thank my mentor, Dr. Xiang-An Li, who accepted me to his lab and gave me the chance to get this degree. Dr. Li was always generous with his time and help during my graduate study. He not only provided me well rounded experience in laboratory work and experiment design, but also encouraged me to think and develop the project independently. Also Dr. Li is a dedicated researcher. His diligence and enthusiasm toward science has made him an amazing role model for scientists. Without his instruction and encouragement, it would not have been possible for me to finish this project.

Also I am truly thankful to other members in my dissertation committee, Dr. Subbarao Bondada, Dr. Kuey Chen, Dr. Bernhard Hennig, Dr. Jianhang Jia and Dr. Brett Spear for their valuable discussions, suggestions and encouragement. Special thanks go to Dr. Bondada. He provided me priceless advice for my experiment design and great assistance in my experiments.

In particular, I would like to thank my colleague and wife, Junting Ai, who not only gave me unconditionally love and encouragement that helped me go through all the difficulties during my graduate studies, but also constantly contributed to my project. None of this would have been possible without her incredible support.

I would also love to thank all other current and past members in Li Lab, Dr. Ling Guo, Dr. Hong Feng and Dr. Qian Cai, for their great support and help for my studies. In particular, I want to thank Dr. Feng for teaching me flow cytometry, the technique I used throughout my whole project.

I also thank Debra Rateri and Deborah Howatt in Dr. Alan Daugherty Lab, Qing Hua in Dr. Dennis Bruemmer Lab, Wei Zhang in Dr. Mary Vore Lab, Greg Bauman and Jennifer Strange in UK flow cytometry core, Dr. Yi Liu in Dr. Gary van Zant Lab, Dr. Francesc Marti, Dr. Beth Garvy and Dr. Maria de Beer from University of Kentucky for their help in particular experiments. I am thankful to Dr. Vishva Dixit from Genentech and Dr. Gregory Sempowski from Duke University for providing materials for the experiments. In particular, I appreciate Dr. Jonathan Ashwell from NIH for his advice for this project. Also I want to thank my friends Jing Liu, Jing Wu, Jing Wei and Shu Gu for their help on proof-reading or statistical analysis in this dissertation.

Last, but by no means least, I would like to express my sincere appreciation to all my family. I especially want to thank my beloved grandmother Xiuyun Zhao, my father Lianjun Zheng and my mother Ruijin Jia who always fully supported my academic career and helped us take care of our daughter Melinda. I also want to express special thanks to our American parents Melinda and Lee Edgerton, who gave us incredible assistance and made us feel at home in Lexington.

Thank you all for your substantial part in my success.

TABLE OF CONTENTS

LIST OF TABLES

LIST OF FIGURES

Chapter 1 Background

1.1 T cell development and homeostasis

1.1.1 Introduction to the immune system

The mammalian immune system can be divided into two branches: the innate immune system and the adaptive immune system. The innate immune system provides the first line of defense against invading pathogens, but is non-specific to pathogens and unable to establish immunological memory. On the contrary, the adaptive immune system is pathogen-specific and can create immunological memory that mounts enhanced responses to pathogens upon re-infection [1, 2]. In the adaptive immune system, the two major players are B cells and T cells. B cells primarily fight against infections by producing antibodies and thereby play a key role in the humoral immunity. B cells can also act as antigen-presenting cells during immune responses [3]. In contrast, T cells are the central player in cell-mediated immunity as T cells can directly kill cells infected with intracellular pathogens or facilitate other cell types, including B cells, to fulfill their immune functions [4, 5]. The detailed characteristics and functions of T cells are discussed below.

1.1.2 Introduction to T cells

Distinguished from other lymphocytes, T cells bear T cell receptors (TCRs) on their surface, which can recognize major histocompatibility complex (MHC)-bound antigens and are highly diverse in binding specificity [6]. The majority of T cells in the immune system express TCRs composed of α- and β-

TCR chains and thus are known as the αβ T cells. In contrast, a minority of T cells express TCRs formed by γ- and δ-TCR chains, which are known as γδ T cells and exert distinct functions from αβ T cells [7, 8]. In this dissertation, T cells will refer to the conventional αβ T cells unless otherwise stated.

Two major classes of T cells that have different effector functions are distinguished by the surface co-receptors CD4 and CD8. $CD8^+$ cells recognize class I MHC molecules and can kill cells infected with intracellular pathogens. Therefore, $CD8^+$ cells are also called cytotoxic T cells or killer T cells. $CD4^+$ T cells recognize class II MHC molecules. These cells are able to provide essential signals to help other immune cells during immune responses and thus are also known as helper T cells [9, 10]. $CD4^+$ T cells can be further divided into several subtypes, such as Th1 cells, Th2 cells, Th17 cells and regulatory T cells. These helper T cell subtypes secrete different cytokines and play various roles in immune processes [11-13].

1.1.3 T cell homeostasis

Both $CD4^+$ and $CD8^+$ T cells contain three major populations, naïve cells, memory cells and effector cells. Naïve T cells are T cells that have not encountered their specific antigens and do not have functional activities. Naïve T cells are characterized by the presence of surface receptor L-selectin (CD62L) [11, 14] and the absence of activation markers such as CD69, CD25 or CD44 [15, 16]. Circulating through peripheral lymphoid tissues, naïve T cells scan MHC/peptide complexes on the surface of antigen presenting cells. Effector T cells can perform T cell functions such as producing cytokines (for $CD4^+$ cells) or

invoking cell killing (for $CD8^+$ cells). They can migrate to the site of infection and directly participate in the removal of antigens [13, 17]. Memory T cells are “experienced” T cells that have previously encountered their cognate antigens and are characterized by the expression of surface marker CD44. Memory T cells can be further divided into two major groups, central memory T cells and effector memory T cells. Central memory T cells express homing receptors, such as CD62L and C-C chemokine receptor type 7 (CCR7), that allow cells to migrate to secondary lymphoid organs. These cells are able to self-renew, but lack immediate effector functions. In contrast, effector memory T cells express molecules required for homing to inflammation tissues and have rapid effector functions [18, 19].

The numbers of naïve T cells, effector T cells and memory T cells are tightly regulated by complex homeostatic mechanisms to ensure optimal immune responses to antigens as well as reduce a risk of damaging self-tissues (Figure 1.1) [13]. Under normal conditions, naïve T cell numbers are maintained in a relatively constant level. Because naïve T cells are long-lived cells that rarely proliferate [20], their homeostasis in the periphery is mainly maintained by controlling survival. Naïve T cells depend on extrinsic signals such as self-peptide+MHC complexes and interleukin-7 (IL-7) to survive [21-24]. Though new T cells are produced continuously from the thymus, all naïve T cells compete for the limited survival signals and a balanced number of naïve T cells are removed by apoptosis [13, 25]. Meanwhile, naïve T cells can give rise to a number of memory-phenotype T cells through a process called homeostatic proliferation.

The homeostatic proliferation of naïve T cells may reflect naïve T cell responses to self-antigens and is responsible for the progressive accumulation of memory T cells as age increases [26]. Unlike naïve T cells, memory T cells are proliferative. Their survival relies on IL-7 and interleukin-15 (IL-15) but not on self-peptide+MHC complexes [21, 27, 28]. Also, the degree of death appears to balance with the cell division to keep the size of memory cells relatively steady under normal circumstances [13, 26].

When the body is invaded by a pathogen, the specific naïve T cells recognize the peptide/MHC complexes on antigen presenting cells and then become activated. Activated T cells undergo clonal expansion, giving rise to thousands of effector T cells with identical binding specificity, which then migrate to the inflammation site to exert their functions. T cell-mediated immune responses are also tightly controlled. On one hand, a small group of effector T cells differentiate into regulatory T cells, which can suppress immune responses and prevent autoimmune problems [29]. On the other hand, after the antigen is cleared, the majority of effector T cells are rapidly removed by apoptosis to avoid damage to self tissues. Only a small group of effector T cells are retained to develop into memory T cells [30-32]. If the memory T cells are exposed to the same antigen, they can rapidly produce a large number of effector T cells, providing a quicker and stronger secondary immune response to clear the invading pathogen [13].

1.1.4 Thymopoiesis

T cells complete their development in the thymus, an organ located anatomically in the anterior superior mediastinum. Generally speaking, cells in the thymus, i.e. thymocytes, can be divided into two major groups, T-lineage cells and stromal cells. Thymic T-lineage cells are cells being “educated” in the thymus. They develop from bone marrow-derived precursors to mature naïve T cells, constituting a majority of thymocytes. Thymic stromal cells include thymic epithelial cells, thymic endothelial cells, dendritic cells and macrophages, which are important in providing a specialized environment to instruct T cell development [33, 34].

Bone marrow-derived progenitors undergo a complex developmental program in the thymus to generate mature naïve T cells (Figure 1.2). The most original T-lineage cells in the thymus are the earliest T progenitors (ETPs), which are derived from bone marrow precursors that enter the thymus via the circulation. ETPs lack most of the surface molecules characteristic of mature T cells but express high levels of the cytokine receptor Kit (cKit or CD117) [35, 36]. After settling in the thymus, ETPs start to proliferate and give rise to downstream T lineage cells. Thymocytes in the early developmental stage including ETPs do not express CD4 or CD8. Thereby these cells are called double negative (DN) thymocytes. During the DN stage of thymopoiesis, T-lineage cells temporarily express surface marker CD25 and down-regulate CD44 expression. Thus, based the expression of CD44 and CD25, the DN cells are further divided to four groups, that is, from immature to mature, $CD44^{+}CD25^{-}$ (DN1) cells, $CD44^{+}CD25^{+}$

(DN2) cells, $CD44^{-}CD25^{+}$ (DN3) cells and $CD44^{-}CD25^{-}$ (DN4) cells. DN1 cells are highly heterogeneous which include ETPs and a variety of non-T-lineage cells. In contrast, nearly all of DN cells in other three stages are T-lineage cells [13, 37, 38]. The rearrangement of TCR-β chain locus occurs in DN2 and DN3 stage. Only thymocytes with successful β chain rearrangements can progress to DN4 stage. This process is regarded as the first checkpoint of T cell development, which is called β selection [39].

Thymocytes passing β selection begin to express CD4 and CD8 to become double positive (DP) thymocytes, which comprise the majority (>80%) of thymocytes [13, 37, 38]. During the DP stage, the TCR-α locus rearranges and a selection process called positive selection occurs. In positive selection, thymocytes are screened for their recognition of MHC molecules. DP thymocytes without a TCR capable of binding MHC molecules are removed by apoptosis. DP thymocytes also undergo negative selection in which they are tested for their reactivity to self-ligands. Cells with high reactivity to self-ligands are eliminated in this selection process. Positive selection and negative selection ensure that only T cells that contain functional TCRs and do not recognize self-antigens are generated from the thymus [40]. DP thymocytes passing two selection processes differentiate to $CD4^{+}$ single positive (4SP) or $CD8^{+}$ single positive (8SP) cells. During the SP stage, thymocytes down-regulate proteins involved in selection processes and begin expressing a series of markers involved in thymocyte egress from the thymus or homing to secondary lymphoid organs. This process is called SP thymocyte maturation [41, 42]. The mature SP thymocytes finally

the egress from the thymus to blood as recent thymic emigrants (RTEs) to maintain the naïve T cell pool [34].

1.1.5 Thymopoiesis and T cell homeostasis

Thymopoiesis plays an essential part in the homeostatic regulation of naïve T cells (Figure 1.3). The contribution of thymopoiesis to maintaining the naïve T cell pool size was revealed in mice or human beings whose thymopoiesis was ablated. In mice, absence of thymopoiesis in mice causes a dramatically decreased naïve T cell pool size and a reduced naïve T cell to memory T cell ratio [43, 44]. The decay of the naïve T cell pool was also reported in thymectomized human beings [45, 46]. The reduction of naïve T cells is thought to be due to successive antigen stimulation that shifts naïve cells to memory cells [44, 47].

More importantly, thymopoiesis plays a key role in replenishing the naïve T cells to maintain a diverse TCR repertoire and optimal T cell functions. A maximally diverse TCR repertoire of naïve T cells is essential for the efficient generation of immune responses to new infections [48, 49]. However, during antigen stimulation or homeostatic proliferation, the clone sizes and relative clonal representation in TCR repertoire can be altered, causing a progressive loss of diversity and accumulation of auto-reactive T cells [50-53]. The biased TCR repertoire can be corrected by RTEs. The newly generated T cells have a competition advantage over the old ones, replacing equal numbers of preexisting naïve T cells in the pool [54]. Through injecting TCR transgenic cells into mice, Tanchot et.al showed that in presence of thymic output, the gradually T cell

substitution results in a decay of preexisting TCR transgenic cells, demonstrating that the RTEs play a critical role in renewing the TCR repertoire [55]. The absence or reduction of thymic output leads to a loss of TCR diversity and accumulation of auto-reactive T cells, which is responsible for the compromised immune responses and autoimmune disorders in thymectomized patients, and aged people or mice [46, 56-59].

T cell production not only maintains TCR diversity, but also is required for optimal naïve T cell functions. When thymopoiesis is absent and the naïve T cell pool is not replenished, naïve T cells live longer and undergo proliferation in an attempt to restore the size of the reduced pool [44, 60, 61]. In this process, T cell function is compromised. In aged or thymectomized mice, T cells show a decreased functional avidity, defective stimulation-induced signaling as well as blunted responsiveness to stimulation [62-64]. Increasing thymopoiesis in aged animals can improve their peripheral T cell functions [65-67]. These observations revealed that thymopoiesis is essential in maintaining optimal T cell functions.

1.1.6 Lymphoid progenitor development and thymic homing

Due to a lack of self-renewal progenitors in the thymus, long-term thymopoiesis depends on continuous settlement of bone marrow progenitors to the thymus [54, 68, 69]. The thymic precursors originally derive from hematopoietic stem cells (HSCs) residing in bone marrow, which are able to self-renew and have the potential to generate all the blood cell types. HSCs are positive for the molecule Sca-1 and cKit, and negative for surface expression of markers found on mature cell types (lineage markers). Thus, they belong to Lin^-

Sca-1^{+}cKit^{+} (LSK) cells in bone marrow. Within LSK cells, HSCs are characterized by the lack of CD135 expression [70, 71]. The first step in the differentiation of HSCs involves the generation of multipotent progenitors (MPPs). Compared with HSCs, MPPs lose the self-renewal capacity and only maintain short-term multilineage reconstituting potential. MPPs also belong to LSK cells but begin to express low levels of CD135 [72, 73]. MPPs then give rise to lymphoid-primed multipotent progenitors (LMPPs), which start to express lymphoid-specific genes and are more committed to lymphoid development. LMPPs are still Lin^{-}Sca-1^{+}cKit^{+}, but distinguished from HSCs and MPPs by their high levels of CD135 expression [74]. LMPPs in turn produce common lymphoid progenitors (CLPs), which possess high lymphoid potential with limited myeloid potential. Compared with their upstream progenitors, CLPs display elevated IL-7 receptor α (IL-7Rα) expression and reduced Sca-1 and cKit expression [75, 76] (figure 1.4).

Bone marrow progenitors can mobilize out of bone marrow into the circulation and then migrate to the thymus through a process called progenitor thymic homing (Figure 1.4) [34, 68]. Though all bone marrow progenitors can be detected in blood [77], only LMPPs and CLPs have the ability to enter the thymus and are closely related with the intrathymic precursors at the molecular level [78, 79]. Consequently, LMPPs and CLPs are believed as the direct ancestors of thymic T-lineage cells. Due to the extremely low numbers of progenitors settling to the thymus, the detailed mechanism of progenitor thymic settling is not completely understood [80, 81]. However, a group of adhesive molecules and

cytokines expressed in thymic endothelial cells, such as P-selectin, CCL21 and CCL25, have been reported to mediate the entry of progenitor cells [68, 82]. Multiple mouse strains with disrupted progenitor thymic homing due to the blockage of the adhesion cascade display reduced thymocyte numbers and impaired thymopoiesis [83, 84], highlighting the essential role of progenitor thymic homing in maintaining normal thymopoiesis.

1.1.7 Age-related thymic involution

Despite being the main site for T cells development, thymus mass and thymic cellularity begins to decrease after adolescence [85-87]. This phenomenon is known as age-related thymic involution. This thymus regression is an evolutionary conserved event, as it occurs in nearly all vertebrates that have a thymus [88]. The age-related thymic involution is characterized by a systematic loss of thymocytes without an obvious blockade in thymocyte differentiation [89]. It has been showed that age-related thymic involution leads to reduced T cell production [90, 91]. Consequently, aged people or mice display a restricted naïve T cell pool, a skewed TCR repertoire and impaired T-cell functions [62, 87, 92, 93], which are believed at least partly responsible for the impaired immune response to newly encountered antigens and increased susceptibility to infections [62, 92]. The reason why the thymus involutes in the elderly has not been fully elucidated, but multiple defects have been suggested to underlie age-related thymic involution, including the loss of developmental potential in aged bone marrow cells[94]; the decline in ETPs and their

proliferative potential [94, 95]; and decreased numbers and altered structure of thymic epithelial cells (TECs) [96-99].

1.1.8 Thymocyte depletion and thymic recovery

In addition to age-related thymic involution, the thymus can also undergo transient and reversible regression under certain circumstances [100]. Transient thymic regression is called acute thymic involution, and is characterized by enhanced thymocyte death and acute loss of DP thymocytes [100-103]. Naturally occurred acute thymic involution is usually associated with stress, under conditions such as infections [104], malfunction [105] and pregnancy [106]. Some therapeutic processes, such as clinical cancer treatments or preparative regimens for bone marrow transplant, can also cause acute thymic involution [102, 107, 108]. Similar to age-related thymic involution, acute thymic involution results in a disrupted thymopoiesis, which is considered deleterious as it decreases the likelihood of infectious agent being cleared and increases the risk of infections by newly encountered antigens [89, 107, 109, 110]. Moreover, the thymic recovery after lymphocyte depletion is a prolonged process, which is the primary obstacle to reconstitute peripheral T cell pool and immune responses in thymic depleted patients [102, 107, 111-113]. How thymic involution is induced and how thymic recovery is regulated still remains incompletely understood [102].

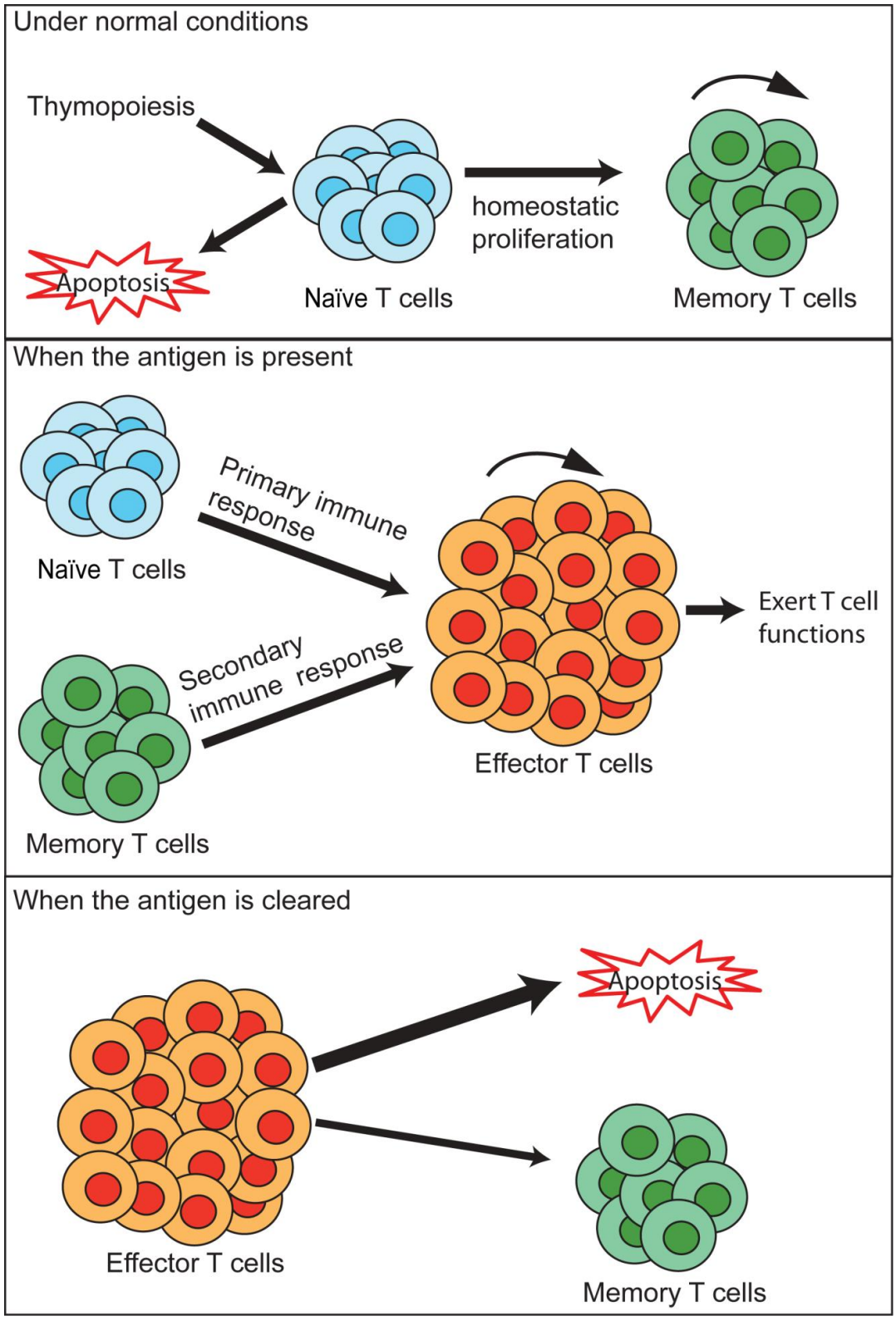
Under normal conditions
Thymopoiesis
Apoptosis
Naïve T cells
homeostatic proliferation
Memory T cells
When the antigen is present
Naïve T cells
Primary immune response
Exert T cell functions
Secondary immune response
Effector T cells
Memory T cells
When the antigen is cleared
Apoptosis
Effector T cells
Memory T cells

Figure 1.1 Regulation of T cell homeostasis.

Under normal circumstances (top), the naïve T cell pool size is maintained by T cell production from the thymus and balanced cell death of existing naïve T cells. In addition, naïve T cells can undergo homeostatic proliferation and be converted to memory T cells. In contrast, the memory T cell pool is mainly maintained by proliferation. During immune responses (middle), naïve T cells are activated and generate large numbers of effector T cells, which can migrate to the inflammation site to fight against pathogens. If the antigen is not new, memory T cells can also generate effector T cells in a quicker and stronger manner. When the antigen is removed (bottom), most effector T cells undergo apoptosis to avoid damages to self-tissues. A small number of effector T cells develop to memory cells to protect against secondary invasions.

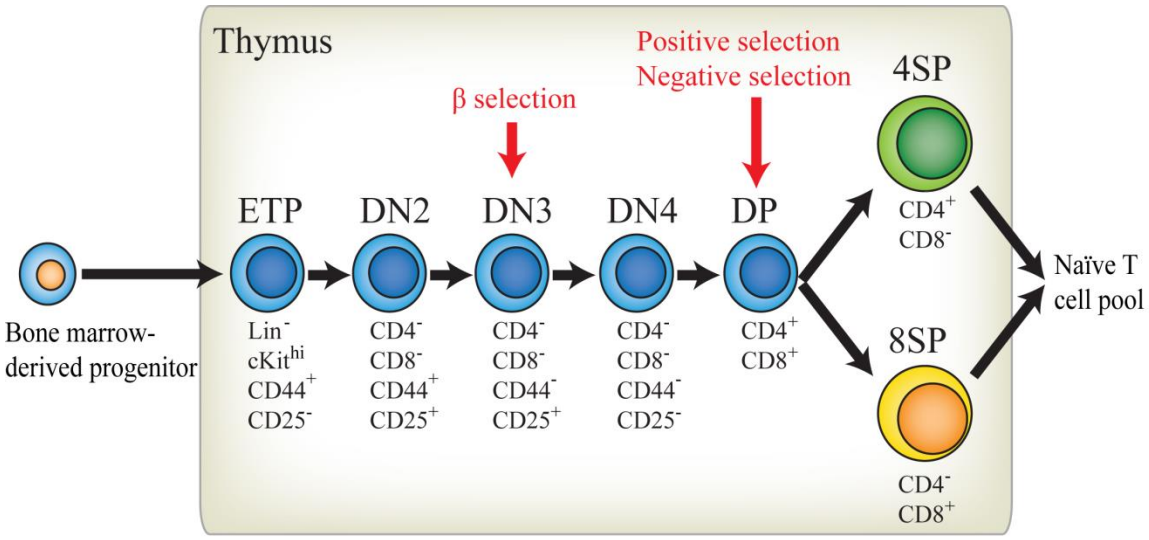

Figure 1.2 T cell development in the thymus.

Bone marrow-derived precursors arrive in thymus as earliest thymic progenitors(ETPs), which then develop from double negative stages(DN; $CD4^-$ $CD8^-$) to double positive stages(DP; $CD4^+CD8^+$) after being screened for the expression of pre-TCR(β selection). DP cells undergo positive selection to delete cells without effective TCR and negative selection to remove cells interact with self-antigens, followed by differentiating into single positive (SP; $CD4^+CD8^-$ or $CD4^-CD8^+$) cells. SP cells, after maturation, exit the thymus as recent thymic emigrants (RTEs).

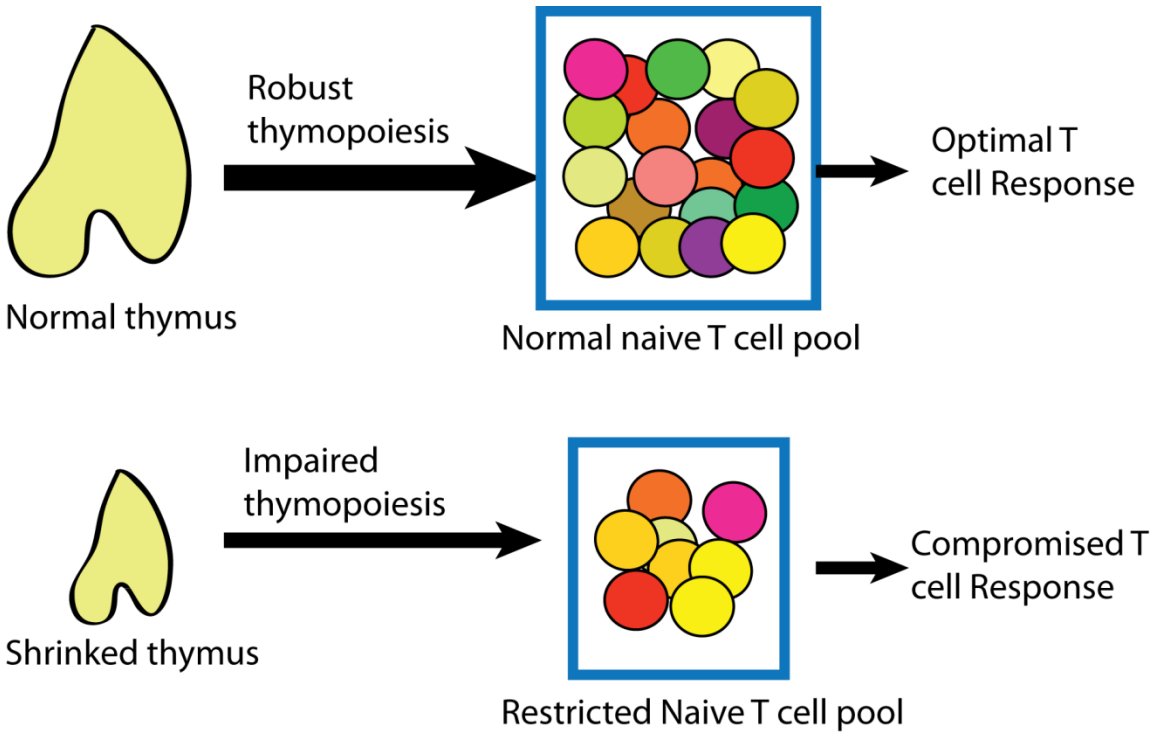

Figure 1.3 Consequences of the impaired thymopoiesis.

Adequate T cell production is essential for maintaining a normal naïve T cell pool size, maximal TCR diversity and optimal T cell responses (upper). Inadequate T cell production leads to decreased naïve T cell numbers, restricted TCR repertoire and impaired T cell responses (bottom).

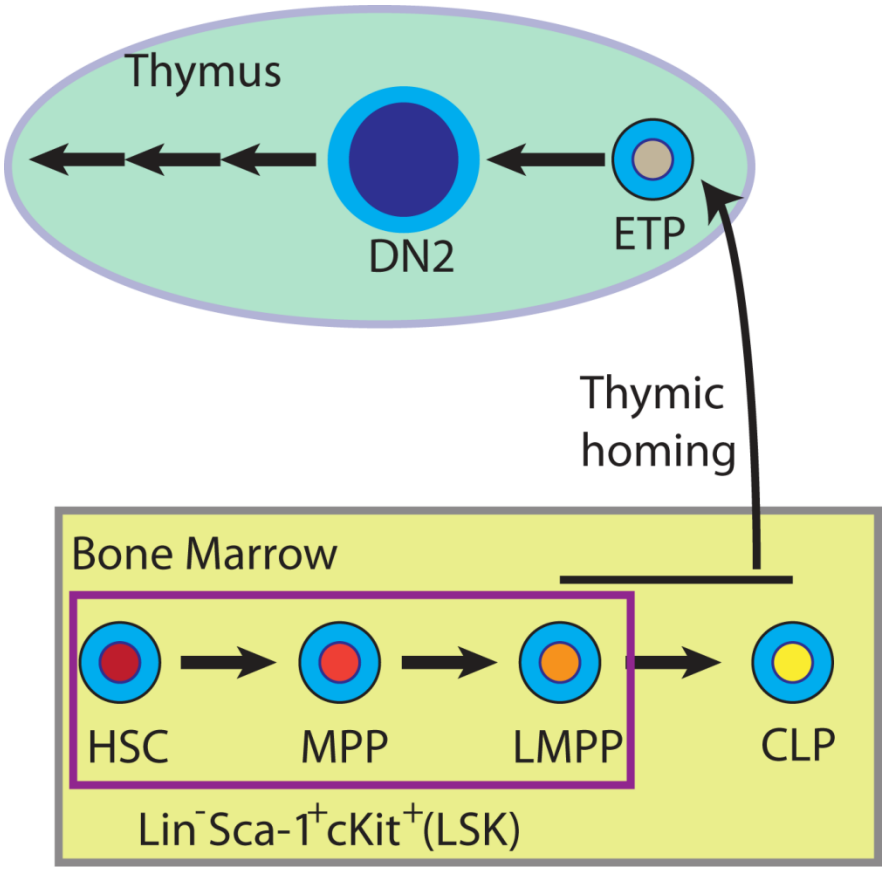

Figure 1.4 Thymic progenitor development and homing.

Thymic progenitors originally derive from hematopoietic stem cells (HSCs) in bone marrow. To generate thymic progenitors, HSCs give rise to multipotent progenitors (MPPs), which then develop to lymphoid-primed multipotent progenitors (LMPPs). HSCs, MPPs and LMPPs are all subgroups of LSK (Lin^- $Sca\text{-}1^+cKit^+$) cells. LMPPs can further develop to common lymphoid progenitors (CLPs). LMPPs and CLPs are able to settle in the thymus via the circulation through a process called progenitor thymic homing, followed by the generation of downstream thymocytes.

1.2 Scavenger receptor class B type I

1.2.1 Overview of SR-BI

Scavenger receptor class B type I (SR-BI) is a 509-amino acid transmembrane protein belonging to the class B scavenger receptor family. As with CD36 and lysosome membrane protein 2 (LIMP2), the other members of this family, SR-BI has a horseshoe-like structure with short N- and C-terminal cytoplasmic domains, two transmembrane domains and a large heavily N-glycosylated extracellular loop (Figure 1.5) [114, 115]. The extracellular domain of SR-BI is predicted to contain a helical bundle which binds with ligands and a tunnel used for substrates delivery [116]. SR-BI also has a splice variant, SR-BII, which differs from SR-BI in its carboxyl terminal and serves as another member of class B scavenger receptor family [117].

Like many other scavenger receptors, SR-BI can recognize a wide range of self- and foreign ligands (Figure 1.5) [118-121]. The self-originated ligands of SR-BI include modified low density lipoprotein (LDL), naïve LDL, high density lipoprotein (HDL), maleylated bovine serum albumin (BSA), anionic phospholipids and apoptotic cells [122-125]. The non-self-ligands include lipopolysaccharide (LPS), lipoteichoic acid (LTA), gram-negative bacteria, gram-positive bacteria and soluble hepatitis c virus (HCV) E2 glycoprotein [126-128]. SR-BI is most abundantly expressed in liver, adrenal gland and ovaries, which is closely related with its major functions (discussed in detail below) [125, 129, 130]. SR-BI is also expressed many other cell types, such as endothelial cells [131], epithelial cells [132], macrophages [133] and lymphocytes [134]. The wide

range of ligands SR-BI can bind and the diverse tissues SR-BI is expressed underlie the multiple functions of SR-BI within the body [135].

1.2.2 Classical function of SR-BI in HDL metabolism

HDLs are the smallest and most dense group of lipoproteins in plasma [136]. HDLs are highly heterogeneous, as they vary in diameter, density and composition [137, 138]. The basic structure of HDLs include two major parts, a core made of hydrophobic lipid, such as cholesteryl ester and triglyceride, and a surface monolayer of phospholipid, free cholesterol and apolipoproteins [138, 139]. HDL cholesterol (HDL-c) is recognized as “good” cholesterol, as it is well documented that the concentration of HDL-c in blood is inversely associated with the risk of cardiovascular diseases [140, 141]. Intense researches on the metabolism and functions of HDLs have revealed that they can exert multiple atheroprotective functions, including mediating cholesterol transportation[142, 143], anti-inflammation[144-146], and anti-oxidation [147, 148].

An essential mechanism by which HDLs protect against cardiovascular disease is mediating cholesterol transport from peripheral tissues via reverse cholesterol transport (RCT) [149]. Due to the inability to degrade cholesterol, peripheral cells must transport excess cholesterol to the liver to prevent cholesterol accumulation. RCT is the process by which HDLs take away cholesterol from peripheral tissues and transport cholesterol to the liver for excretion [150]. Blockage of RCT causes cholesterol accumulation in peripheral tissues, which leads to elevated risk for arthrosclerosis [151]. In addition to transporting cholesterol to the liver, HDLs are also responsible for delivering

cholesterol to steroidogenic tissues, such as the adrenal gland, providing cholesterol as sources for steroid synthesis [152-154].

In 1996, SR-BI was identified as the first HDL receptor as it was reported that SR-BI not only binds HDL but also mediates selective cholesterol uptake from HDL [125]. Later it was confirmed that SR-BI is a physiological HDL receptor. In mice, overexpression of SR-BI decreases plasma HDL levels [155] and the deficiency of SR-BI causes hypercholesterolemia and accumulation of large HDL particles in the circulation [156]. In humans, SR-BI mutations also lead to elevated HDL concentrations in plasma and altered cholesterol metabolism in macrophages [157, 158]. Nowadays, it has is well known that SR-BI is a key mediator in HDL metabolism and plays multiple roles in RCT (Figure 1.6) [159, 160].

The primary role of SR-BI in RCT is that it is the sole molecule mediating cholesterol uptake from HDL in the liver, where SR-BI is most abundantly expressed [125, 161-163]. In this process, cholesterol and other lipids are selectively delivered to cells without endocytosis or degradation of lipoprotein particles [164, 165]. Consequently, this process is called selective cholesterol uptake. Hepatic SR-BI-mediated selective uptake is a key determinant of the efficiency of RCT, as revealed by hepatic overexpression of SR-BI decreases plasma HDL-c concentration and increases biliary cholesterol secretion [155, 166, 167]; hepatic-specific down-regulation or knockout of SR-BI elevates plasma HDL-c levels [168-170]. SR-BI also plays a role in mediating selective cholesterol uptake in steroidogenic tissues, such as the adrenal gland [161].

Adrenal SR-BI-mediated selective uptake is essential for adrenal steroidogenesis, which is highlighted by recent findings that adrenal-specific disruption of SR-BI in mice results in glucocorticoid insufficiency [171].

HDL takes cholesterol from peripheral tissues in interstitial space and then delivers cholesterol to the liver via blood. Thus, in RCT, HDL needs to travel between interstitial fluid and blood to deliver cholesterol. Recent publications indicate that SR-BI is involved in HDL transport. To enter the interstitial fluid, lipid-poor HDL in blood crosses aortic endothelial cells by transcytosis [172, 173]. Silencing SR-BI in endothelial cells decreases the binding of HDL by 50% and reduces HDL transcytosis, indicating that endothelial SR-BI participates in this movement [173]. After loading cholesterol from peripheral cells, lipid-rich HDL returns to blood via lymphatic vessels [174, 175]. Lymphatic endothelium-expressed SR-BI mediates the uptake and transcytosis of HDL to lymphatic vessels. Blocking SR-BI significantly reduces the transport of HDL from the periphery to blood in mice [174], indicating that SR-BI is an essential determinant in the process that returns HDL to blood .

SR-BI plays a role in mediating free cholesterol efflux from peripheral cells to HDL. The role of SR-BI in cholesterol efflux was elucidated by the observations that in cell lines, the cholesterol efflux rate from cells to HDL correlates with the SR-BI expression levels [176, 177], and macrophages from SR-BI-deficient mice or patients carrying functional SR-BI mutations display reduced capability of effluxing cholesterol to HDL [157, 178]. However, one group reported that SR-BI deficiency in macrophages does not impair RCT *in vivo*

[179]. How SR-BI-mediated cholesterol efflux in macrophages and other cell types physiologically affects RCT still remains incompletely understood.

1.2.3 SR-BI and atherosclerosis

As SR-BI is a key player in RCT, it is not surprising that SR-BI plays a protective role against atherosclerosis. The systemic role of SR-BI in protecting against atherosclerosis was demonstrated by manipulating SR-BI expression in animal models. In mice, modest SR-BI overexpression decreases the development of the diet-induced fatty streak lesions [180], whereas attenuation or ablation of SR-BI expression increases diet-induced aortic atherosclerosis [178, 181, 182]. Moreover, the absence of SR-BI in apolipoprotein E (ApoE)-deficient background spontaneously induces accelerated atherosclerosis, early onset occlusive coronary artery disease, and premature death [183]. These data clearly indicate a protective role of SR-BI against atherosclerosis.

Interestingly, though the atheroprotective effects of SR-BI are thought mainly attributed to its roles in cholesterol transport, several other atheroprotective properties of SR-BI are also identified [184-187]. For example, SR-BI expressed in hematopoietic cells plays a role in protection against atherosclerosis, since the absence of SR-BI expression in hematopoietic cells leads to elevated atherosclerosis [178, 182, 188-190]. SR-BI expressed in macrophages seems to provide the major atheroprotective effect, which is supported by the observation that the absence of macrophage SR-BI impairs cholesterol homeostasis [191] and exaggerates cytokine secretion in macrophages [189, 192]. Meanwhile, SR-BI-facilitated bidirectional cholesterol

efflux influences foam cell formation. Though hematopoietic SR-BI deficiency alone does not cause foam cell accumulation, it exaggerates foam cell accumulation when hematopoietic ATP-binding cassette transporter A1(ABCA1) is absent, suggesting that SR-BI may serve as a compensatory route of cholesterol efflux to decrease foam cell formation [190, 193].

HDL can also protect against atherosclerosis through its anti-oxidative properties. This anti-oxidative benefit is mainly attributed to two HDL-bound antioxidative enzymes, paraoxonase 1 (PON1) and platelet-activating factor acetylhydrolase (PAF-AH) [139, 143, 148]. SR-BI deficiency decreases PON1 and PAF-AH activity, causing an increased oxidative stress *in vivo* [194]. In addition, SR-BI was reported to participate in the pathway in which PON1 directly dampens macrophage inflammatory responses [195], suggesting that SR-BI deficiency may increase atherosclerosis through impairing anti-oxidative property of HDL. SR-BI expressed in endothelial cells also contributes to reducing atherosclerosis. Endothelial SR-BI not only mediates HDL-induced endothelial cell migration and repair [196], but also induces the production of the anti-atherogenic molecule NO in response to HDL [197, 198].

1.2.4 SR-BI as a multi-functional receptor

In addition to mediating cholesterol transport and protecting against atherosclerosis, SR-BI is able to perform several other functions in multiple systems. Currently identified roles of SR-BI include controlling induced steroid production, preventing female infertility, maintaining normal erythropoiesis and platelet functions, and a series of functions in immunity.

SR-BI-mediated selective cholesterol uptake from HDL is an essential pathway to supply exogenous cholesterol to the adrenal gland [161, 199-202], which is shown by the depletion of cholesterol storage in adrenal gland of SR-BI-deficient mice [156]. Because of the existence of other pathways that can supply cholesterol to adrenal, such as endogenous cholesterol synthesis [203] and LDL receptor-mediated cholesterol uptake [204], the adrenal functions of SR-BI-null mice appear unaffected under normal conditions [205-207]. However, the deficient mice exhibit a lack of inducible glucocorticoid production in response to ACTH or stress [206-208], indicating that SR-BI-mediated cholesterol uptake is required for inducible glucocorticoid production. Patients carrying missense mutations of SR-BI also display marked reductions in urinary steroid secretion and decreased responses to corticotrophin stimulation, indicating that SR-BI is also essential in maintaining normal adrenal function in humans [157].

The absence of SR-BI in mice also causes female infertility which is believed to be a result of the defective oocytes that display abnormal morphology and arrested development *in vitro* [209]. Meanwhile, the SR-BI deficiency-induced abnormal HDLs are also linked to the female infertility. Normalization of the HDL particles in SR-BI$^{-/-}$ mice by disrupting apolipoprotein A-I (apoA-I), probucol treatment or hepatic SR-BI expression relieves the female infertility [210, 211]. In contrast, in spite of the lipid storage depletion [209], SR-BI-null ovaries are not responsible for the female infertility, since SR-BI$^{-/-}$ ovaries transplanted to ovariectomized SR-BI$^{+/+}$ mice display normal functions[210].

The loss of SR-BI in mice leads to abnormalities in erythrocytes and platelets. For erythrocytes, SR-BI-deficient mice show accumulation of reticulocytes in the circulation and a blockage in erythrocyte development in spleen [212, 213]. For platelets, SR-BI deficiency causes abnormal platelet morphologies, elevated rates of platelet clearance from the circulation and a defect in ADP-induced platelet aggregation in mice [214-216]. The abnormalities in erythrocytes and platelets are at least partly induced by the SR-BI deficiency-induced hypercholesterolemia; and are thought to be the reason for anemia and increased susceptibility to thromobosis [212, 214, 217].

1.2.5 Roles of SR-BI in immunity

SR-BI-deficient mice exhibit several phenotypic changes in the immune system (Figure 1.7), such as increased susceptibility to septic death, impaired lymphocyte homeostasis and reduced HCV infection [135]. Based on these major immunological phenotypes, multiple functions of SR-BI in immunity have been discovered in recent years.

A well-documented role of SR-BI in immunity is in protection against septic death. SR-BI deficiency causes significantly elevated death rate in sepsis, as shown by our observations that LPS injection induced 90% fatality in SR-BI-deficient mice, whereas all wild-type littermates survived [218]; and cecal ligation and puncture (CLP) induced 100% fatality in SR-BI-deficient mice, compared with 21% fatality in controls [207]. In addition to the increased death rate, during sepsis, SR-BI$^{-/-}$ mice have multiple defects including uncontrolled inflammatory cytokine production, delayed LPS clearance and augmented tissue damage [206,

207]. These observations indicate that SR-BI provides essential protection against sepsis.

Further investigations revealed that SR-BI can exert multiple protective functions against septic death [135]. The primary leading factor to the elevated mortality in sepsis of SR-BI$^{-/-}$ mice is thought to be the impaired inducible steroid synthesis in the adrenal gland. After LPS injection, supplementation of corticosterone in drinking water normalizes cytokine production and rescues survival rate of SR-BI$^{-/-}$ mice; and adrenalectomy abolishes the differences in inflammatory cytokine production between wild-type and SR-BI-deficient mice [206]. Under CLP challenge, though corticosterone supplementation in drinking water does not increase the survival rate of SR-BI$^{-/-}$ mice [207], adrenalectomized SR-BI$^{+/+}$ mice transplanted with SR-BI$^{-/-}$ adrenal show higher fatality than those transplanted with SR-BI$^{+/+}$ adrenal, suggesting that the insufficiency of multiple adrenal-derived steroids instead of corticoids alone is responsible for decreased survival rate during sepsis [219].

SR-BI deficiency also leads to elevated macrophagic inflammatory responses in mice [192, 207]. Hematopoietic SR-BI deficiency causes higher cytokine productions in response to LPS, indicating that macrophage SR-BI helps control inflammatory responses *in vivo*.[192]. The uncontrolled inflammatory responses of macrophages are a contributing factor to the elevated septic death of SR-BI-null mice, as shown by that overexpression of an SR-BI mutant in SR-BI-deficient mice, which normalizes macrophagic cytokine

production without restoring corticosterone generation, significantly improves their survival under CLP challenge [207, 220].

As a scavenger receptor able to recognize foreign ligands, SR-BI can bind LPS and mediate its removal [126]. Hepatocytes from SR-BI-null mice display a decreased ability to uptake LPS *in vitro*, resulting in decreased hepatic LPS uptake and increased plasma LPS retention after LPS injection *in vivo* [206]. In the CLP model, SR-BI-deficient mice also show higher plasma LPS concentrations, providing further support that SR-BI deficiency decelerates LPS clearance [207]. Interestingly, during early stages of sepsis, SR-BI-deficient mice display lower plasma LPS concentrations than their wild-type counterparts, suggesting that SR-BI-mediated LPS uptake may also be essential for transporting LPS from the inflammation site to blood [207]. ScarbII179N mice, whose SR-BI expression is specifically decreased by 90% in the liver [168], show elevated mortality under CLP challenge associated with impaired hepatic LPS uptake, but normal corticosterone production and macrophagic inflammatory response, indicating that the SR-BI-mediated hepatic LPS uptake is also critical in protecting against septic death [221]. In addition, SR-BI can also protect against NO-induced cytotoxicity. The lack of SR-BI-mediated protection against NO-induced cytotoxicity is believed to be responsible for the increased tissue damage during sepsis [218].

Though its functions are mostly considered beneficial, SR-BI is utilized by HCV in the process of cell entry [222]. The involvement of SR-BI in HCV entry was elucidated by the fact that down-regulating or blocking SR-BI in hepatocytes

decreases HCV infectivity *in vitro* [223-227] and the deficiency or blockage of SR-BI in humanized mice reduces HCV infection *in vivo* [228-230]. Therefore, SR-BI is regarded as a promising target to treat HCV infection [231].

Initially it was thought SR-BI mediates HCV entry through direct binding [128]. However, later research indicated that HCV entry involves the lipid transfer functions of SR-BI [222, 232-235] but is probably not dependent on the SR-BI-HCV binding [228, 235, 236]. Notably, SR-BI may be important in initiating the host defense during HCV infection because dentritic cells also depend on SR-BI to uptake HCV [237]. The detailed role of SR-BI in HCV infection and how this receptor can be used to prevent HCV infection requires further investigation.

1.2.6 SR-BI and adaptive immunity

In recent years, several players in RCT, including ApoA-I, ATP-binding cassette transporter G1 (ABCG1) and Liver X receptor (LXR) have been identified as modulators in adaptive immunity [139, 238-242]. For example, the absence of ApoA-I, the major protein in HDL [136, 243] induces cholesterol accumulation in T cells, causing T cell expansion and hyperactivation in skin lymph nodes associated with an autoimmune phenotype in LDL receptor (LDLR)-deficient mice fed with an atherogenic diet [239, 240]. Similarly, deficiency of ABCG1, a key transporter mediating cholesterol efflux in RCT [244, 245], causes increased cholesterol accumulation in T-lineage cells, resulting in increased thymocyte and peripheral T cell proliferation in mice [241]. Our group investigated the role of SR-BI in adaptive immunity using SR-BI-deficient mice

and were the first to report that the loss of SR-BI causes impaired lymphocyte homeostasis [134].

SR-BI-deficient mice display significant lymphocyte expansion in spleen resulting in significantly enlarged spleen sizes. Notably, the lymphocyte expansion is imbalanced, as SR-BI-deficient mice exhibit a 30% decrease in the T/B cell ratio. Meanwhile, the SR-BI deficiency also causes lymphocyte hyperactivation and hyperproliferation. As a consequence of the impaired lymphocyte homeostasis, aged SR-BI-deficient mice suffer from profound autoimmune disorders. With these data, we demonstrated that SR-BI is essential in maintaining lymphocyte homeostasis and preventing autoimmunity [134].

The adaptive immune defects of SR-BI-deficient mice are at least partly attributed to their abnormal HDL, which is larger in size and characterized by the accumulation of free cholesterol [156]. Functionally, SR-BI-deficient HDL shows a reduced ability to mediate selective cholesterol uptake [246], decreased anti-oxidative enzyme activity [194], and is responsible for female infertility [210, 211]. We found that the dysfunctional HDL from SR-BI-null mice partly loses the inhibitory effects on anti-CD3-stimulated T cell proliferation and LPS-induced B cell proliferation of normal HDL, indicating that SR-BI can indirectly influence lymphocyte function through regulating HDL properties [134]. Intriguingly, we recently reported that HDL from SR-BI-deficient mice is also dysfunctional in enhancing glucocorticoid-induced thymocyte apoptosis, which contributes to the increased septic death of SR-BI-null mice, providing another clue of how HDL functions in adaptive immunity [247].

The mechanism by which normal/dysfunctional HDL modulates lymphocyte proliferation is not yet fully understood. Several pieces of evidence have implied that HDL may affect lymphocyte proliferation through regulating its cholesterol contents, as seen in leukocytes [139] and hematopoietic progenitors [248]. Bensinger et al. reported that during T cell activation, the LXR pathway controlling cholesterol export is suppressed and the pathway controlling cholesterol synthesis is induced, suggesting that T cell cholesterol homeostasis is altered during the activation process [242]. Pharmaceutically activating LXR pathways inhibits activation-induced T cell proliferation while absence of LXRβ causes a proliferative advantage of T cells [242]. Importantly, LXR modulates T cell function via ABCG1, the transporter mediating cholesterol efflux from cells to HDL [242]. The ABCG1 deficiency also causes increased proliferation of T cells in mice [241], together suggesting that ABCG1-mediated cholesterol efflux to HDL inhibits T cell proliferation. In SR-BI-deficient mice, the HDL may be dysfunctional in acquiring cholesterol from lymphocyte via ABCG1, which causes the proliferative advantage. Further investigations are warranted to test this possibility.

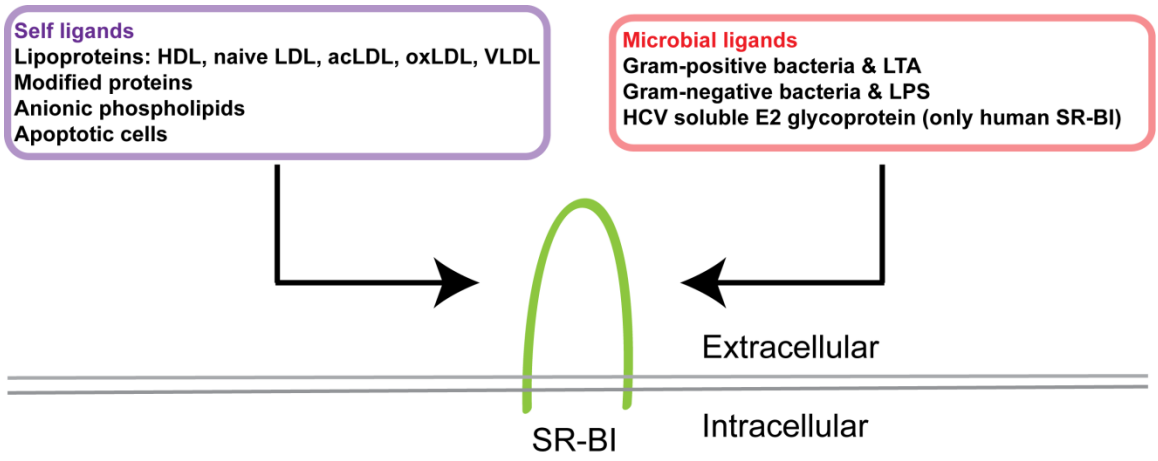

Figure 1.5 General structures and ligands of SR-BI.

SR-BI has a horse-shoe structure with two short intracellular domains, two transmembrane domains and a large extracellular loop. It can bind a variety of self-molecules or microbial ligands.

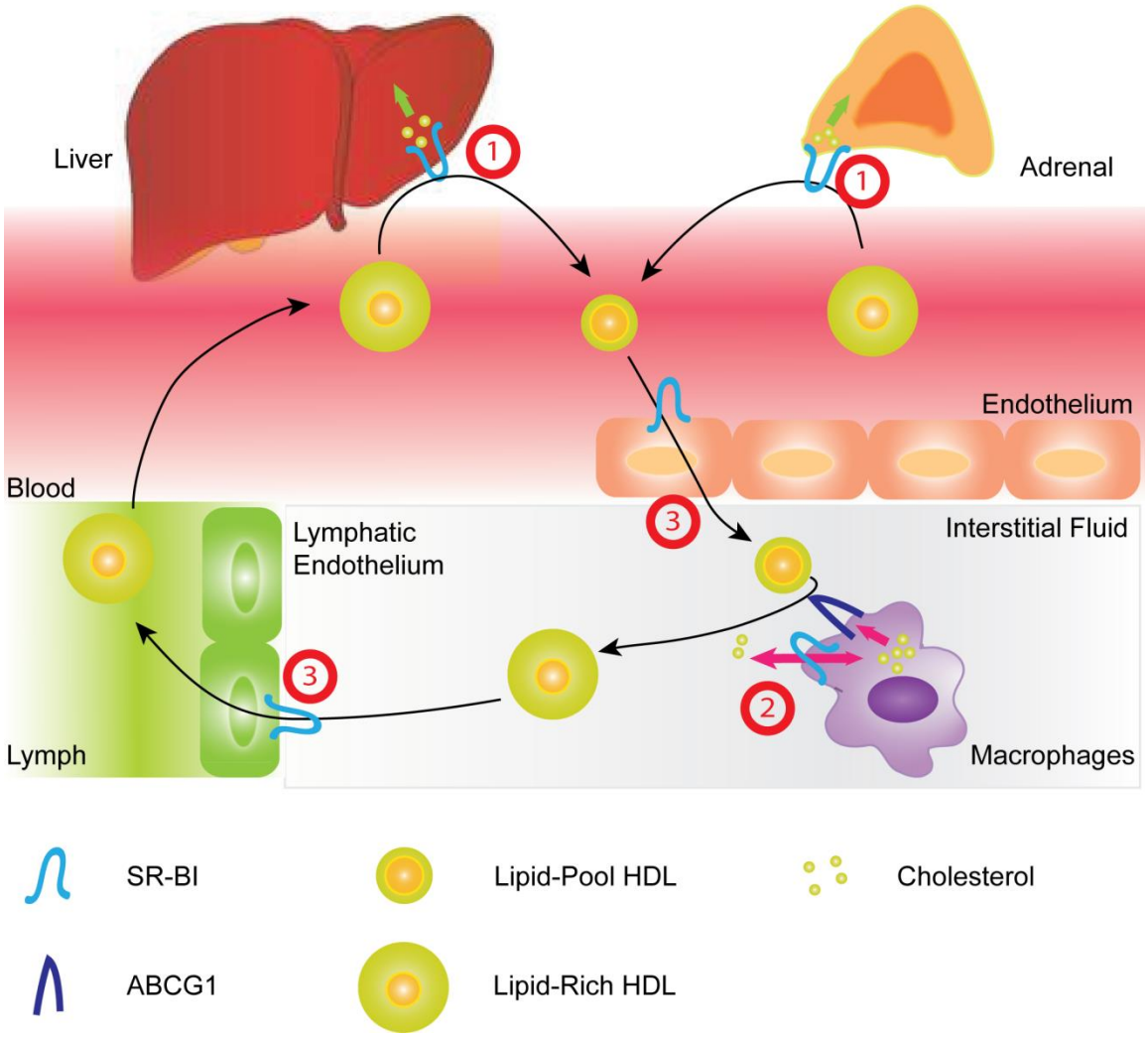

Figure 1.6 Multiple roles of SR-BI in RCT.

In RCT, HDL loads cholesterol from peripheral tissues (shown as macrophage in figure) via ATP-binding cassette transporters and delivers cholesterol to liver for disposal or to steroidogenic tissues, such as adrenal gland, for steroidogenesis. The roles SR-BI plays in RCT including 1, mediating selective cholesterol uptake in liver or steroidogenic tissues; 2, facilitating cholesterol efflux in peripheral tissues and 3, mediating HDL transport between blood and interstitial fluid.

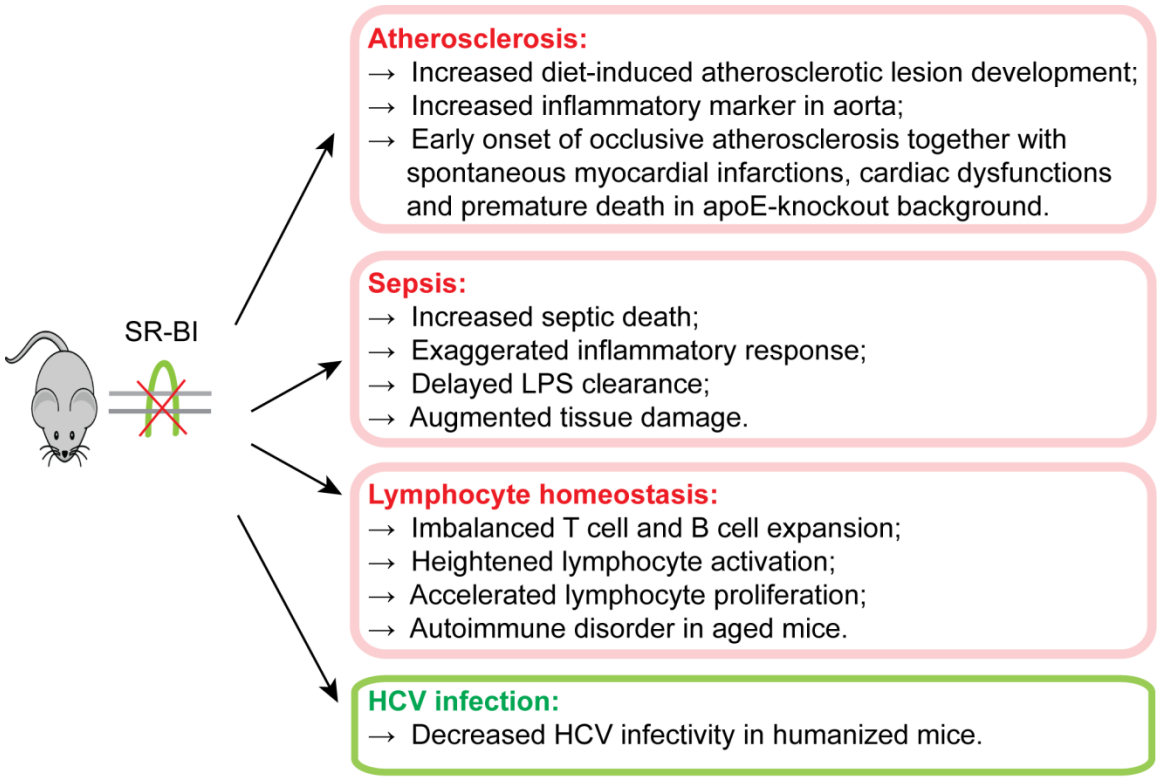

Figure 1.7 Major immune phenotypes of SR-BI-deficient mice.

SR-BI deficiency causes several defects in immunity including increased susceptibility to atherosclerosis, elevated susceptibility to sepsis and impaired lymphocyte homeostasis (shown in red). SR-BI deficiency also has beneficial effects in mice as it decreases HCV infection (shown in green) [135].

1.3 Synopsis of the project

During the past few years, our group has been intensively working on investigating the multiple roles of SR-BI in immunity. We were the first to report that SR-BI-deficient mice have impaired lymphocyte homeostasis and that SR-BI deficiency-induced dysfunctional HDL is the leading cause of lymphocyte expansion, hyperactivation and hyperproliferation [134, 135]. However, as the SR-BI-null HDL is dysfunctional in inhibiting the stimuli-induced proliferation of both T cells and B cells, it is not likely responsible for the decrease in T cell/ B cell ratio. Thus, SR-BI should play additional roles in maintaining lymphocyte homeostasis in addition to preventing lymphocyte expansion by keeping normal HDL functions.

In an effort to identify the additional roles of SR-BI in adaptive immunity, we focused on T cell development. Interestingly, by comparing the phenotypes of SR-BI-null mice with mice whose T cell production is decreased, we found that in addition to the decrease in T cell/B cell ratio, several other phenotypes of SR-BI-null also potentially result from reduced T cell production, including the decreased percentage of naïve T cells, blunted T cell response to stimuli and autoimmune problems. These observations led us to hypothesize that SR-BI deficiency causes impaired thymopoiesis, which contributes to the lymphocyte imbalance in SR-BI-null mice. In chapter 3, we tested this hypothesis by evaluating thymus size and thymic output. We observed significantly reduced thymus size and markedly declined thymic output in SR-BI-null mice, clearly indicating that SR-BI deficiency impairs thymopoiesis in mice. Importantly, by

assessing peripheral T cells and their function in young age SR-BI-null mice, we elucidated that SR-BI deficiency also impairs T cell homeostasis and responses, demonstrating that SR-BI plays a role in maintaining lymphocyte homeostasis by maintaining an optimal T cell production.

Next, we sought to elucidate the mechanism by which SR-BI deficiency impaired thymopoiesis. As the first step, described in chapter 4, we analyzed thymocyte subtypes in SR-BI-null mice in order to understand which steps of thymopoiesis SR-BI plays a role in. We observed that SR-BI-null mice do not show any significant change in the percentages of thymocyte subtypes except for a remarkable decrease in the portion of ETPs, suggesting that SR-BI deficiency reduces the progenitor entry into the thymus but does not influence other downstream steps in thymopoiesis. To determine whether or not SR-BI deficiency affects progenitor entry into the thymus, we analyzed bone marrow progenitor development and progenitor thymic homing, two major steps upstream of ETPs in T cell development, in SR-BI-null mice. Although we did not detect any defect in progenitor development in the absence of SR-BI, we found that fewer circulating bone marrow progenitors settle into the thymus in SR-BI-null mice, demonstrating that SR-BI deficiency impairs thymopoiesis though impacting bone marrow progenitor thymic homing. As SR-BI-null mice display decreased percentage of ETPs and impaired progenitor thymic homing, we hypothesized that SR-BI deficiency leads to delayed thymic recovery after thymocyte depletion. Using the sublethal irradiation model, we observed that SR-

BI-null mice exhibit impaired thymic recovery, indicating SR-BI is also required for thymic regeneration.

In chapter 5, we investigated how the absence of SR-BI induces defects in T cell development. First, we utilized bone marrow transplantation models to investigate the role of hematopoietic and non-hematopoietic SR-BI in thymopoiesis. We found that non-hematopoietic SR-BI deficiency is the leading factor to the impaired thymopoiesis whereas hematopoietic SR-BI deficiency does not cause any disadvantages in T cell development. Next, to evaluate the contribution of SR-BI deficiency-induced hypercholesterolemia to the impaired thymopoiesis, we manipulated plasma cholesterol concentration in SR-BI$^{-/-}$ mice. Exaggerating hypercholesterolemia of SR-BI-null mice does not worsen thymic hypocellularity, nor does relieving hypercholesterolemia correct thymic hypocellularity, indicating that the defects in thymus are not induced by SR-BI deficiency-induced hypercholesterolemia. We also did not observe cholesterol accumulation in thymic macrophages of SR-BI-null mice, excluding the possibility that SR-BI deficiency induces impaired thymopoiesis through cholesterol accumulation and the subsequent NLRP3 inflammasome activation. Interestingly, using adrenal transplantation models, we found that mice with adrenal SR-BI deficiency display reduced thymus size, declined ETP percentage and impaired thymic regeneration, demonstrating that absence of SR-BI in adrenal is the leading cause to the impaired thymopoiesis.

Taken together, we identified a previously unrecognized role of SR-BI in thymopoiesis. We conclude that 1: SR-BI deficiency impairs bone marrow

progenitor thymic homing, which further causes reduced thymus size, decreased ETP percentage, declined T cell production and delayed thymic recovery, 2: The reduced T cell production induced by SR-BI deficiency impairs peripheral T cell homeostasis and functions, and 3: Adrenal SR-BI plays a major role in maintaining normal thymopoiesis and thymic regeneration.

Chapter 2 Materials and Methods

2.1 Mice

2.1.1 General information

SR-BI$^{+/-}$ (B6;129S2-*Srb1*^{tm1Kri}/J), Rag-1$^{-/-}$ (B6.129S7-*Rag1*^{tm1Mom}/J), CD45.1(B6.SJL-*Ptprc*^{a} *Pepc*^{b}/BoyJ), LDLR$^{-/-}$ (B6.129S7-*Ldlr*^{tm1Her}/J) and C57BL/6J mice were purchased from the Jackson Laboratory. Because of the female infertility due to SR-BI deficiency [210], SR-BI$^{-/-}$ mice were generated by breeding SR-BI$^{+/-}$ mice, and the SR-BI$^{+/+}$ littermates were used as controls. Rag-1$^{-/-}$, CD45.1 and C57BL/6J mice were all maintained by sibling mating. Mice were kept and bred in a temperature-controlled room with 12-hour light and 12-hour dark diurnal cycle at the animal facility of the University of Kentucky. All mice were housed in filter-topped cages and were fed a standard laboratory diet (0.015% wt/wt cholesterol, 5.7% wt/wt fat, Harlan Tekland 2018) if not otherwise stated. Animal care and experiments were all approved by the Institutional Animal Care and Use Committee of the University of Kentucky.

2.1.2 Generation of SR-BI/Rag-1 double knockout mice

To generate SR-BI$^{-/-}$Rag-1$^{-/-}$ mice, male SR-BI$^{-/-}$ mice and female Rag-1$^{-/-}$ mice were first cross-bred to generate SR-BI$^{+/-}$Rag-1$^{+/-}$ F1 offspring, which were subsequently intercrossed to generate F2 offspring. SR-BI$^{+/-}$Rag-1$^{-/-}$ mice in F2 offspring were selected and intercrossed. Generated SR-BI$^{-/-}$Rag-1$^{-/-}$ and SR-BI$^{+/+}$Rag-1$^{-/-}$ offspring were used for experiments, while the SR-BI$^{+/-}$Rag-1$^{-/-}$ offspring were further intercrossed to maintain the strain.

2.1.3 Generation of SR-BI-null mice in C57BL/6J background

Most SR-BI-null mice used in this project were in a C57BL/6J/129 mixed background. However, these mice could not be used in bone marrow transplantation or bone marrow transfer experiments together with CD45.1 mice that were in the C57BL/6J background. Thus, we backcrossed SR-BI$^{+/-}$ mice with C57BL/6J mice for more than 10 generations. After backcrossing, the SR-BI$^{+/-}$ offspring were selected and intercrossed to generate SR-BI$^{-/-}$ and SR-BI$^{+/+}$ mice in C57BL/6J background.

2.1.4 Generation of SR-BI/LDLR double knockout mice

To generate SR-BI$^{-/-}$LDLR$^{-/-}$ mice, male SR-BI$^{-/-}$ mice and female LDLR$^{-/-}$ mice were first cross-bred to generate SR-BI$^{+/-}$LDLR$^{+/-}$ F1 offspring, which were subsequently intercrossed to generate F2 offspring. SR-BI$^{+/-}$LDLR$^{-/-}$ mice in F2 offspring were selected and intercrossed. Generated SR-BI$^{-/-}$LDLR$^{-/-}$ mice were used for experiments, while SR-BI$^{+/-}$LDLR$^{-/-}$ mice were further intercrossed to maintain the strain.

2.1.5 Genotyping of mice

2.1.5.1 Preparation of tail genomic DNA

When necessary, the genotypes of mouse offspring were determined by polymerase chain reaction (PCR) with tail genomic DNA before they were weaned. Briefly, ~0.4cm tail tips were cut from mice at the age of 14-19 days and digested with 100μL 0.4μg/μL proteinase K in 55˚C water bath for 16~18 hours. The digested tails were then centrifuged at 2,000 rpm for 5 min at room temperature and heated at 95 °C for ten minutes to deactivate the proteinase K.

The solution was diluted by 5-fold volume of ddH_2O and centrifuged again at 2,000 rpm, 5 min at 4 °C. The supernatant containing the genomic DNA was used as the template for PCR.

2.1.5.2 Preparation of liver genomic DNA

The genotypes of all experimental mice were confirmed using DNA from liver tissues after mice were sacrificed. To isolate the genomic DNA, approximately 30mg liver tissue was cut into small pieces and incubated with 600µL digestion buffer (116µL 0.5M pH=8.0 EDTA + 484µL Nuclei lysis solution + 4µL 20mg/mL proteinase K solution) in 55˚C water bath for 18-20 hours. After digestion, the protein was precipitated by adding 200µL Protein Precipitation Solution and incubating on ice for 5 minutes. The solution was then centrifuged at 12,000rpm for 5 minutes at 4°C, before the supernatant was mixed with isoproterenol at a ratio of 1:1. The mixed solution was centrifuged again at 12,000rpm for 5 minutes at 4°C. After the centrifuge, the pellet was washed with 70% ethanol and dissolved in 400µL ddH_2O. The final solution contained the genomic DNA and was used as the template for PCR.

2.1.5.3 PCR genotyping of SR-BI

SR-BI wild-type and knockout alleles in mice were amplified as described previously [249]. The primer sequences for amplifying SR-BI alleles were 5'-GAT-GGG-ACA-TGG-GAC-ACG-AAG-CCA-TTC-T-3' (named as AB2) and 5'-TCT-GTC-TCC-GTC-TCC-TTC-AGG-TCC-TGA-3' (named as AB3). The reaction system was made of 10µL Taq Red Mix (Bioline), 1µL 10µM AB2 primer, 1µL 10µM AB3 primer, 1µL DNA template and 7µL ddH_2O. The PCR machine

settings were: step 1: 5 minutes at 95°C; step 2: 30 seconds at 95°C, 30 seconds at 58°C, 2 minutes at 72°C, 35 cycles; step 3: 10 minutes at 72°C. After reaction, PCR products were analyzed using 1.5% agarose gels. The 1.0kb amplified DNA band was from the wild-type allele and the 1.5kb one was from the knockout allele (Figure 2.1).

2.1.5.4 PCR genotyping of Rag-1

In the process of generating SR-BI$^{-/-}$Rag-1$^{-/-}$ mice, Rag-1 alleles were genotyped in mice. The protocol to amplify the Rag-1 alleles was modified from the protocol suggested by Jackson Lab. Briefly, to amplify the wild-type allele of Rag-1, two primers, 5'- GAG-GTT-CCG-CTA-CGA-CTC-TG -3' (named as oIMR1746) and 5'- CCG-GAC-AAG-TTT-TTC-ATC-GT -3' (named as oIMR3104) were used. The reaction system was made of 10μL Taq Red Mix, 0.5μL 10μM oIMR1746 primer, 0.5μL 10μM oIMR3104 primer, 1μL DNA template and 8μL ddH_2O. The PCR machine settings were: step 1: 2 minutes at 95°C; step 2: 30 seconds at 95°C, 30 seconds at 58°C, 30 seconds at 72°C, 35 cycles; step 3: 2 minutes at 72°C. Later, PCR products were analyzed using 2.0% agarose gels. A 474 bp band was amplified if the wild-type Rag-1 allele was present (Figure 2.2).

The PCR reaction to amplify the mutant allele of Rag-1 was the same with the one to amplify the wild-type allele except that a primer 5'-TGG-ATG-TGG-AAT-GTG-TGC-GAG-3' (oIMR8162) was used to replace oIMR1746. The amplified DNA product from the mutant allele was 530bp (Figure 2.2).

2.1.5.5 PCR genotyping of LDLR

In the process of generating SR-BI$^{-/-}$LDLR$^{-/-}$ mice, LDLR alleles were genotyped in mice. The protocol to amplify the LDLR alleles was modified from the protocol suggested by Jackson Lab. Briefly, two primers used to amplify the wild-type allele of LDLR were 5'- CCA-TAT-GCA-TCC-CCA-GTC-TT-3' (named as oIMR3349) and 5'- GCG-ATG-GAT-ACA-CTC-ACT-GC-3' (named as oIMR3350). Two primers used to amplifying the mutant allele of LDLR were oIMR 3349 and 5'- AAT-CCA-TCT-TGT-TCA-ATG-GCC-GAT-C-3' (named as oIMR0092). The reaction system was made of 0.5μL GoTaq (Promega), 4μL 5X reation buffer (Promega), 0.4μL dNTP (Promega), 1.6μL Mg^{2+} (Promega), 0.5μL 10 μM oIMR0092, 0.5μL 10 μM oIMR3349, 0.5μL 10 μM oIMR3350, 1μL DNA template and 11μL ddH_2O. The PCR machine settings were: step 1: 3 minutes at 94°C; step 2: 30 seconds at 94°C, 1 minute at 65°C, 1 minute at 72°C, 35 cycles; step 3: 2 minutes at 72°C. Later, amplified PCR products were analyzed using 2.5% agarose gels. A 167 bp band was amplified from wild-type LDLR allele and a 350 band was amplified from the mutant LDLR allele (Figure 2.3).

2.2 Mouse treatments

2.2.1 BrdU injection

5-bromo-2'-deoxyuridine (BrdU) is an analog of thymidine which can be integrated into newly synthesized DNA of cells during proliferation. BrdU that is incorporated into the DNA can be detected with its specific antibody and thus can be used to monitor cell proliferation *in vivo* and *in vitro* [250-252]. For *in vivo* BrdU labeling, we gave mice two intraperitoneal injections of 1mg BrdU in 200μL

sterile PBS. The injections were spaced 24 hours apart and 24 hours after the second injection, the mice were sacrificed and the BrdU incorporation in cells was detected (BrdU detection procedure described in chapter 2.3.5).

2.2.2 Bone marrow transplantation

Bone marrow transplantation was performed as described previously [253, 254]. Briefly, recipient mice (13~20 weeks) were maintained on antibiotic water (4μg/mL sulfratrim) for one week before irradiation. Then, the recipient mice were irradiated with two doses of 400Rads from a cesium source that was delivered 3 to 4 hour apart. After irradiation, 5 million bone marrow cells obtained from femurs of 5~6-week-old donor mice (bone marrow cell isolation procedure described in chapter 2.3.1.5) were suspended in 100μL PBS and injected via tail vein into the irradiated recipient mice. After bone marrow transplantation, mice were maintained on antibiotic water for another 4 weeks, and then changed on regular water for 2 weeks before being sacrificed.

2.2.3 Short-term homing assay

The short-term homing assay is commonly used to investigate the thymic progenitor settlement in mice [83, 255]. Briefly, 20 million bone marrow cells from 5-week-old SR-BI$^{+/+}$ mice labeled with carboxyfluorescein succinimidyl ester (CFSE, labeling procedure described in chapter 2.5) were suspended in 100μL PBS and injected to non-irradiated 5-week-old SR-BI$^{+/+}$ or SR-BI$^{-/-}$ mice via tail vein. The mice were maintained on regular water and normal diet for two days before analysis.

2.2.4 Long-term homing assay

The long-term homing assay was conducted to study the contribution of circulating bone marrow progenitors to thymopoiesis [255]. In this assay, 20 million bone marrow cells from 6-week-old CD45.1 mice suspended in 100μL PBS were injected to non-irradiated SR-BI$^{+/+}$ or SR-BI$^{-/-}$ mice in C57BL/6J background (6~26 weeks) via tail vein. The mice were maintained on regular water and normal diet for two weeks before analysis.

2.2.5 Sublethal irradiation

Sublethal irradiation in mice mimics the whole body irradiation in patients which is a preparative regimen for hematopoietic stem cell transplantation and causes acute thymic atrophy. Sublethal irradiation thus is widely used for investigating thymocyte recovery after thymocyte depletion [111, 256, 257]. In this project, 8~10-week-old mice were irradiated with a single dose of 450 Rads from a cesium source. Then the irradiated mice were maintained on regular water and normal diet for 4 days, 7 days or 14 days before analysis.

2.2.6 High fat diet feeding

The high fat diet used in this project contains 15.8% by weight fat, 1.25% by weight cholesterol and 0.5% by weight sodium cholate (Harlan Tekland), which is widely used for elevating cholesterol concentrations in mice [258, 259]. After being weaned at the age of 3 weeks, the mice were immediately fed with the high fat diet. The mice fed on normal diet described in chapter 2.1.1 were used as control.

2.2.7 Probucol administration

Probucol is a cholesterol lowering drug [260, 261] which was reported to relieve the hypercholesterolemia in SR-BI$^{-/-}$ mice and normalize several adverse effects of SR-BI deficiency [210, 262]. Probucol (Sigma) was dissolved in ethanol at 55°C water bath before being sprayed on normal diet at 0.2% by weight. Then the probucol-added diet was dried for one week before use. After being weaned at the age of 3 weeks, mice were immediately fed with the probucol diet. The mice on normal diet described in 2.1.1 were used as control.

2.2.8 Adrenal transplantation

The procedure of adrenal transplantation was previously described [171, 263]. Briefly, at day 8 after birth, the donor mice (offspring of SR-BI$^{+/-}$ breeders) were genotyped using tail tips. At day 9, the SR-BI$^{+/+}$ or SR-BI$^{-/-}$ donor mice were euthanized using CO_2 and their adrenal glands were harvested. The SR-BI$^{+/+}$ recipient mouse (10-12 weeks) was anesthetized by isoflurane inhalation. After anesthetization, the adrenal glands of the recipient were removed bilaterally and one donor adrenal gland was put under the right kidney capsule through a slit made by tweezers. After the right kidney was returned, the incisions were sutured. After the surgery, the recipient was maintained on water containing 0.9% NaCl, before they were used for experiments 6 weeks later.

2.3 Flow cytometry

2.3.1 Preparation of single cell suspensions

2.3.1.1 Spleen

The spleens were isolated and weighed immediately after mice were sacrificed. Isolated spleen (if the spleen was less than 100mg, the whole spleen was used; otherwise, a 70-100mg piece of spleen was used) was placed in a stomacher bag (Seward) in the presence of 10mL RPMI 1640 (Gibco) containing 5% FBS (Gibco) and disrupted using Stomacher 80 (Seward). Later, the suspension was moved to a 50mL centrifuge tube (BD Biosciences) through a 100μm cell strainer (BD Biosciences). Then 5mL RPMI 1640 containing 5% FBS was added to wash the stomacher bag and transferred to the same centrifuge tube through the strainer. After the wash was added, the cell suspension was centrifuged at 1,500 rpm for 5 minutes at 4˚C. The supernatant was discarded and the cells were incubated with 5mL ACK lysis buffer (0.15 M NH_4Cl, 10 mM $KHCO_3$, 0.1 mM EDTA, pH=7.4) at room temperature to deplete erythrocytes. After 5 minutes incubation, 10mL PBS w/o calcium and magnesium (Gibco) was added to cease the lysis. 100μL of the cell suspension after lysis was immediately diluted and counted, before the cells were centrifuged at 1,500 rpm for 5 minutes. Then the cells were washed again with PBS w/o calcium and magnesium before they were suspended in 5mL RPMI 1640 containing 5% FBS to make the final suspension.

2.3.1.2 Thymus

Thymus was isolated, weighed and placed in a 60mm culture dish (BD Biosciences) immediately after the mouse was sacrificed. The isolated thymus was then mechanically disrupted through a 100μm cell strainer into 10mL RPMI 1640 containing 5% FBS. The cell suspension was transferred into a 15mL centrifuge tube (BD Biosciences). 5 mL RPMI 1640 containing 5% FBS was added to wash the dish and strainer, and then transferred to the same centrifuge tube. After the wash was added, the cell suspension was centrifuged at 1,500 rpm for 5 minutes at 4˚C. The cells were suspended in 5mL RPMI 1640 containing 5% FBS to make the final suspension.

2.3.1.3 Lymph nodes

Mesenteric lymph nodes were isolated and weighed immediately after a mouse was sacrificed. 2-4 lymph nodes were used for making single cell suspensions following the method that was described in chapter 2.2.1.2. The cells were finally suspended in 2mL RPMI 1640 containing 5% FBS.

2.3.1.4 Blood

Blood was collected from mouse by abdominal arterial puncture. To prevent coagulation, the needles were pre-rinsed with 0.5M EDTA (Sigma) and the collected blood was immediately mixed with 20μl 0.5M EDTA in a 1.5mL EP tubes. 300uL anti-clotted blood was added to 5mL ACK lysis buffer in a 50mL centrifuge tube to remove red blood cells. 5 minutes after incubation, 45mL PBS w/o calcium and magnesium was added to cease lysis and the cells were immediately centrifuged at 1,500 rpm for 5 minutes at 4˚C. The pellet was

resuspended with 1mL RPMI 1640 containing 5% FBS to make the final suspension.

2.3.1.5 Bone marrow

Two femurs were removed immediately after a mouse was sacrificed. After both ends of a femur were cut, 5 mL RPMI 1640 containing 5% FBS was used to flush out the bone marrow cells into a 15mL centrifuge tube. Bone marrow cells from two femurs of one mouse were pooled together and then moved into a 50mL centrifuge tube through a 100μm cell strainer. The cells were centrifuged at 1,500 rpm for 5 minutes at 4˚C and resuspended in 1mL RPMI 1640 containing 5% FBS to make the final suspension.

2.3.2 Cell counting

For splenocytes, 100μL cell suspension was diluted 10-fold with RPMI 1640 containing 5% FBS immediately after lysis and then counted using a counting chamber. For thymocytes, 100μL final cell suspension was diluted 10-fold, 20-fold or 50-fold with RPMI 1640 containing 5% FBS and then counted using a counting chamber. For lymph node cells and whole blood cells, 10μL final cell suspension was directly counted without dilution with a counting chamber. The number of lymph node cells was normalized to cells per 2 lymph nodes. The concentration of blood cells was shown as cells per mL blood. For bone marrow cells, 10μL final cell suspension was 100-fold diluted with RPMI 1640 containing 5% FBS and then counted using a counting chamber.

2.3.3 Surface marker antibody staining

The antibodies used in this project are listed in Table 1. For most assays in this project, $5x10^5$ cells were first incubated with 0.25μg anti-mouse CD16/CD32 in 30μL FACS staining buffer (PBS w/o calcium and magnesium containing 1% BSA) for 10 minutes at 4˚C to block Fc receptors. Then 20μL FACS staining buffer containing fluorescent dye-labeled antibodies (0.125μg per antibody) was added to make a final volume of 50μL and the cells were incubated at 4˚C 30 minutes. After incubation, the cells were washed twice with 500μL FACS staining buffer. Finally the stained cells were suspended in 250μL FACS staining buffer and analyzed with FACSCalibur or LSRII flow cytometer (BD Biosciences). The generated data were analyzed with FlowJo software (Treestar).

For TUNEL, BrdU or filipin staining assay, 1 million cells were stained with 0.25μg of antibody in 100μL staining buffers and washed with doubled volume of buffers before subsequent staining. For ETP staining or bone marrow progenitor analysis, 5~15 million cells were stained and washed with proportionally increased volume of buffers and antibodies. The stained cells were suspended in 1~1.5mL FACS staining buffer before analysis.

2.3.4 TUNEL apoptosis detection assay

Terminal deoxynucleotidyl transferase dUTP nick end labeling (TUNEL) is a widely used method for detecting DNA fragmentation which is an essential marker for cell apoptosis [264, 265]. Briefly, 1 million cells were first stained with antibodies recognizing surface antigens as described in chapter 2.2.3, followed

by incubation with 100μL BD Cytofix/Cytoperm solution (BD Biosciences) for 20 minutes at room temperature. After washing twice with 1x BD Perm/Wash buffer (BD Biosciences), the cells were incubated with 50μL TUNEL reaction mixture (Roche) that was prepared following the manufacture instructions for 45 minutes at 37˚C. Finally the cells were washed twice with FACS staining buffer, suspended in 500μL FACS staining buffer and analyzed with flow cytometer.

2.3.5 BrdU incorporation detection

The BrdU incorporation was evaluated using a commercial BrdU kit (BD bioscience) following instructions of the manufacture. Briefly, 1 million cells were first stained with antibodies recognizing surface antigens as described in chapter 2.2.3, followed by incubation with 100μL BD Cytofix/Cytoperm solution for 20 minutes at room temperature. After washing twice with 1x BD Perm/Wash buffer, the cells were incubated with 100μL BD Cytoperm Permeabilization Buffer Plus for 10 minutes at room temperature and again washed twice with 1x BD Perm/Wash buffer. After the wash, the cells were suspended in 100μL BD Cytofix/Cytoperm solution and incubated for 5 minutes, before they were washed twice with 1x BD Perm/Wash buffer. Later, the fixed cells were incubated with 100μL 300μg/mL DNase in PBS for 1 hour at 37˚C to expose the incorporated BrdU. After the DNase was washed away with 1x BD Perm/Wash buffer, the cells were stained with 1:50 APC-conjugated anti-BrdU antibodies in 50μL 1x BD Perm/Wash buffer. Finally, the cells were washed with FACS staining buffer twice and suspended in 250μL FACS staining buffer before analysis.

2.3.6 Filipin staining

Filipin is a highly fluorescent compound that specifically binds cholesterol. Thus it can be used as a probe to evaluate the level of cholesterols [191, 266, 267]. One million thymocytes of mice were first stained with surface markers and then incubated with 100μL BD Cytofix/Cytoperm solution (BD Biosciences) for 20 minutes at room temperature. After washing twice with 1x BD Perm/Wash buffer (BD Biosciences), the cells were incubated with 100μL 100μg/mL filipin (Sigma) in 1x BD Perm/Wash buffer for 1 hour at 37˚C. Finally the cells were washed twice, suspended in 100μL PBS and analyzed with flow cytometer.

2.4 T cell receptor excision circles detection

T cell receptor excision circles (TRECs) are circular DNA molecules generated during TCR rearrangements which lack the ability to replicate. These molecules were diluted during T cell proliferation and thus nicely correlated with T cell production [90, 268, 269]. To detect TRECs in T cells, splenocytes of mice were stained with surface antibodies as described in chapter 2.2.3. Then $CD4^+$ and $CD8^+$ splenocytes were sorted with an iCyt Synergy sorter system (Sony). The cell lysate was prepared by incubating 10,000 cells/μL isolated cells with 0.4μg/μL proteinase K (QIAGEN) at 55˚C for one hour, followed by inactivating proteinase at 95˚C for 15 minutes. The lysate from 50,000 cells (5μL) was added to a quantitative PCR (qPCR) reaction.

The qPCR was performed using a LightCycler 480 Instrument (Roche). The forward primer to amplifying TRECs was 5’-CAT-TGC-CTT-TGA-ACC-AAG-CTG-3’ and the reverse primer was 5’-TTA-TGC-ACA-GGG-TGC-AGG-TG-3’.

The probe was 5'-FAM-CAG-GGC-AGG-TTT-TTG-TAA-AGG-TGC-TCA-CTT-Black hole Quencher-1-3' (synthesized by Integrated DNA Technologies). The reaction system was modified from previous report [90] and contained 12.5μL LightCycler 480 Probes Master (Roche), 1μL 0.5μM forward primer, 1μL 0.5μM reverse primer, 1μL 12.5μM probe, 4.5μ H_2O and 5μL templates. The qPCR program was set as: step 1: 10 minutes at 95°C; step 2: 15 seconds at 95°C, 1 minute at 60°C, single data collection, 45 cycles; step 3: 37°C, hold.

The standard curves for murine TRECs were generated by using standard mouse TRECs plasmids, which were a generous gift from Dr. Gregory D. Sempowski, Duke University Medical Center [90]. For each real-time PCR assay, stock dilutions of 10^7, 10^6, 10^5, 10^4, 10^3 and 10^2 plasmids per 5uL were run in triplicate to generate standard curves. TREC frequency of isolated cells was determined in triplicate and expressed as the number of TRECs per 100 cells. The total number of TRECs of a given population was calculated by multiplying the TREC frequency by the number of that population.

2.5 CFSE labeling

CFSE is a widely used fluorescent cell staining dye for *in vivo* cell tracing [270]. In this project, we used CFSE-labeled bone marrow cells in the short-term homing assay (described in 2.2.3). We labeled bone marrow cells with CFSE using a commercial kit (Molecular Probes). Briefly, bone marrow cells were first suspended in PBS containing 0.1% BSA at a concentration of 20 million cells per mL. Then 2μL 5mM CFSE stock solution per mL of cells was added to make a final CFSE concentration of 10μM, followed by incubation with cells at 37°C for

10 minutes. The staining was quenched by adding 5 volumes of ice-cold PBS and incubation on ice for 5 minutes. After washing cells three times with PBS, the cells were suspended in PBS at the concentration of 20 million cells per 100μL before being injected into mice.

2.6 in vitro *T cell activation*

Splenocytes or lymph node cells from mice were plated at a concentration of 4 x 10^6 cells per mL in a 96-well plate and cultured in RPMI 1640 medium supplemented with 10% FBS, 5 mM L-glutamine (Gibco), 100 units/mL penicillin, 100 μg/mL streptomycin, and 50μM 2-mercaptoethanol (2-ME). For anti-CD3 stimulation, the plates were incubated with 100μL anti-CD3 (eBioscience) in PBS at indicated concentrations overnight and washed twice with 100 μL PBS before use. For proliferation assay, 5μg/mL pre-bound anti-CD3 were used to stimulate T cells and 10 μM BrdU was added to track new born cells. After 96 hours incubation at 37°C, BrdU incorporation in T cells was analyzed by FACS. For activation assays, cells were stimulated with indicated concentrations of pre-bound anti-CD3 and soluble anti-CD28 (eBioscience). Forty-eight hours later, CD69 expression in T cells was evaluated.

2.7 Plasma cholesterol determination

Fresh anti-coagulated blood was drawn by tail bleeding or from abdominal aorta from mice and used to determine plasma cholesterol concentrations. Quantitative determination of plasma total cholesterol was performed with enzymatic colorimetric method following the instruction from manufacturer (Wako Pure Chemical Industries, Ltd).

2.8 Western blot

The thymi from 5-week-old mice were first lysed with cell lysis buffer (cell signaling) in the presence of proteinase inhibitor (Sigma), before being centrifuged at 12,000 rpm for 15 minutes at 4°C. The protein concentration in the supernatant was determined by Lowry protein assay [271] with a commercial kit (Biorad). Then, 100μg (by protein) cell lysate was loaded and resolved in a 12.5% polyacrylamide gel. After the gel electrophoresis, the protein in the gel was electrically transferred to a polyvinylidene fluoride (PVDF) membrane, which was then blocked with 5% milk in Tris-Buffered Saline with Tween 20 (TBST, 50mM Tris, 150mM NaCl, 0.05% Tween 20, pH=7.6) at room temperature for 1 hour and incubated with 1:10000 anti-caspase 1 (4B4, a gift from Dr. Vishva Dixit, Genentech) in 5% milk/TBST at room temperature for 1 hour. After washing for three times with 0.25% milk/TTBS, the membrane was incubated with 1:1000 peroxidase-conjugated anti-Rat IgG in 0.25% milk/TTBS for 1 hour at room temperature. After washing three times with 0.25 milk/TTBS, the membrane was incubated with peroxidase substrates (Thermo Scientific) for 5 minutes before the chemiluminescence was detected.

Then the membrane was stripped with stripping buffer (Thermo Scientific) and blotted with 1:500 anti-β-tublin (E7-c, Developmental Studies Hybridoma Bank). After washing, the membrane was incubated with 1:5000 peroxidase-conjugated anti-mouse IgG and detected as described upon.

2.9 Statistic analysis

In this dissertation, data were all shown as mean ± standard error. Comparison of two groups was by 2-tailed Student's t-test. P values for survival curves were determined from the Kaplan-Meier survival curves by use of the Log-Rank test utilizing SAS software. Means were considered different at $p < 0.05$.

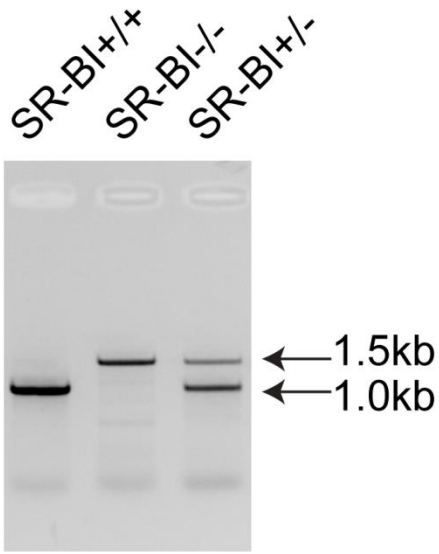

Figure 2.1 Genotyping for SR-BI alleles.

PCR system for SR-BI genotyping was set up as described in 2.1.5.3. Fifteen microliter amplified DNA product was resolved in a 1.5% agarose gel under 100 volts for 30 minutes.

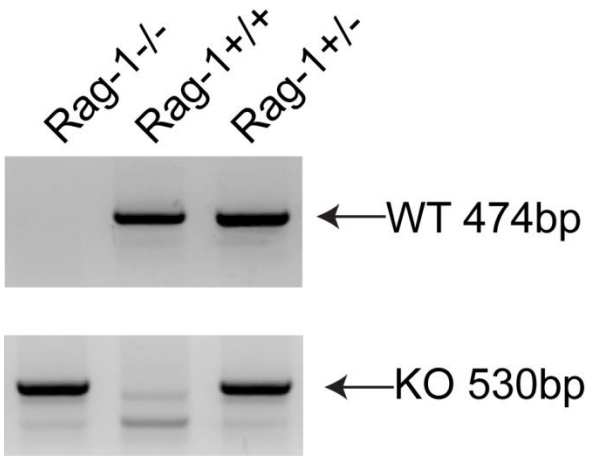

Figure 2.2 Genotyping for Rag-1 alleles.

PCR system for Rag-1 genotyping was set up as described in 2.1.5.4. Ten microliter amplified DNA product was resolved in a 2.0% agarose gel under 100 volts for 30 minutes.

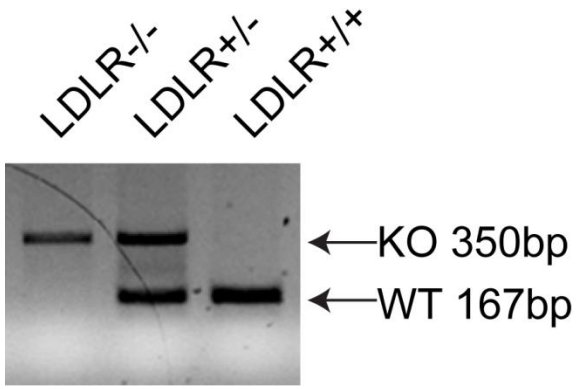

Figure 2.3 Genotyping for LDLR alleles.

PCR system for LDLR genotyping was set up as described in 2.1.5.5. Ten microliter amplified DNA product was resolved in a 2.5% agarose gel under 100 volts for 30 minutes.

Table 2.1 Antibodies used for flow cytometry.

Antigen	Clone	Format	Source	Note
BrdU	-	APC	BD Biosciences	Proliferation marker
B220	RA3-6B2	FITC	Biolegend	Lineage marker for ETP and bone marrow progenitor staining
CD2	RM2.5	FITC	Biolegend	Lineage marker for bone marrow progenitor staining
CD3ε	17A2	FITC	BD Biosciences	Lineage marker for ETP and bone marrow progenitor staining
CD4	GK1.5	APC	Biolegend	Thymocyte and peripheral T cell subset staining
CD4	GK1.5	FITC	Biolegend	Lineage marker for bone marrow progenitor staining
CD4	GK1.5	PE	Biolegend	Thymocyte and peripheral T cell subset staining
CD8α	53.67	FITC	Biolegend	Lineage marker for ETP and bone marrow progenitor staining; Thymocyte and peripheral T cell subset staining
CD8α	53.67	PE-cy5	BD Biosciences	Thymocyte and peripheral T cell subset staining
CD8β	53.58	FITC	Biolegend	Lineage marker for ETP staining
CD11b	M1/70	FITC	Biolegend	Lineage marker for ETP and bone marrow progenitor staining
CD11b	M1/70	PerCP-cy5.5	BD Biosciences	Thymic macrophage staining
CD11c	n148	FITC	Biolegend	Lineage marker for ETP staining
CD16/ CD32	93	Purified	BD Biosciences	Fc blocking
CD19	6D5	FITC	Biolegend	Lineage marker for ETP and bone marrow progenitor staining
CD25	PL61	APC	Biolegend	Thymocyte subset staining
CD44	1M7	PE-cy5	Biolegend	Thymocyte and peripheral T cell subset staining
CD45	30-F11	APC	BD Biosciences	For blood lymphocyte staining
CD45.1	A20	PE-cy7	Biolegend	Bone marrow transplantation and thymic homing assay
CD45.2	104	APC-cy7	Biolegend	Bone marrow transplantation and thymic homing assay
CD62L	MEL-14	PE-cy7	Biolegend	Thymocyte and peripheral T cell subset staining
CD69	H1.2F3	PE	BD Biosciences	Thymocyte subset staining; activation marker
CD135	A2F10	APC	Biolegend	Bone marrow progenitor staining

Table 2.1 Antibodies used for flow cytometry (continued).

Antigen	Clone	Format	Source	Note
CD135	A2F10	APC	Biolegend	Bone marrow progenitor staining
cKit	2B8	PE	Biolegend	Bone marrow progenitor and ETP staining
F4/80	BM8	PE	eBioscience	Thymic macrophage staining
GR-1	RB6-8C5	FITC	Biolegend	Lineage marker for ETP and bone marrow progenitor staining
IL-7Rα	A7-R34	APC-cy7	Biolegend	Bone marrow progenitor staining
NK1.1	PK136	FITC	Biolegend	Lineage marker for ETP and bone marrow progenitor staining
Sca-1	D7	PE-cy7	Biolegend	Bone marrow progenitor staining
TCR-β	H57	FITC	Biolegend	Lineage marker for ETP staining
TCR-γ/δ	GL3	FITC	Biolegend	Lineage marker for ETP staining
Ter119	Ter119	FITC	Biolegend	Lineage marker for ETP and bone marrow progenitor staining

Chapter 3 SR-BI is required for maintaining normal thymopoiesis and peripheral T cell homeostasis

3.1 Introduction

Our group previously reported that SR-BI deficiency results in impaired lymphocyte homeostasis in mice [134]. The key features of the impaired lymphocyte homeostasis in SR-BI-deficient mice include lymphocyte expansion, lymphocyte hyperactivation, lymphocyte hyperproliferation and a decrease in T cell to B cell ratio. Later, we identified that the HDL from SR-BI$^{-/-}$ mice is dysfunctional in inhibiting stimuli-induced proliferation of both T cells and B cell, which is responsible for the lymphocyte expansion, hyperactivation and hyperproliferation in the deficient animal [134]. However, the dysfunctional HDL is not likely responsible for the reduced percentage of T cells, suggesting SR-BI probably plays additional roles in preventing lymphocyte imbalance.

Several pieces of evidence have suggested an additional role of SR-BI in adaptive immunity in maintaining normal thymopoiesis. In addition to the decrease in T cell/B cell ratio, SR-BI-null mice display several other phenotypes potentially resulting from reduced T cell productions. First, SR-BI-deficient mice show a reduced percentage of naïve populations and increased portion of memory population in T cells [134], which is commonly seen in mice whose T cell production is decreased [43, 44]. Second, T cells from SR-BI-deficient mice display reduced cytokine production in response to stimuli *in vitro* [134], which might be the consequence of the inadequate refreshment of the T cell pool by newly generated T cells that is known to cause T cell senescence and impaired T

cell functions to stimuli [62-64]. Third, aged SR-BI-deficient mice have autoimmune problems [134], which might also be contributed by decreased thymopoiesis that is known to cause accumulation of autoimmune T cells in the periphery [50-53]. These observations implied that SR-BI might modulate T cell development.

We hypothesized that SR-BI deficiency impairs thymopoiesis, which contributes to the lymphocyte imbalance in SR-BI-null mice. To test this hypothesis, in this chapter, we first analyzed thymus weight and thymic cellularity of SR-BI-deficient mice at different ages and observed that SR-BI deficiency causes reduced thymus size in mice. Next, we evaluated T cell production by detecting TRECs in mice and found that SR-BI deficiency causes declined T cell production. The reduced thymus size and declined T cell production of SR-BI-null mice together indicate that SR-BI deficiency impairs thymopoiesis in mice. By assessing the peripheral T cell homeostasis of mice, we found that the decline of T cell production in the deficient mice leads to narrowed naïve T cell pool in the periphery and compromised T cell functions at young ages. Results from these studies indicate that SR-BI is required in maintaining normal thymopoiesis and peripheral T cell homeostasis.

3.2 Results

3.2.1 SR-BI deficiency leads to reduced thymus weight in mice

To understand if SR-BI plays a role in modulating thymus size, we first evaluated thymus weight of SR-BI$^{-/-}$ mice after puberty (around 5 weeks), when thymus size declines as age increases [87, 272]. As shown in Figure 3.1A and 3.1B, though an age-related decrease in thymus mass was observed in both groups, SR-BI$^{-/-}$ mice display significantly lower thymus weight than age-matched SR-BI$^{+/+}$ controls until 32 weeks. In older ages (>32 weeks), the reduction in thymus weight of SR-BI$^{-/-}$ mice was not observed, as thymus weight of both groups has declined to a low level. This group of data indicates that SR-BI deficiency causes a reduction in thymus weight in mice.

3.2.2 SR-BI deficiency results in decreased thymic cellularity in mice

We also assessed thymocyte number of SR-BI$^{-/-}$ mice after puberty. In line with the lower thymus weight, the deficient mice exhibit markedly smaller thymic cellularity than with age-matched controls (Figure 3.2A and 3.2B). Notably, the reduction in thymic cellularity could still be observed when the SR-BI$^{-/-}$ mice were over 40 weeks. This group of data show that SR-BI deficiency results in reduced thymic cellularity in mice.

3.2.3 SR-BI modulates thymus size in a gender-independent manner

It is well documented that in both humans and mice, females have larger thymic size and higher-grade thymopoiesis than males, indicating gender is an essential factor influencing the thymus [272, 273]. Thus, we next analyzed if SR-BI influences thymus size in a gender-dependent manner. We observed that in

both male and female group, SR-BI$^{-/-}$ mice exhibit significantly reduced thymus weight in early ages (<16 weeks for female and <40 weeks for male) and remarkably decreased thymocyte counts compared with their SR-BI$^{+/+}$ counterparts (Figure 3.3). These observations reveal that the effect of SR-BI on thymus size is not gender-dependent.

3.2.4 SR-BI does not affect thymus size before puberty

We then asked when SR-BI deficiency begins to affect thymus size in mice. To answer this question, we examined thymus weight and thymic cellularity in mice before puberty (1 week of age) and during puberty (5 weeks of age). Consistent with former observations, 5-week-old SR-BI$^{-/-}$ mice display significant reductions in both thymus weight and thymocyte counts compared with 5-week-old SR-BI$^{+/+}$ mice (Figure 3.4A and 3.4B). However, neither thymus weight nor thymic cellularity of 1-week-old SR-BI$^{-/-}$ mice is significantly lower than those of their SR-BI$^{+/+}$ littermates (Figure 3.4A and 3.4B), indicating that SR-BI does not affect thymus size before puberty.

3.2.5 SR-BI deficiency causes a decline in thymic T cell output

T cell production from the thymus is usually correlated with thymus size [274]. Thus, we next hypothesized that the SR-BI deficiency induces reductions in thymic T cell export associated with the decrease of thymus size. To test this, we determined TRECs in CD4^{+} and CD8^{+} splenocytes isolated from mice. As expected, the frequency of TRECs in both CD4^{+} and CD8^{+} cells from SR-BI$^{-/-}$ mice is lower (Figure 3.5A and 3.5B), indicating that the frequency of newly generated T cells is decreased by SR-BI deficiency. More importantly, the

absolute numbers of TRECs are decreased by 26% and 22% respectively in $CD4^+$ and $CD8^+$ splenocytes of SR-$BI^{-/-}$ mice (Figure 2.5C and 2.5D), indicating that the loss of SR-BI also reduces the number of RTEs. This group of data indicate that SR-BI deficiency reduces thymic T cell output in addition to lowering thymus size.

3.2.6 SR-BI deficiency leads to narrowed naïve T cell pool in the periphery

Continuous T cell output from the thymus is essential in maintaining peripheral T cell homeostasis. Inadequate T cell production narrows naïve T cell pool and compromises T cell functions in the periphery [62, 92]. Though 20-week-old SR-$BI^{-/-}$ mice show reduced percentage of naïve population in T cells, their naïve T cell numbers are not decreased [134], which may result from increased T cell proliferation induced by dysfunctional HDL. To further investigate how SR-BI deficiency-impaired thymopoiesis affects peripheral T cell homeostasis, we evaluated CD62L and CD44 expression in T cells from lymph nodes, spleen and blood in younger mice.

We found that in lymph nodes from 5-week-old SR-$BI^{-/-}$ mice, the percentages of the naïve ($CD62L^{hi}CD44^-$) cells in $CD4^+$ and $CD8^+$ population are all significantly reduced compared with SR-$BI^{+/+}$ controls, while the portion of memory T cells ($CD62L^{hi}CD44^+$, central memory T cells and $CD62L^{low}CD44^+$, effector memory T cells) is elevated, in line with the observations in 20-week-old mice (Figure 3.6A-3.6D). However, the numbers of lymph node naïve cells in $CD4^+$ and $CD8^+$ population are also reduced by 34% and 36% respectively in the 5-week-old deficient mice, indicating that their naïve T cell pool size is narrowed

(Figure 3.6F and 3.6G). Shrinkage in the naïve T cell pool of SR-BI$^{-/-}$ lymph nodes is not due to heightened T cell activation, since the total number of memory T cells is not increased (Figure 3.6 F and 3.6G). The decrease in the number of naïve T cells results in a marginal reduction in total T cell numbers in lymph nodes from 5-week-old SR-BI$^{-/-}$ mice (Figure 3.6E).

The SR-BI deficiency-induced reductions in lymph node naïve T cell counts were also observed in 13-week-old mice. Though compared with 5-week-old group, the percentage of naïve cells in T cells in both SR-BI$^{+/+}$ and SR-BI$^{-/-}$ mice is declined in 13-week-old group (Figure 3.7A and 3.7B, in comparison with Figure 3.6B and 3.6D), the T cells from SR-BI$^{-/-}$ lymph nodes display lower portion of naïve subsets than those from SR-BI$^{+/+}$ counterparts (Figure 3.7A and 3.7B). Meanwhile, the total numbers of naïve cells in CD4^{+} and CD8^{+} population are reduced by 50% in lymph nodes from 13-week-old SR-BI$^{-/-}$ mice (Figure 3.7C and 3.7D). These findings from 5-week-old and 13-week-old mice together indicate that the absence of SR-BI narrows the naïve T cell pool in lymph nodes.

We also assessed the naïve T cell pool in spleens and blood of 5-week-old SR-BI$^{-/-}$ mice. Consistent with the observations from lymph nodes, SR-BI$^{-/-}$ mice show remarkable decreases in naïve T cell percentage (Figure 3.8A-3.8D) and marginal reductions in naïve T cell number in spleen (Figure 3.8E and 3.8F). Importantly, a dramatic decline in the blood naïve T cell concentrations was detected in SR-BI$^{-/-}$ mice compared with SR-BI$^{+/+}$ mice (Figure 3.8G). These observations support our conclusion that SR-BI deficiency-impaired thymopoiesis result in a narrowed naïve T cell pool in mice.

3.2.7 SR-BI deficiency leads to increased proliferation of naïve T cells

Naïve T cells rarely proliferate under normal conditions. However, reduced naïve T cells in the periphery can increase naïve T cells proliferation as a compensatory mechanism to maintain the relative steady naïve T cell pool size [17]. Thus, we hypothesized that SR-BI deficiency-reduced T cell output results in an increase in the proliferation of naïve T cells. To test this hypothesis, we injected BrdU to mice and analyzed BrdU incorporation in naïve $CD4^+$ cells. As expected, SR-$BI^{-/-}$ mice show 40% and 30% decreases in the $BrdU^+$ percentage of naïve $CD4^+$ cells in spleen (Figure 3.9A and Figure 3.9B) and lymph nodes (Figure 3.9C and Figure 3.9D) compared with SR-$BI^{+/+}$ mice, though the decrease does not reach statistically significance in lymph nodes (Figure 3.9A and Figure 3.9B). These observations further support that SR-BI deficiency reduced T cell production and impaired peripheral T cell homeostasis.

3.2.8 SR-BI deficiency causes compromised T cell function

Reduced T cell production is also known to compromise T cell functions in the periphery [62, 92]. Thus, we determined if the declined T cell output in SR-$BI^{-/-}$ mice results in impaired T cell functions. For this purpose, we activated splenocytes from mice with anti-CD3 *in vitro*, and detected the proliferation of T cells using BrdU. As expected, we found significantly lower $BrdU^+$ percentage in $CD4^+$ (Figure 3.10A and 3.10B) and $CD8^+$ (Figure 3.10C and 3.10D) cells in SR-$BI^{-/-}$ group than SR-$BI^{+/+}$ controls. Moreover, the counts of newborn ($BrdU^+$) $CD4^+$ and $CD8^+$ cells are dramatically (>70%) decreased in SR-$BI^{-/-}$ group (Figure

3.10E and 3.10F), indicating that T cells from SR-BI$^{-/-}$ mice have impaired stimuli-induced proliferation of T cells.

To further confirm that the SR-BI deficiency causes T cell dysfunctions in response to stimuli, we assessed the activation status of SR-BI$^{-/-}$ T cells after incubation with TCR ligand by detecting the expression of the T cell activation marker CD69 (Figure 3.11). Forty-eight hours after cell culture, though in the absence of stimuli, T cells from SR-BI$^{+/+}$ and SR-BI$^{-/-}$ mice show low and comparable levels of CD69 expression, in the presence of stimuli SR-BI$^{-/-}$ T cells show markedly reduced level of CD69 expression in comparison with SR-BI$^{+/+}$ T cells (Figure 3.11 A-D). This group of data reveals that T cells from SR-BI$^{-/-}$ mice have compromised stimuli-induced activation.

Previously, we also reported that SR-BI$^{-/-}$ T cells display reduced IL-4 secretion in response to TCR ligand engagement [134], demonstrating SR-BI deficiency also renders T cells dysfunctional in stimuli-induced cytokine secretion. Altogether, this group of data elucidates that SR-BI deficiency causes compromised T cell functions associated with decreased T cell production and the impaired peripheral T cell homeostasis.

3.3 Summary

In this chapter, we tested our hypothesis that SR-BI deficiency caused impaired thymopoiesis, which contributed to the lymphocyte imbalance in SR-BI-null mice. By assessing thymus weight and thymic cellularity of SR-BI$^{-/-}$ mice (Figure 3.1 and 3.2), we found that absence of SR-BI in mice causes a reduction in thymus size. Notably, the adverse effect of SR-BI deficiency on thymus size is not gender-dependent (Figure 3.3) and initiates around puberty (Figure 3.4). By detecting TRECs in isolated T cells from mice, we revealed that SR-BI deficiency decreases T cell output (Figure 3.5). Reduced thymus size and thymic output together lead us to conclude that SR-BI deficiency impaired thymopoiesis in mice. By examining the T cell homeostasis in mice at young ages, we observed that SR-BI-null mice display a narrowed naïve T cell pool size (Figure 3.6, 3.7 and 3.8) and increased naïve T cell proliferation (Figure 3.9). These observations indicate that SR-BI deficiency leads to impaired T cell homeostasis in the periphery. Finally, by evaluating T cell responses to stimuli *in vitro*, we found that SR-BI deficiency also compromises T cell functions (Figure 3.10 and 3.11). Altogether, in this chapter, we identify SR-BI as a novel modulator in thymopoiesis. Our data clearly indicate that SR-BI is required in maintaining normal thymopoiesis and optimal peripheral T cell homeostasis in mice.

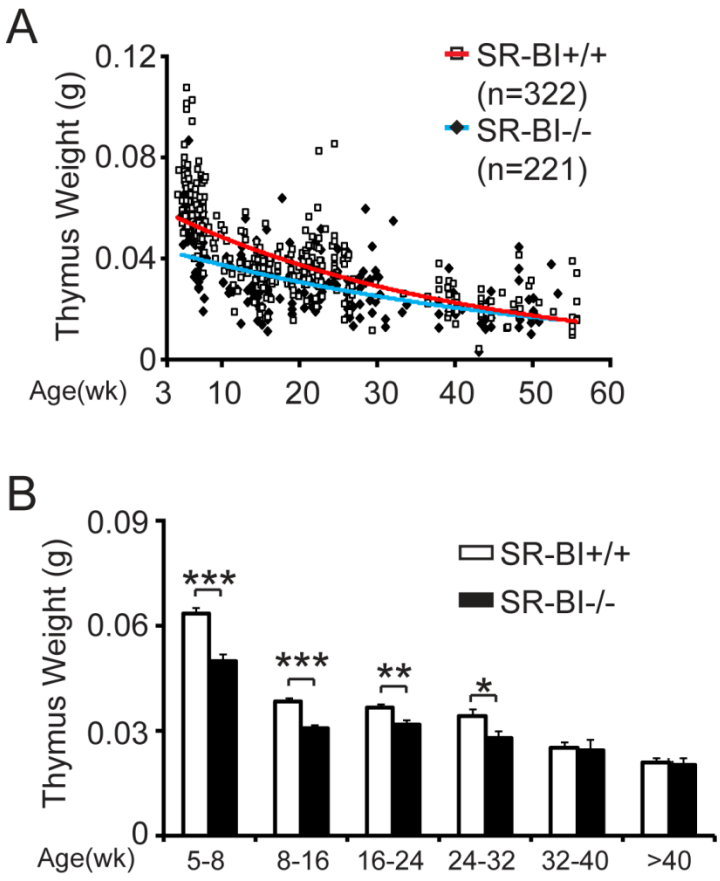

Figure 3.1 SR-BI deficiency reduces thymus weight in mice.

The thymi of mice without any treatment were isolated and weighed. A) The age-related changes in thymus weight of SR-BI$^{+/+}$ (n=322) and SR-BI$^{-/-}$ (n=221) mice after puberty are displayed. B) The weight of SR-BI$^{-/-}$ (n=221) thymi is grouped by age and compared with age-matched SR-BI$^{+/+}$ (n=322) controls. *, $p<0.05$; **, $p<0.01$; ***, $p<0.001$.

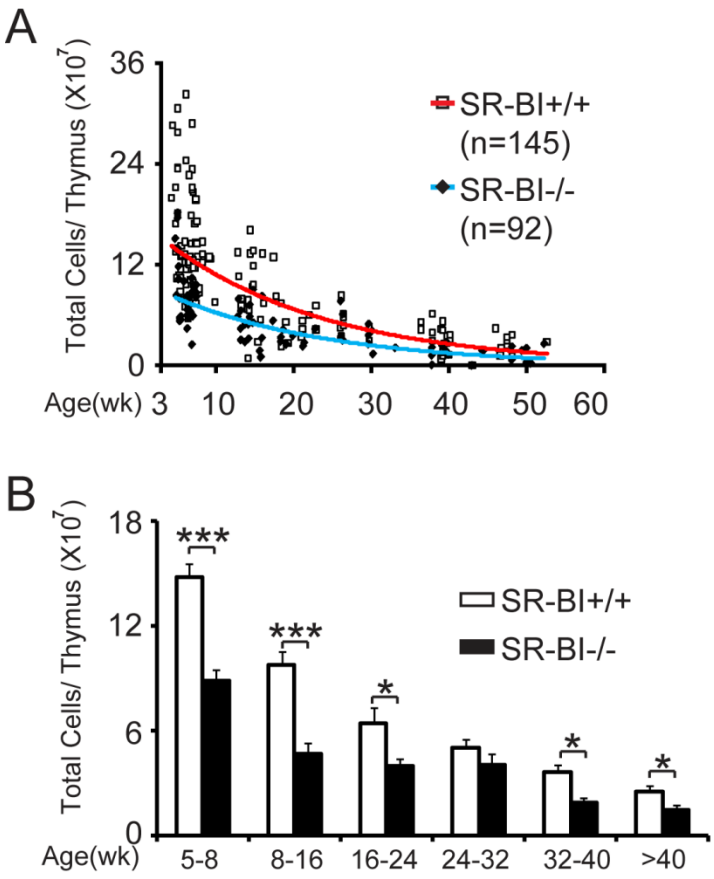

Figure 3.2 SR-BI deficiency decreases thymic cellularity in mice.

The thymi of mice were mechanically disrupted through 100μm cell strainers and re-suspended with 5mL medium. The thymocyte suspension was then diluted and counted using a counting chamber. The total thymocyte number in the 5mL suspension was regarded as the thymic cellularity of mice. A) The age-related changes in the thymic cellularity of SR-BI$^{+/+}$ (n=145) and SR-BI$^{-/-}$ (n=92) mice after puberty are shown. B) The thymic cellularity of SR-BI$^{-/-}$ (n=92) mice is grouped by age and compared with age-matched SR-BI$^{+/+}$ (n=145) controls. *, $p<0.05$; ***, $p<0.001$.

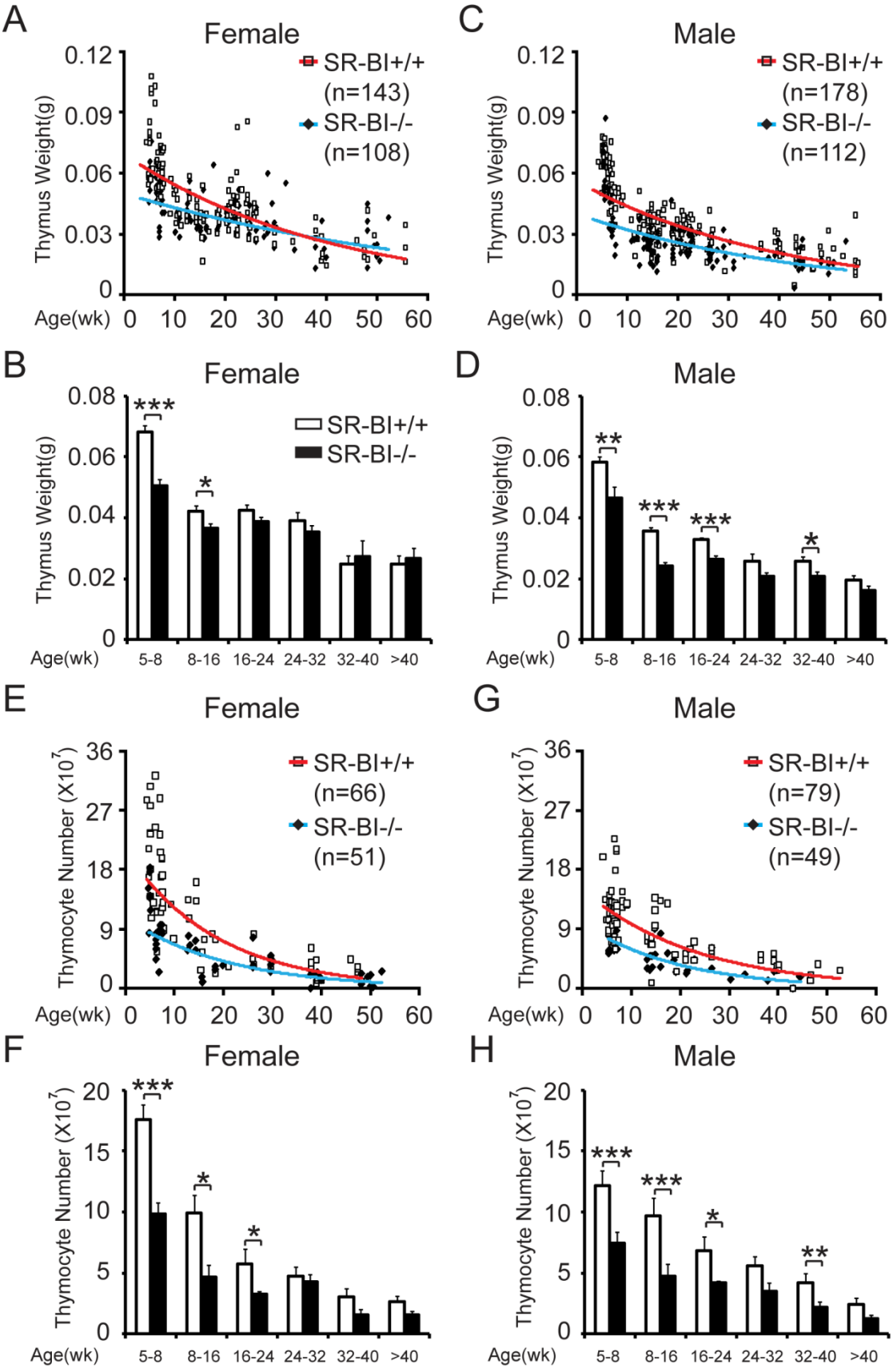
A
Female
SR-BI+/+ (n=143)
SR-BI-/- (n=108)
Thymus Weight(g)
Age(wk)
C
Male
SR-BI+/+ (n=178)
SR-BI-/- (n=112)
B
Female
SR-BI+/+
SR-BI-/-
5-8
8-16
16-24
24-32
32-40
>40
D
Male
E
Female
SR-BI+/+ (n=66)
SR-BI-/- (n=51)
Thymocyte Number (X10^7)
G
Male
SR-BI+/+ (n=79)
SR-BI-/- (n=49)
F
Female
H
Male

Figure 3.3 SR-BI deficiency reduces thymus size in both males and females.

A)-D) Reduced thymus weight was detected in both female (A and B) and male (C and D) SR-BI$^{-/-}$ mice compared with SR-BI$^{+/+}$ controls. E)-H) Decreased thymic cellularity was observed in both female (E and F) and male (G and H) SR-BI$^{-/-}$ mice compared with SR-BI$^{+/+}$ controls. *, $p<0.05$; **, $p<0.01$; ***, $p<0.001$.

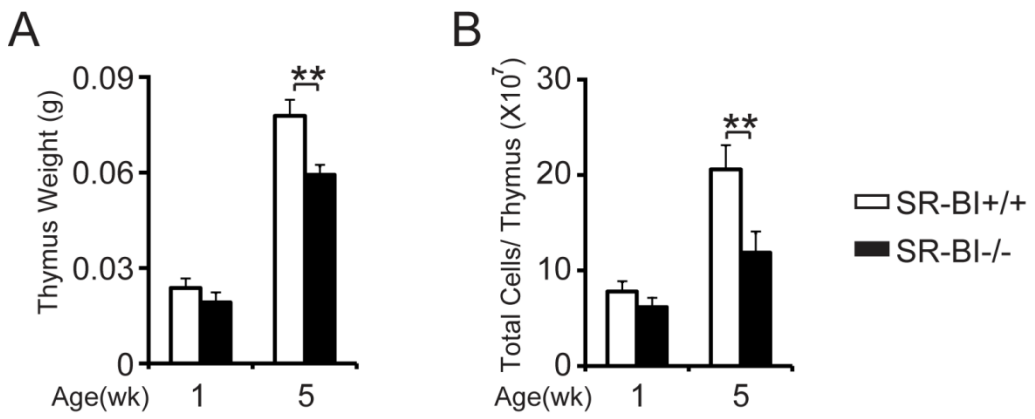

Figure 3.4 SR-BI deficiency does not decrease thymus size before puberty.

A) 5-week-old but not 1-week-old SR-BI$^{-/-}$ mice exhibit lower thymus weight than age-matched SR-BI$^{+/+}$ mice. n=5-8 per group. B) 5-week-old but not 1-week-old SR-BI$^{-/-}$ mice display reduced thymocyte counts compared with age-matched SR-BI$^{+/+}$ mice. n=5-8 per group. **, $p<0.01$.

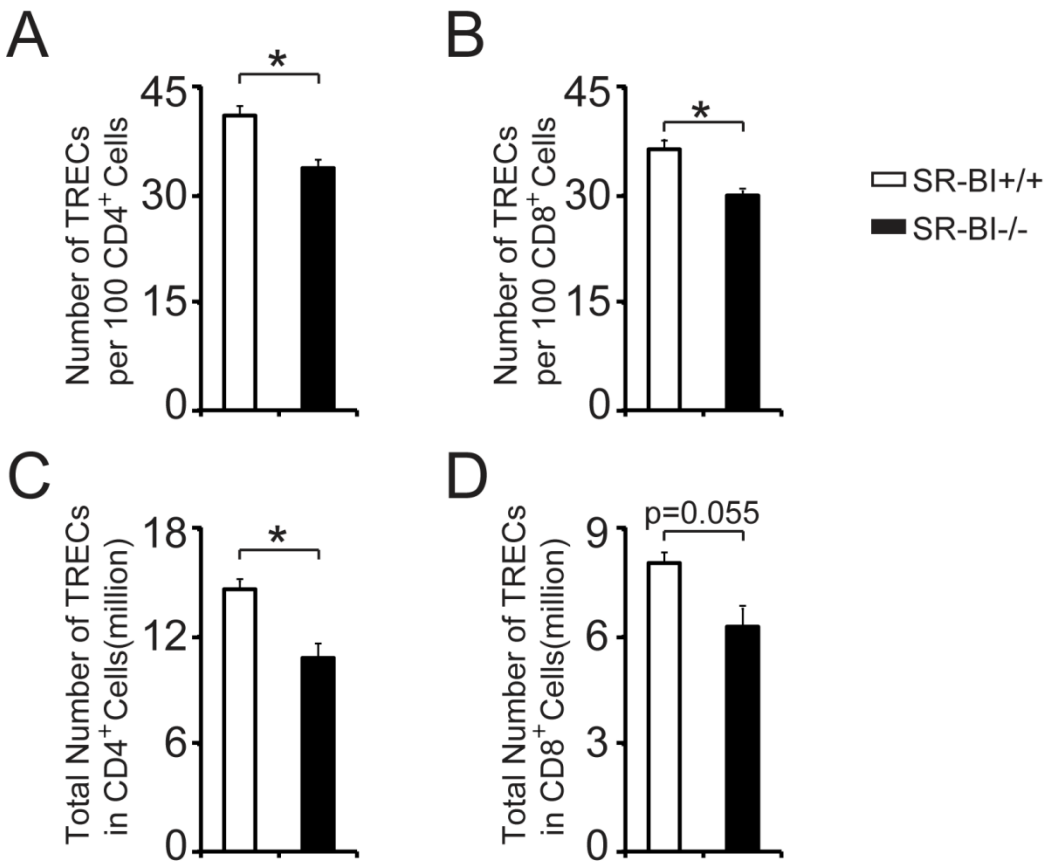

Figure 3.5 SR-BI deficiency reduces T cell output from thymus.

$CD4^+$ and $CD8^+$ splenocytes were sorted from 13-week-old $SR\text{-}BI^{+/+}$ and $SR\text{-}BI^{-/-}$ mouse by flow cytometry and then lysed with proteinase K. The lysates from 50,000 cells were used for TREC detection with quantitative PCR. A)-B) The frequency of TRECs is showed as TREC numbers per 100 $CD4^+$ or $CD8^+$ cells. C)-D) The total number of TRECs of a given population was calculated by multiplying the TREC frequency by the number of cells. n=3 per group with triplicate measurements. *, $p<0.05$.

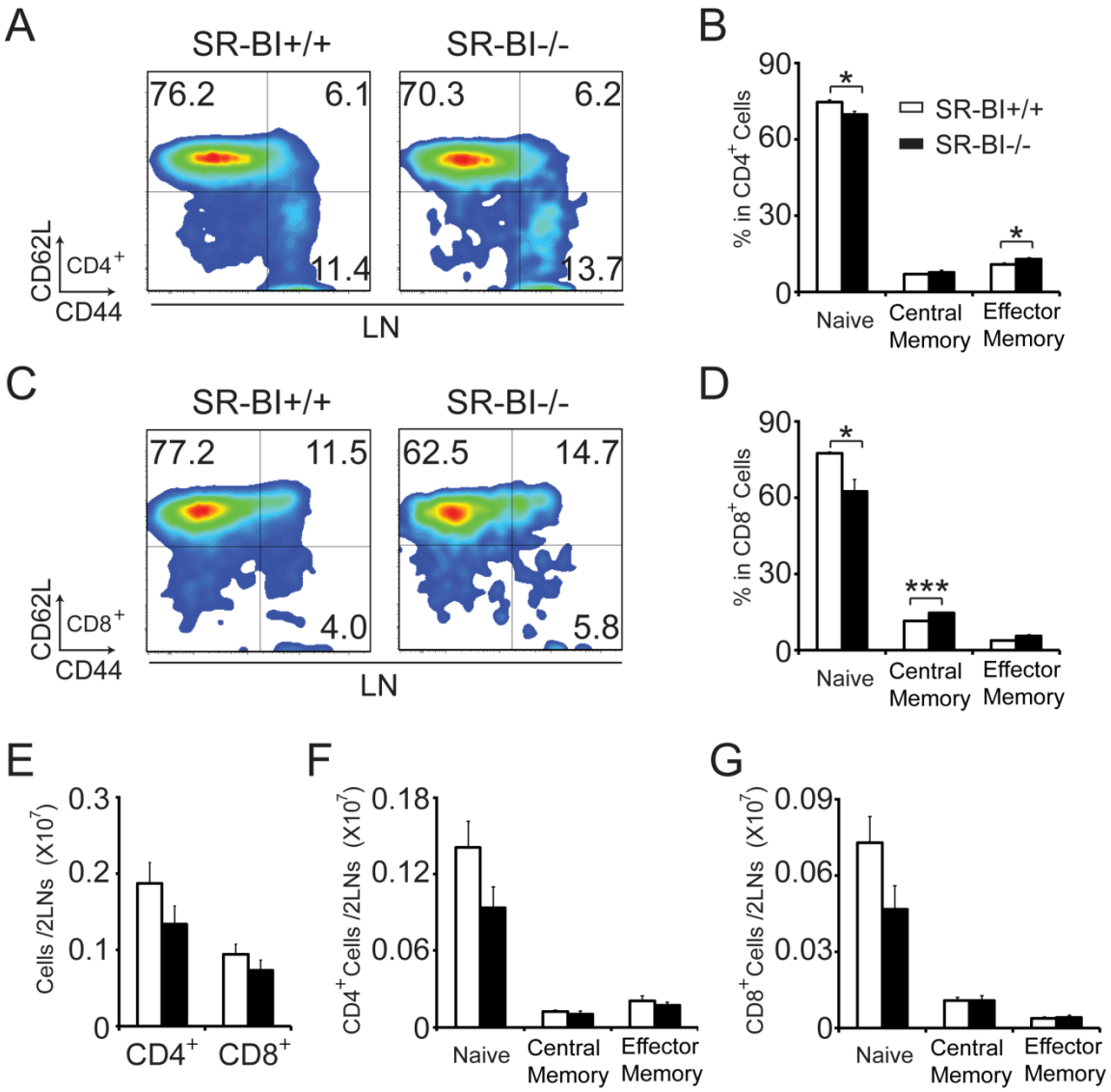

Figure 3.6 SR-BI deficiency reduces naïve T cell pool in lymph nodes of 5-week-old mice.

Mesenteric lymph nodes from 5-week-old SR-BI$^{+/+}$ and SR-BI$^{-/-}$ mice were mechanically disrupted through 100μm cell strainers and stained with a panel of fluorescent-labeled antibody. Cells were then analyzed by flow cytometry. A)-D) Based on expression of CD62L and CD44, three major cell subtypes of CD4^{+} (A and B) or CD8^{+} (C and D) cells were gated: naïve cells (CD62L^{hi}CD44^{-}), central memory cells (CD62L^{hi}CD44^{+}) and effector memory cells (CD62L^{lo}CD44^{+}). E)

The total number of $CD4^+$ or $CD8^+$ cells of a given mouse was calculated by multiplying its $CD4^+$ or $CD8^+$ percentage in total viable lymph node cells by the number of lymph node cells. F)-G) The total number of a $CD4^+$ or $CD8^+$ subtype in a given mouse was calculated by multiplying its percentage in $CD4^+$ or $CD8^+$ cells by the $CD4^+$ or $CD8^+$ cell numbers. n=5-6 per group. *, $p<0.05$; ***, $p<0.001$.

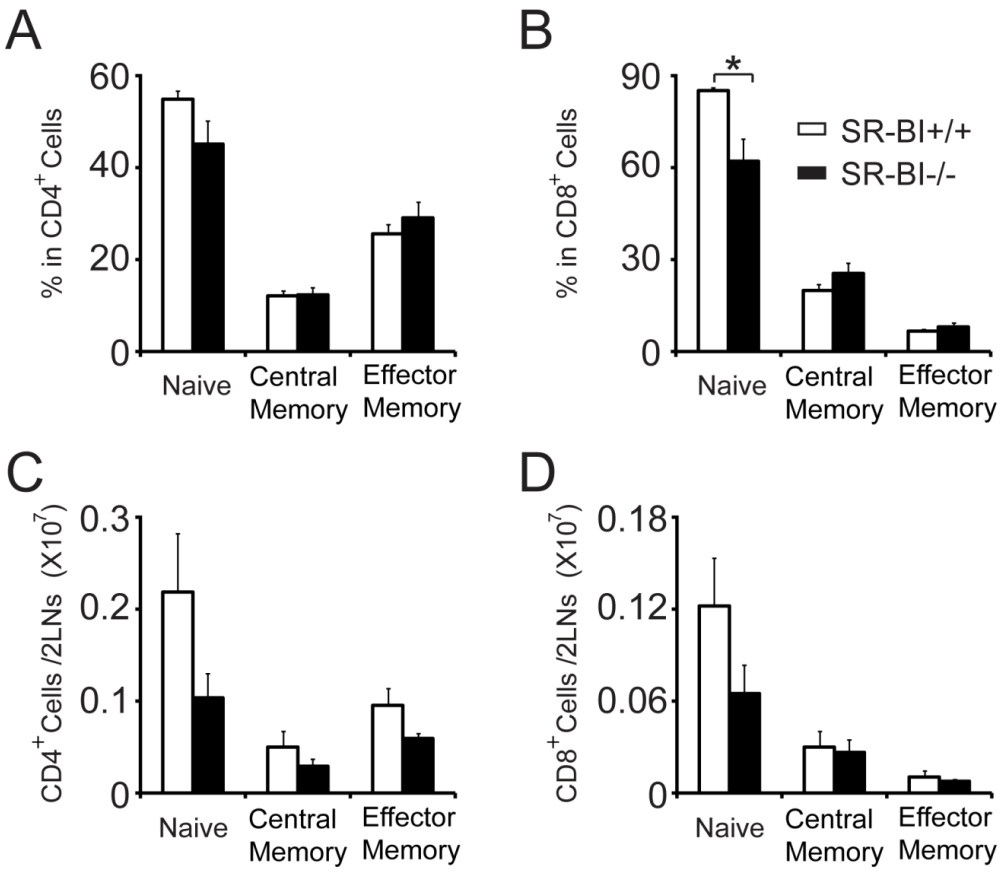

Figure 3.7 SR-BI deficiency reduces naïve T cell pool in lymph nodes of 13-week-old mice.

Mesenteric lymph nodes from 13-week-old SR-BI$^{+/+}$ and SR-BI$^{-/-}$ mice were mechanically disrupted through 100μm cell strainers and stained with a panel of fluorescence-labeled antibody. Cells were then analyzed by flow cytometry. A)-B) Based on expression of CD62L and CD44, three major cell subtypes in CD4^{+} (A) or CD8^{+} (B) cells were gated: naïve cells (CD62L^{hi}CD44^{-}), central memory cells (CD62L^{hi}CD44^{+}) and effector memory cells (CD62L^{lo}CD44^{+}). C)-D) The total number of a CD4^{+} or CD8^{+} subtype of a given mouse was calculated by multiplying its percentage in CD4^{+} or CD8^{+} cells by the CD4^{+} or CD8^{+} cell numbers. n=5 per group. *, $p<0.05$.

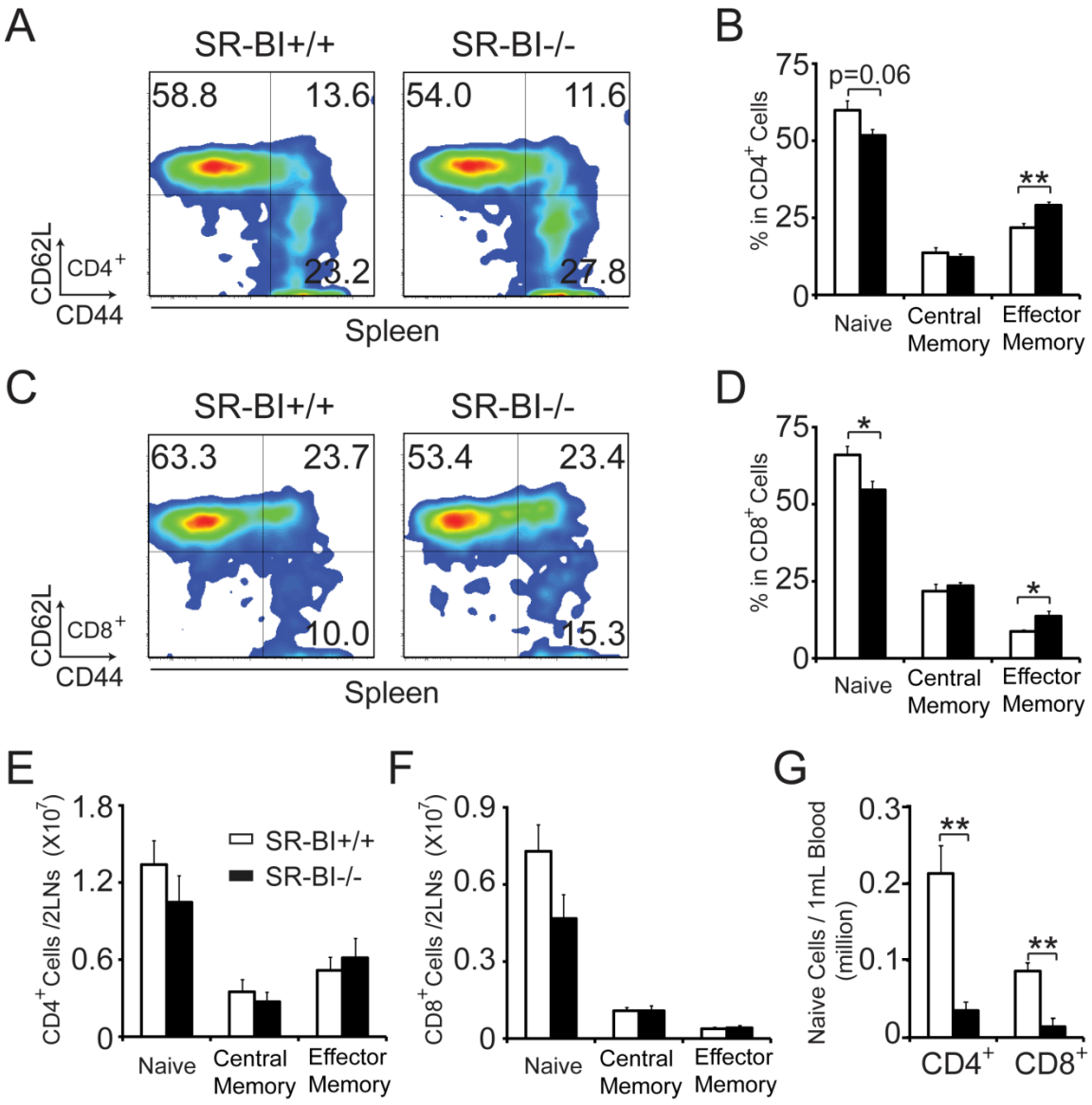

Figure 3.8 SR-BI deficiency reduces naïve T cell pool in spleen and blood of 5-week-old mice.

A)-D) Spleens from SR-BI$^{+/+}$ and SR-BI$^{-/-}$ mice were disrupted with a stomacher, incubated with ACK lysis buffer to deplete erythrocytes and stained with a panel of fluorescent-labeled antibody. Cells were the analyzed by flow cytometry. Based on expression of CD62L and CD44, three major cell subtypes in CD4^{+} (A-B) and CD8^{+} (C-D) cells were gated: naïve cells (CD62L^{hi}CD44^{-}), central memory

cells ($CD62L^{hi}CD44^{+}$) and effector memory cells ($CD62L^{lo}CD44^{+}$). E)-F) The total number of a $CD4^{+}$ or $CD8^{+}$ subtype of a given mouse was calculated by multiplying its percentage in $CD4^{+}$ or $CD8^{+}$ cells by the splenic $CD4^{+}$ or $CD8^{+}$ cell numbers. n=5-6 per group. G) anti-clotted blood from $SR\text{-}BI^{+/+}$ and $SR\text{-}BI^{-/-}$ mice was first incubated with ACK lysis buffer to remove erythrocytes, stained with a panel of fluorescent-labeled antibody and analyzed with a flow cytometer. The naïve cells were defined as $CD62L^{hi}CD44^{-}$ population in $CD4^{+}$ or $CD8^{+}$ cells. The concentration of naïve cells was calculated by multiplying the percentage of naïve T cells $CD45^{+}$ blood cells by the $CD45^{+}$ cell concentration of the mouse. n=5-6 per group. *, $p<0.05$; **, $p<0.01$.

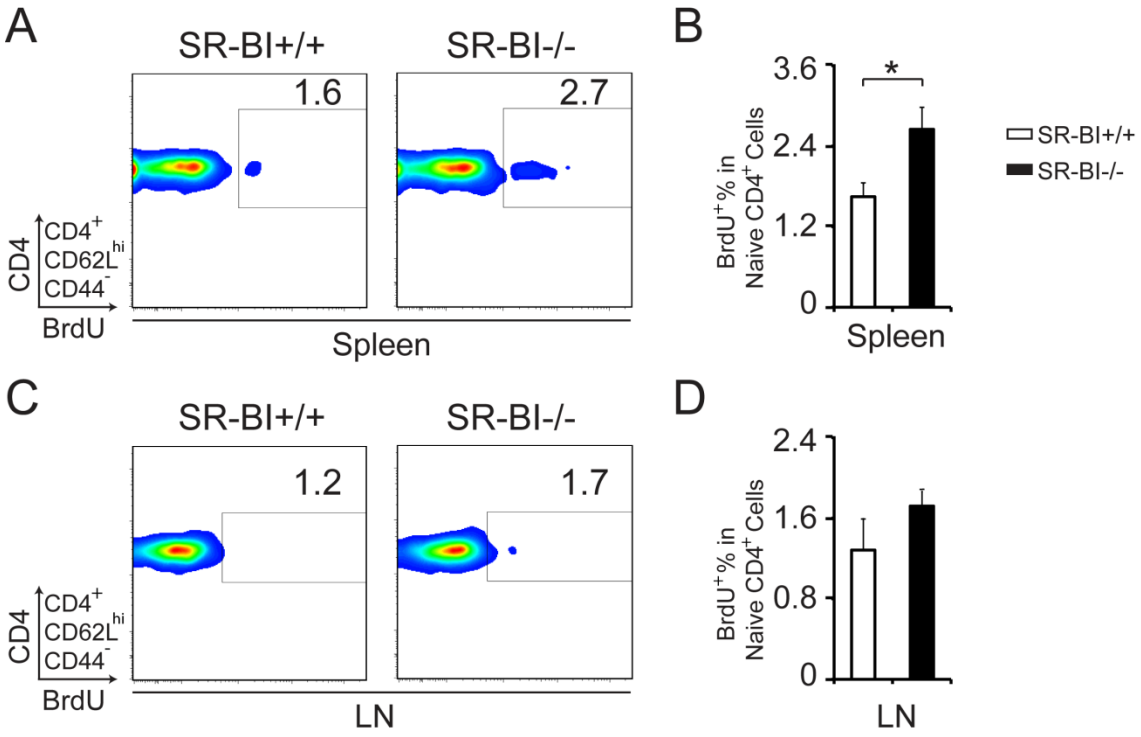

Figure 3.9 SR-BI deficiency increases naïve T cell proliferation.

Five-week-old SR-BI$^{+/+}$ and SR-BI$^{-/-}$ mice were given two i.p. injections (spaced 24 hours apart) of 1mg BrdU in 1mL sterile PBS. Forty-eight hours after the first injection, mice were sacrificed. A)-B) BrdU incorporation in naïve CD4^{+} T cells (CD4^{+}CD62L^{hi}CD44^{-}) from spleens of mice was analyzed. n=7-8 per group. C)-D) BrdU incorporation in naïve CD4^{+} T cells (CD4^{+}CD62L^{hi}CD44^{-}) from lymph nodes of mice was analyzed. n=5 per group. *, $p<0.05$.

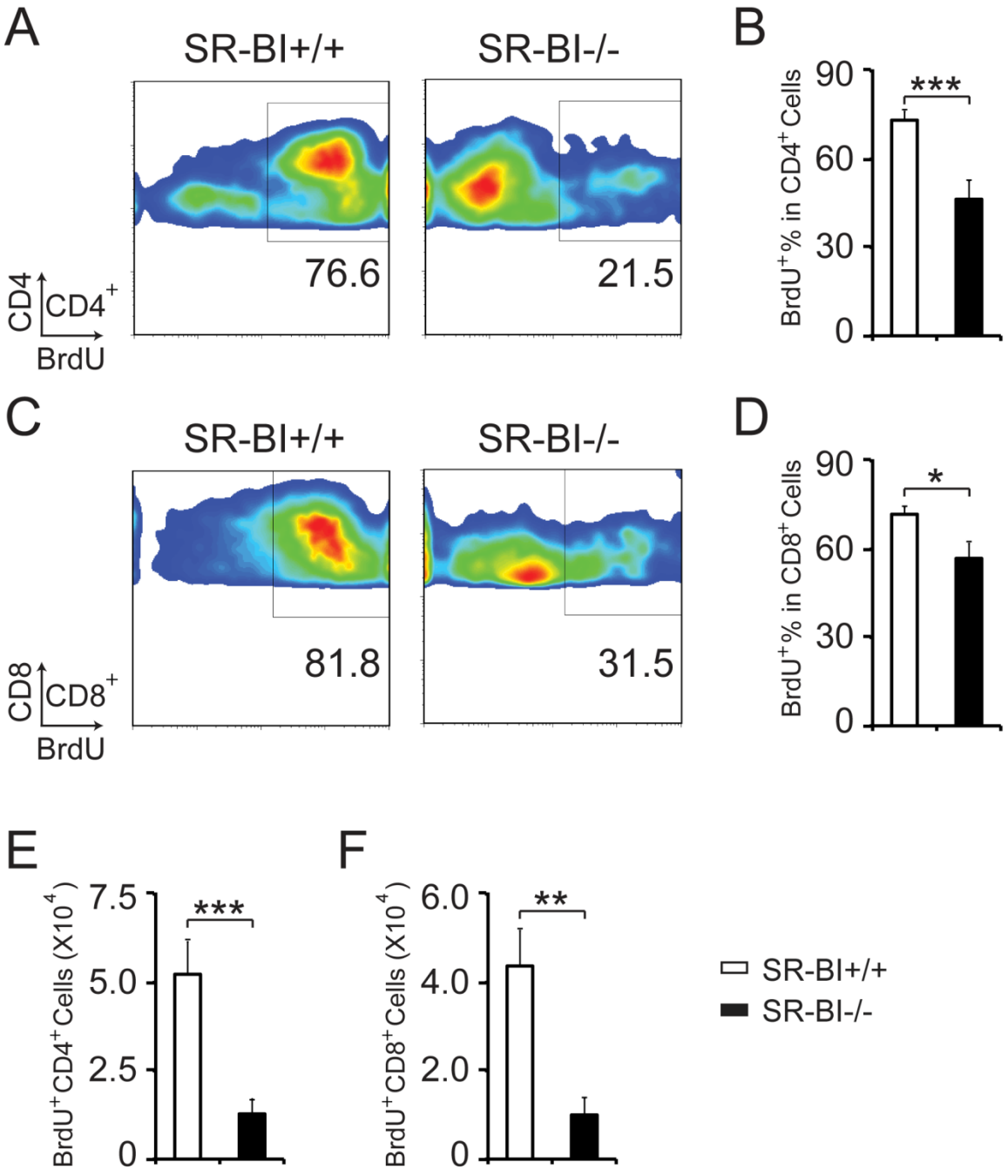

Figure 3.10 SR-BI deficiency impairs stimuli-induced proliferation of T cells.

Eight hundred thousand splenocytes from SR-BI$^{+/+}$ or SR-BI$^{-/-}$ mice (8-12 weeks) were incubated with 20μM BrdU in the presence of 5μg/mL pre-bound anti-CD3

for four days. A)-D) The incorporation of BrdU in cultured $CD4^+$ (A and B) and $CD8^+$ (C and D) T cells was analyzed. E)-F) The total number of $BrdU^+CD4^+$ or $BrdU^+CD8^+$ populations were calculated by multiplying its percentage in cultured cells by total cell numbers in cell cultures after 4-day incubation. n=14 per group. *, $p<0.05$; ***, $p<0.001$.

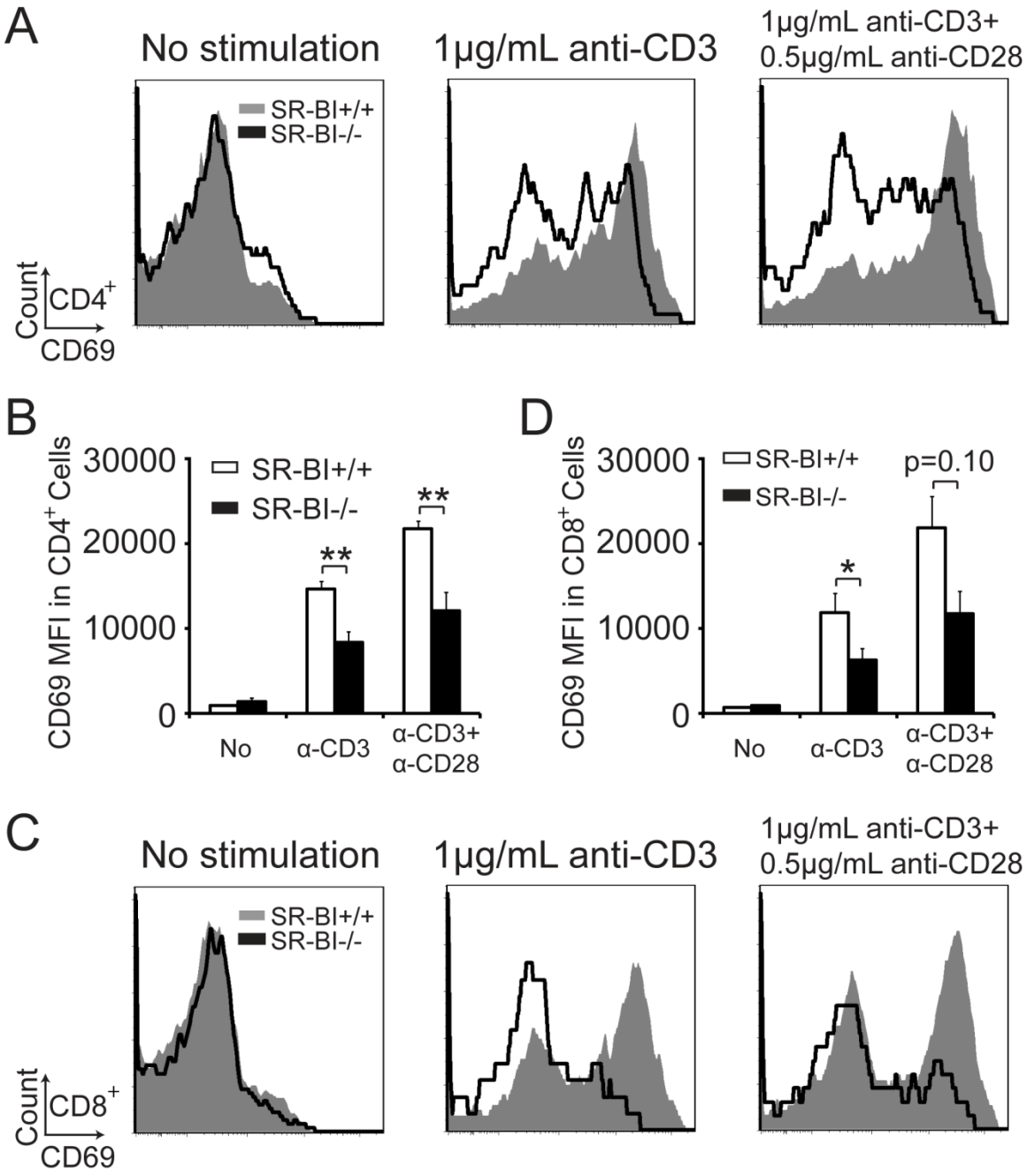

Figure 3.11 SR-BI deficiency impairs stimuli-induced activation of T cells.

Two hundred thousand lymph node cells from SR-BI$^{+/+}$ or SR-BI$^{-/-}$ mice (8 weeks) were incubated with 20μM BrdU in presence of indicated concentrations of pre-bound anti-CD3 and soluble anti-CD28. A)-D) After 48-hour incubation, the level

of CD69 expression in $CD4^+$ (A and B) and $CD8^+$ (C and D) cells was detected. MFI: mean fluorescence intensity. n=3 per group. *, $p<0.05$; **, $p<0.01$.

Chapter 4 SR-BI is required in maintaining normal bone marrow progenitor thymic homing and thymic regeneration

4.1 Introduction

T lineage cells in the thymus undergo an established program in which they develop from bone marrow-derived progenitors to mature naïve T cells. The key events in thymopoiesis include the entry of bone marrow progenitors in thymus; β-selection and generation of DP thymocytes; positive and negative selections; generation and maturation of SP thymocytes and the export of mature T cells from the thymus. Based on surface marker expression, thymocytes in different developing stages can be distinguished. The percentage of thymocyte subsets under normal conditions remains relatively stable. Alterations in the percentage of one or more thymocyte subset are seen as indicators of changes in T cell development [33, 34, 40].

Our data in chapter 3 indicates that SR-BI is a novel player in thymopoiesis as SR-BI deficiency causes reduced thymus size and decreased thymic output. However, the underlying mechanism for this is not understood. To investigate the mechanism by which SR-BI modulates thymopoiesis, in this chapter we analyzed thymocyte subtypes in SR-BI-deficient mice at young ages in an effort to understand which steps in thymopoiesis are affected by SR-BI. We found that the intrathymic T cell developmental program is intact in SR-BI$^{-/-}$ mice, as no alterations in the percentage of major thymocyte subsets was observed in the deficient mice. Interestingly, we found that SR-BI-null mice display a

significant reduction in the percentage of ETPs, suggesting that SR-BI deficiency reduces progenitor thymic entry in mice.

Changes in the ETP population of SR-BI-null mice led us to hypothesize that SR-BI deficiency impairs thymopoiesis by affecting bone marrow-derived progenitors upstream of ETPs. Starting from the HSCs in bone marrow, T lineage progenitors experience two major developmental events before giving rise to downstream cells in the thymus [77]. The first is the lymphoid progenitor development in bone marrow, in which progenitors develop from HSCs to LMPPs and CLPs to gain the ability of entering thymus. The second is the bone marrow progenitor thymic homing, in which progenitors move out of bone marrow and migrate to the thymus via the circulation. Reduced progenitor entry into the thymus has been shown to decrease the portion of ETPs and lead to thymic hypocellularity [83, 84]. Thus, to test our hypothesis, we evaluated bone marrow progenitor development and progenitor thymic homing in SR-BI$^{-/-}$ mice. We found that the absence of SR-BI does not affect lymphoid progenitor development in bone marrow, but impairs progenitor thymic homing, demonstrating that SR-BI deficiency causes impaired thymopoiesis in mice by inducing reduced bone marrow progenitor settlement in the thymus.

Acute thymus involution can be induced by several factors and the thymic recovery is slow [68, 275]. As SR-BI is required in maintaining normal thymus size and function, we also tested whether SR-BI plays a role in modulating thymic recovery after thymocyte depletion. Thymus regeneration in early stages depends on intrathymic precursors [276] and in the long term requires the

migration of bone marrow progenitors [277]. Due to the decreased portion of ETPs and impaired thymic homing of SR-BI$^{-/-}$ mice, we hypothesized that SR-BI deficiency impairs thymus regeneration after thymocyte depletion. To test this, we induced thymocyte depletion with sublethal irradiation in mice and evaluated subsequent thymic recovery. We observed SR-BI-null mice display delayed thymic regeneration after irradiation.

Taken together, this data revealed that SR-BI deficiency impairs thymopoiesis by decreasing progenitor thymic homing. Also, our results indicate that SR-BI deficiency delays thymic recovery after thymocyte depletion.

4.2 Results

4.2.1 SR-BI deficiency does not alter CD4/CD8 profile in the thymus

To investigate the mechanism by which SR-BI modulates thymopoiesis, we initially stained thymocytes from 5-week-old SR-BI$^{+/+}$ and SR-BI$^{-/-}$ with anti-CD4 and anti-CD8. Based on the expression of these two markers, thymocytes can be divided to DN, DP, 4SP and 8SP populations. We chose mice at 5 weeks because at this age thymocyte number peaks and the reduction of thymic cellularity in SR-BI$^{-/-}$ mice is significant. We observed a normal CD4/CD8 profile in the SR-BI$^{-/-}$ thymi compared with the SR-BI$^{+/+}$ counterparts (Figure 4.1A and 4.1B). The number of each population is reduced coordinately with the total thymocyte number in the deficient mice (Figure 4.1 C). These findings are consistent with our former observations in 6-week-old and 25-week-old mice [134].

4.2.2 SR-BI deficiency does not change DN1-4 profile in the thymus

As a step further, we evaluated the DN1-4 profile of mice. We divided the DN population into DN1, DN2, DN3 and DN4 cells based on the expression of CD25 and CD44. We did not detect any difference in the percentage of the four DN subsets in the deficient mice (Figure 4.2A and 4.2B), indicating SR-BI deficiency does not affect the DN1-4 profile. Similarly, the numbers of all DN subtypes are decreased due to the decline in total thymocyte numbers (Figure 4.2C).

4.2.3 SR-BI deficiency does not affect selection processes in thymopoiesis

We evaluated if SR-BI deficiency affects selection processes, i.e. β-selection, positive selection and negative selection in mice. To determine if SR-BI deficiency influences β-selection, we evaluated TCR-β expression in DN cells. SR-BI$^{-/-}$ show comparable TCR-β expression in DN cells with SR-BI$^{+/+}$ mice (Figure 4.3A), which together with the observation that the percentages of DN subsets are unaltered in SR-BI$^{-/-}$ mice indicate that loss of SR-BI does not cause any defect in β-selection.

We next assessed if SR-BI modulates selections in DP stage by distinguishing the pre- and postselection DP thymocytes using expression of CD69 and TCR-β [278]. Both SR-BI$^{-/-}$ and SR-BI$^{+/+}$ mice exhibit ~10% CD69^{+}TCR-β^{+} (postselection) cells in the DP population (Figure 4.3B and 4.3C). Meanwhile, the TCR-β expression in 4SP and 8SP population is also identical in SR-BI$^{-/-}$ and SR-BI$^{+/+}$ thymi (Figure 4.3D and 4.3E). These observations indicate that SR-BI deficiency is not likely to influence positive selection or negative selection.

4.2.4 SR-BI deficiency does not impair γδ T cell development

Most T cells are αβ T cells because they express αβ TCR chains. In contrast, a small group of T cells possess a distinct TCR, namely γδ TCR, and thus are called γδ T cells, which also develop in the thymus [7]. We investigated if SR-BI deficiency results in a defect in the development of γδ T cells associated with thymic hypocellularity. As shown in Figure 4.4, we found that the γδ TCR expression in DN cells is comparable in SR-BI$^{+/+}$ and SR-BI$^{-/-}$ thymi,

demonstrating that SR-BI deficiency does not influence γδ T cell development in the thymus.

4.2.5 SR-BI deficiency does not influence single positive thymocyte maturation process

We next evaluated if SR-BI plays a role in SP thymocyte maturation. To this purpose, we distinguished immature and mature SP thymocytes by the expression of CD69 and CD62L. In either 4SP (Figure 4.5A and 4.5B) or 8SP (Figure 4.5C and 4.5D) thymocytes, SR-BI$^{-/-}$ mice do not show significant changes in the percentage of immature (CD69^{+}CD62L^{lo}) and mature (CD69^{-} CD62L^{hi}) subtypes compared with SR-BI$^{+/+}$ counterparts, indicating that SR-BI does not affect in SP thymocyte maturation process.

4.2.6 SR-BI deficiency causes reduced apoptosis of DN thymocytes

We also evaluated if SR-BI deficiency influences thymocyte apoptosis as elevated thymocyte apoptosis is able to induce thymic hypocellularity in mice. For this purpose, we detected the DNA strand breaks in thymocytes by TUNEL analysis. As shown in Figure 4.6A, SR-BI$^{-/-}$ mice display slightly lower rather than higher TUNEL^{+} percentage in total thymocytes than SR-BI$^{+/+}$ mice (Figure 4.6A), formally excluding the possibility that SR-BI deficiency impairs thymopoiesis by inducing elevated thymocyte apoptosis. TUNEL analysis in thymocyte subtypes revealed that the decreased apoptotic cell accumulation in SR-BI$^{-/-}$ thymocytes is mainly found in the DN population, since the TUNEL^{+} percentage in DN cells is 25% lower in SR-BI$^{-/-}$ mice than in SR-BI$^{+/+}$ mice (Figure 4.6A and 4.6B). In contrast, the TUNEL^{+} percentages in DP, 4SP and 8SP population are

comparable between SR-BI$^{+/+}$ and SR-BI$^{-/-}$ mice. These data indicate that SR-BI deficiency causes decreased apoptosis in DN thymocytes.

4.2.7 SR-BI deficiency results in decreased proliferation of DN2 thymocytes

SR-BI deficiency could also possibly cause reduced thymus size by decreasing thymocyte proliferation. To test this possibility, we injected mice with BrdU and evaluated thymocyte proliferation by measuring BrdU incorporation. As shown in Figure 4.7A, SR-BI$^{-/-}$ mice do not show significant decline in BrdU^{+} percentage in thymocytes, indicating that SR-BI deficiency does not cause thymic hypocellularity by reducing thymocyte proliferation. Interestingly, by detecting the proliferation of thymocyte subsets, we found that SR-BI$^{-/-}$ mice exhibit a significantly reduced BrdU^{+} portion in DN2 thymocytes compared with SR-BI$^{+/+}$ controls. In DN3 thymocytes, SR-BI$^{-/-}$ mice also show a strong decreasing trend in proliferation, though statistical significance is not reached. In contrast, for DN1 cells, DN4 cells (Figure 4.7A), DP cells, 4SP cells and 8SP cells (Figure 4.7B), the BrdU^{+} percentage is not altered by the absence of SR-BI. These data indicate that SR-BI deficiency results in a decrease in the proliferation of DN2 and DN3 thymocytes.

4.2.8 SR-BI deficiency decreases the percentage of ETPs

The decreased apoptosis of DN thymocytes and the reduced proliferation of DN2 and DN3 thymocytes may be linked because β selection occurs in the DN2 and DN3 stages when cells that fail to express functional TCR-β are removed by apoptosis. Given that the percentages of thymocyte populations before and after β selection are not changed in SR-BI-null mice, we speculated

that fewer DN2 cells are generated to enter β selection in SR-BI-null mice, which results in the reduction in the proliferation of early DN subsets. DN2 thymocytes are direct descendants of ETPs, which are a small subset of DN1 cells. Thus, next we evaluated if SR-BI deficiency affects ETPs in mice. The gating strategy for ETPs is shown in Figure 4.8A. The mature thymocytes were first excluded by a panel of lineage markers (anti-CD3ε, CD8α, CD8β, B220, CD19, CD11b, CD11c, GR-1, NK1.1, Ter119, TCR-β and TCR-γ/δ) and then the ETP was gated as the $CD25^{-}CD44^{+}cKit^{hi}$ population in the Lin^{-} cells [279]. Although SR-$BI^{-/-}$ thymi exhibit comparable Lin^{-} and $Lin^{-}CD25^{-}$ fractions with SR-$BI^{+/+}$ controls, their ETP percentage in $Lin^{-}CD25^{-}$ population and in all thymocytes is reduced by 50% and 40%, respectively (Figure 4.8A and B), together with a 65% decrease in the number of ETPs (Figure 4.8C). These results clearly indicate that SR-BI deficiency-induced thymic hypocellularity is accompanied by a decrease in the portion of ETPs.

4.2.9 SR-BI deficiency does not impair thymopoiesis through affecting lymphoid progenitor development in bone marrow

As SR-BI deficiency leads to dramatically reduced portion of ETPs, the most primitive population in thymocytes, we hypothesized that SR-BI deficiency affects T cell development upstream of ETPs. To test this hypothesis, at first we evaluated bone marrow lymphoid progenitor development in mice. The gating strategy of bone marrow lymphoid progenitors is shown in Figure 4.9A. Briefly, a group of lineage markers (anti-CD2, CD3ε, CD4, CD8α, B220, CD19, CD11b, GR-1, NK1.1 and Ter119) were first used to exclude mature cells. LSK cells were

then distinguished as the Sca-1^{+}cKit^{+} population in Lin^{-} cells and Sca-1^{int}cKit^{int} population (f1) was meanwhile gated. HSCs, MPPs and LMPPs were gated in the LSK population based on the expression of CD135 [280]. CLPs were defined as IL7R^{+} population in f1 population [281]. In 5-week-old SR-BI$^{-/-}$ mice, we did not detect any significant difference in either percentages or numbers of gated bone marrow progenitors compared with SR-BI$^{+/+}$ mice (Figure 4.9A-4.9C), indicating that SR-BI deficiency does not affect lymphoid progenitor development in bone marrow.

4.2.10 SR-BI deficiency causes decreased progenitor homing to the thymus

We next evaluated if SR-BI deficiency impairs bone marrow progenitor thymic homing. To this purpose, we injected 20 million CFSE-labeled SR-BI$^{+/+}$ bone marrow cells into non-irradiated SR-BI$^{+/+}$ and SR-BI$^{-/-}$ mice, and examined the seeding of labeled bone marrow cells within the thymus two days later. In this short-term progenitor homing assay, though comparable concentrations of CFSE^{+} cells were found in the blood of SR-BI$^{-/-}$ and SR-BI$^{+/+}$ mice two days after injection (Figure 4.10A), 34% fewer labeled bone marrow cells were detected in the thymi of SR-BI$^{-/-}$ mice (Figure 4.10B). These observations reveal that absence of SR-BI impairs the entry of bone marrow progenitors into the thymus.

4.2.11 SR-BI deficiency leads to a reduced contribution of circulating progenitors to thymopoiesis

To determine how the reduced bone marrow progenitor entry into the thymus in SR-BI$^{-/-}$ mice contributes to the downstream T cell development, we conducted the long-term homing assay, in which 20 million CD45.1^{+} bone

marrow cells were injected into non-irradiated mice and thymocyte subtypes derived from injected CD45.1^{+} bone marrow cells were analyzed two weeks later. As expected, the percentage and number of CD45.1^{+} thymocytes are both significantly lower in the deficient mice than control mice (Figure 4.11A-C), indicating that the contribution of circulating bone marrow progenitors to thymopoiesis is impaired by SR-BI deficiency. Interestingly, despite the reduced numbers, the CD45.1^{+} cells in SR-BI$^{-/-}$ thymi show a similar CD4/CD8 profile with those in SR-BI$^{+/+}$ mice (Figure 4.11D-E), indicating the downstream development of settled progenitors is intact in the deficient mice. The numbers of CD45.1^{+} thymocyte subtypes are all significantly reduced in SR-BI$^{-/-}$ mice (Figure 4.11F). These findings indicate that SR-BI deficiency impairs thymopoiesis by affecting the thymic homing process of bone marrow progenitors.

4.2.12 SR-BI deficiency impairs thymic recovery after sublethal irradiation

Because the ETPs and progenitor thymic homing are essential for thymic regeneration [68, 277], we proposed that SR-BI deficiency results in impaired thymic recovery after thymocyte depletion. Indeed, using CLP, a model inducing sepsis and thymocyte depletion in mice [282], we had observed that SR-BI$^{-/-}$ mice show much smaller thymi and lower thymic cellularity than SR-BI$^{+/+}$ mice 7 days after the surgery, which implies that SR-BI deficiency leads to delayed thymic regeneration (unpublished data). However, CLP is not a good model for studying the role of SR-BI in thymic recovery because it has been shown that CLP induces dramatic thymocyte apoptosis in SR-BI$^{+/+}$ mice but not in SR-BI$^{-/-}$ mice 18 hours after surgery [247], suggesting that SR-BI deficiency may also affect CLP-

induced thymocyte apoptosis. To induce the same levels of thymocyte depletion in SR-BI$^{+/+}$ and SR-BI$^{-/-}$ mice, we utilized the sublethal irradiation model, which is widely used for investigating thymic recovery [111, 256, 257].

Four days after irradiation, SR-BI$^{+/+}$ and SR-BI$^{-/-}$ mice show equally low levels of thymocyte numbers (Figure 4.12A), indicating that in contrast to CLP-induced thymocyte apoptosis, SR-BI deficiency does not affect irradiation-induced thymocyte apoptosis. From day 4 to day 7 post irradiation, thymic cellularity of SR-BI$^{+/+}$ mice is increased by 8.4-fold while that of SR-BI$^{-/-}$ mice is only elevated by 3.1-fold (Figure 4.12A), indicating that the thymic recovery after irradiation is impaired in the deficient mice. At day 14 after irradiation, the thymocyte counts of SR-BI$^{-/-}$ mice are still 32% lower than those of SR-BI$^{+/+}$ controls (Figure 4.12A). We also analyzed the thymic CD4/CD8 profile at day 7 after irradiation. Consistent with former observations in SR-BI$^{-/-}$ mice and in long-term homing assay, we found that 7 days post irradiation, SR-BI$^{-/-}$ mice show a comparable CD4/CD8 profile with SR-BI$^{+/+}$ mice (Figure 4.12B), demonstrating that during thymic recovery, the T cell development is normal inside SR-BI$^{-/-}$ thymi. Similarly, the number of DN, DP, 4SP and 8SP thymocytes were all significantly decreased associated with total thymocyte counts in the deficient mice (Figure 4.12C). Altogether, these data indicate that SR-BI deficiency impairs thymic recovery after sublethal irradiation.

4.3 Summary

In this chapter, we investigated different steps of T cell development to understand which step of thymopoiesis is modulated by SR-BI. First, we examined thymocyte subsets in 5-week-old mice and found that SR-BI deficiency does not cause any obvious blockage in intrathymic T cell development, as shown by normal percentages of thymocyte subsets (Figure 4.1, 4.2, 4.4 and 4.5) and unaltered TCR-β expression in all thymocyte subsets (Figure 4.3) in SR-BI-null mice. Furthermore, we did not observe increased apoptosis (Figure 4.6) or decreased proliferation (Figure 4.7) of thymocytes in SR-BI-deficient mice, excluding the possibility that SR-BI deficiency causes thymic hypocellularity via affecting thymocyte apoptosis or proliferation. Interestingly, we observed a remarkable decrease in the portion of ETP in SR-BI$^{-/-}$ thymi (Figure 4.8), suggesting that SR-BI deficiency impairs thymopoiesis by affecting progenitor entry into thymus.

We then studied bone marrow progenitor development and thymic homing, two key steps upstream of ETPs in T cell development in mice. By flow cytometry analysis of the bone marrow lymphoid progenitors in mice, we found SR-BI deficiency does not cause any blockage in lymphoid progenitor development (Figure 4.9). Interestingly, by injecting labeled bone marrow cells into the circulation of mice, we observed that 2 days later fewer bone marrow cells homing to the thymus in SR-BI$^{-/-}$ mice (Figure 4.10), demonstrating that SR-BI deficiency impairs bone marrow progenitor thymic homing. The reduction of bone marrow progenitor settlement further results in decreased number of downstream

thymocytes, as shown by that 2 weeks after the labeled bone marrow cell injection, SR-BI$^{-/-}$ mice show 60% fewer thymocytes derived from labeled bone marrow cells (Figure 4.11). These data reveal that SR-BI deficiency impairs bone marrow progenitor thymic homing, which results in the defects in thymopoiesis.

Finally, we investigated if SR-BI deficiency has any effect on thymic regeneration utilizing the sublethal irradiation model. We found that although the thymic cellularity of SR-BI$^{+/+}$ and SR-BI$^{-/-}$ mice is decreased into an equally low level 4 days after irradiation, the thymocyte numbers of SR-BI$^{-/-}$ mice are 63% lower than those of SR-BI$^{+/+}$ mice 7 days after irradiation (Figure 4.12), indicating that SR-BI is also required for normal thymic regeneration.

Taken together, our results indicate that SR-BI deficiency impairs thymopoiesis by impairing bone marrow progenitor thymic homing and SR-BI is required for rapid thymic regeneration after thymocyte depletion.

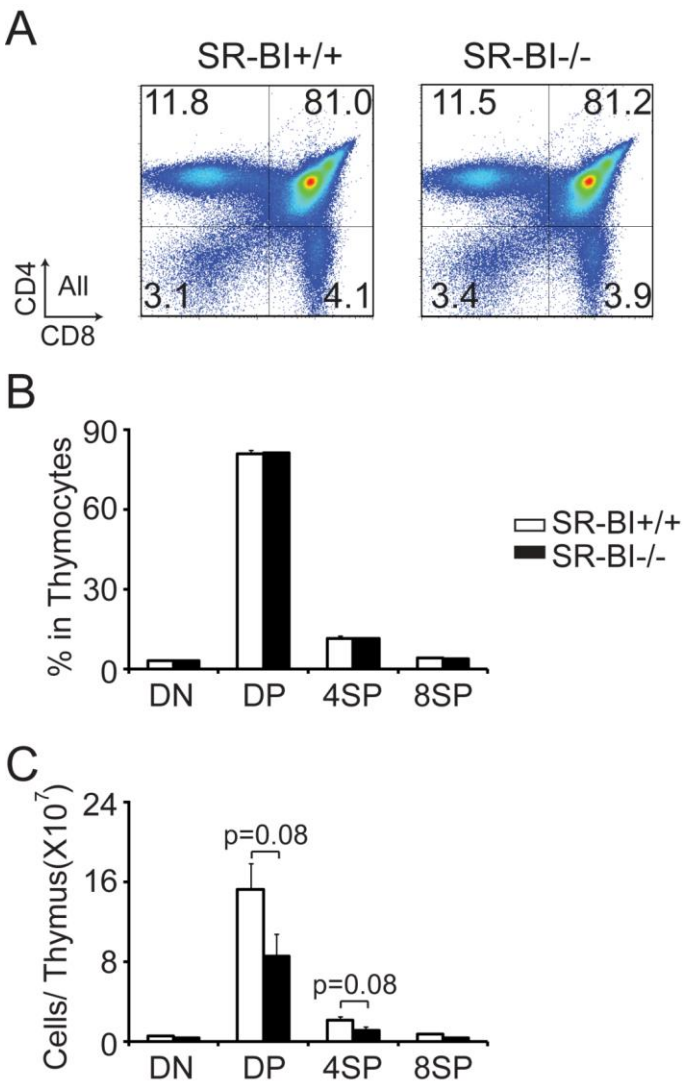

Figure 4.1 SR-BI deficiency does not affect the CD4/CD8 profile in mice.

A)-B) Thymocytes from 5-week-old mice were stained with anti-CD4 and anti-CD8 to distinguish double negative (DN, $CD4^-CD8^-$), double positive (DP, $CD4^+CD8^+$), CD4 single positive (4SP, $CD4^+CD8^-$) and CD8 single positive (4SP, $CD4^-CD8^+$) populations. C) The number of each population was calculated by multiplying its percentage in viable thymocytes by the number of viable thymocytes. n=5-6 per group.

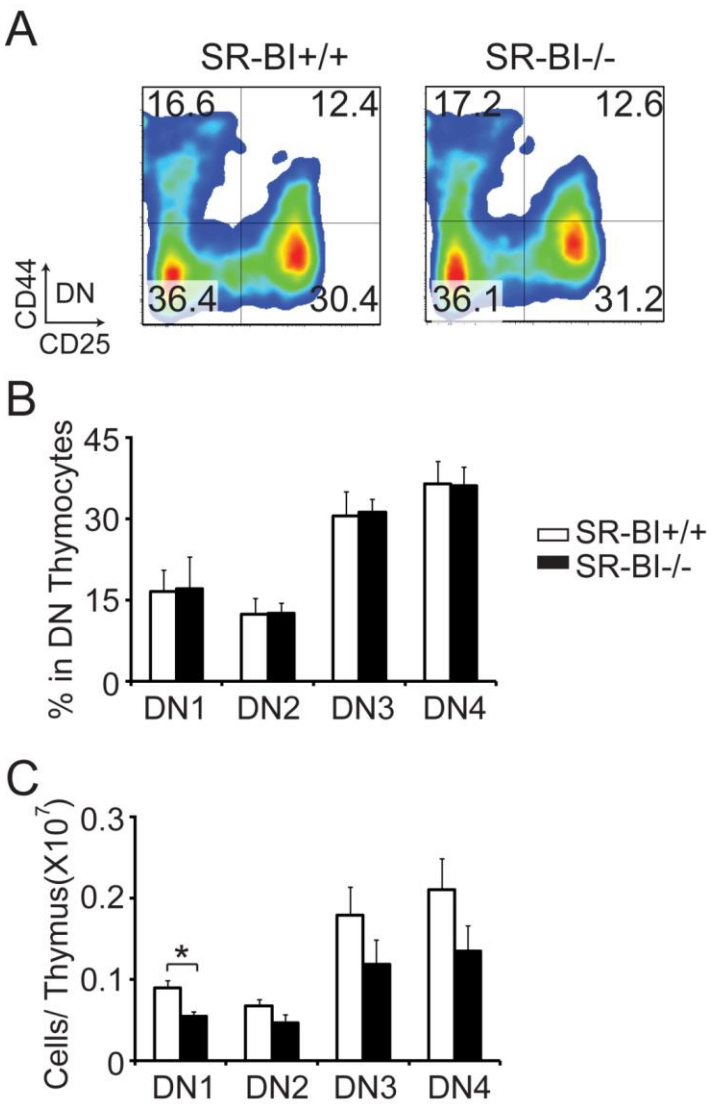

Figure 4.2 SR-BI deficiency does not affect the DN1-4 profile in mice.

Thymocytes from 5-week-old SR-BI$^{+/+}$ or SR-BI$^{-/-}$ mice were stained with a panel of fluorescence-labeled antibody. A)-B) The DN population was divided into four subtypes (DN1, CD25^{-}CD44^{high}; DN2, CD25^{+}CD44^{high}; DN3, CD25^{+}CD44^{low}, and DN4, CD25^{-}CD44^{low}) according to the expression of CD44 and CD25. C) The number of each population was calculated by multiplying its percentage in DN thymocytes by the total number of DN thymocytes. n=5-6 per group. *p<0.05.

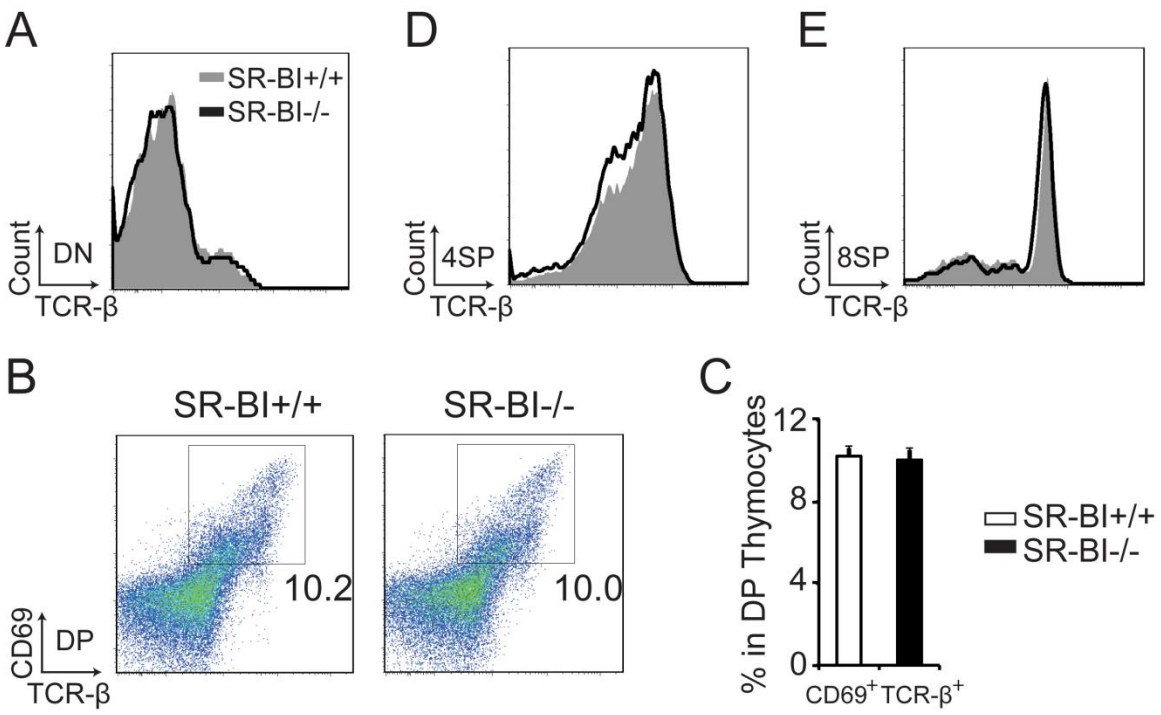

Figure 4.3 SR-BI deficiency does not impair selections during thymopoiesis.

Thymocytes from 5-week-old SR-BI$^{+/+}$ or SR-BI$^{-/-}$ mice were stained with a panel of fluorescence-labeled antibody. A) The TCR-β expression was evaluated in DN population. B)-C) The postselection population in DP cells was defined as CD69^{+} TCR-β^{+} cells. D)-E) The TCR-β expression was evaluated in 4SP and 8SP population. Representative gating figures are shown. n=3 per group.

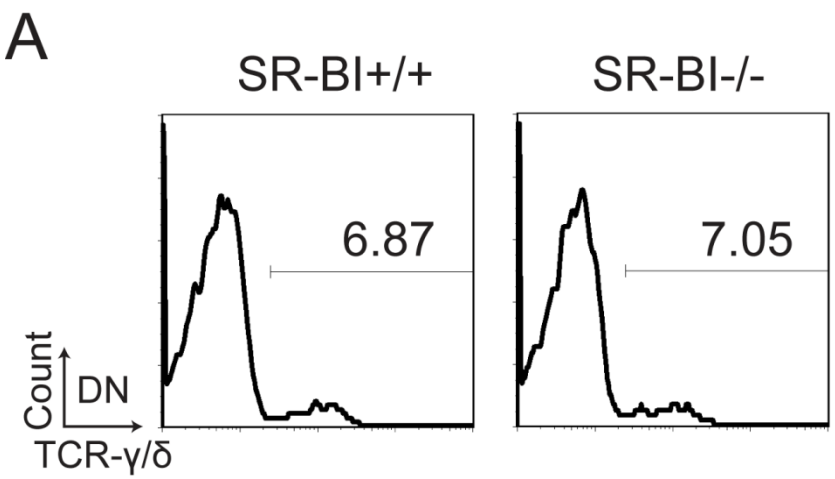

Figure 4.4 SR-BI deficiency does not affect γδ T cell development.

Thymocytes from 5-week-old SR-BI$^{+/+}$ or SR-BI$^{-/-}$ mice were stained with a panel of fluorescence-labeled antibody. The TCR-γ/δ expression was evaluated in DN population. Representative gating plots are shown. n=3 per group.

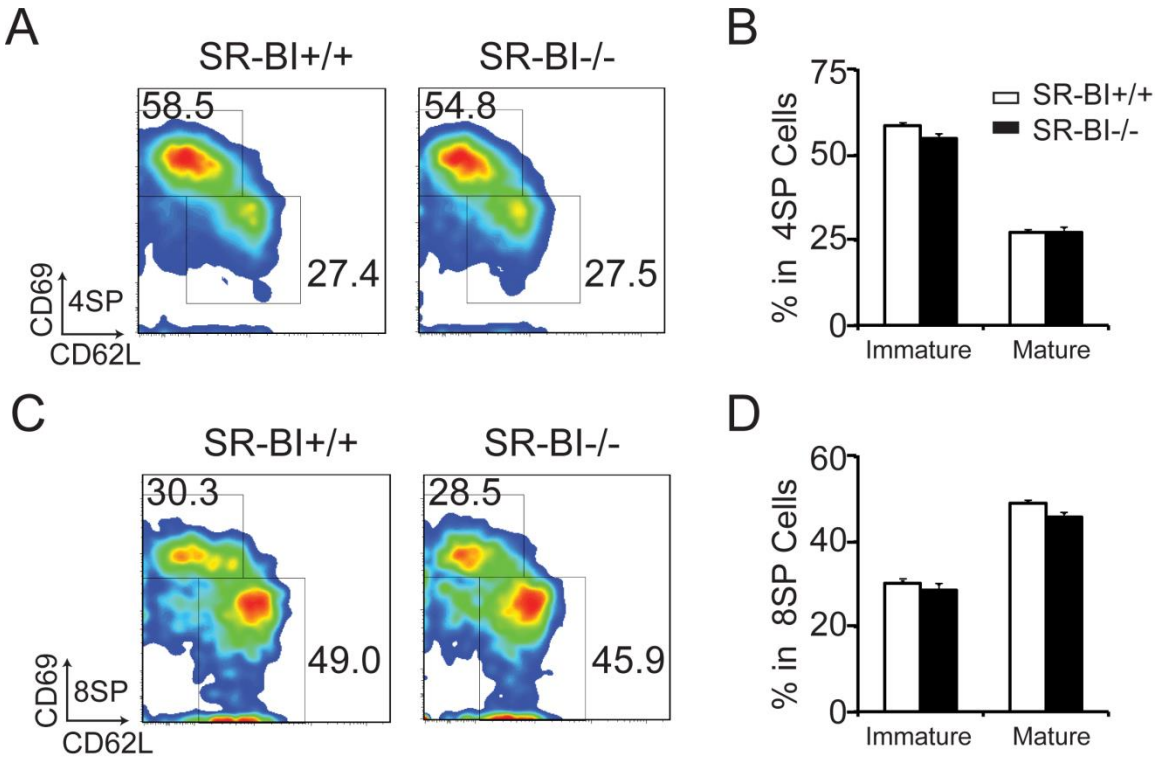

Figure 4.5 SR-BI deficiency does not affect γδ T cell development.

The maturation process of 4SP (A and B) or 8SP (C and D) thymocytes from 5-week-old mice was evaluated by CD69 and CD62L expression. The immature population was defined as $CD62L^{lo}CD69^{+}$ SP cells. The mature population was defined as $CD62L^{hi}CD69^{-}$ SP cells. n=5-6 per group.

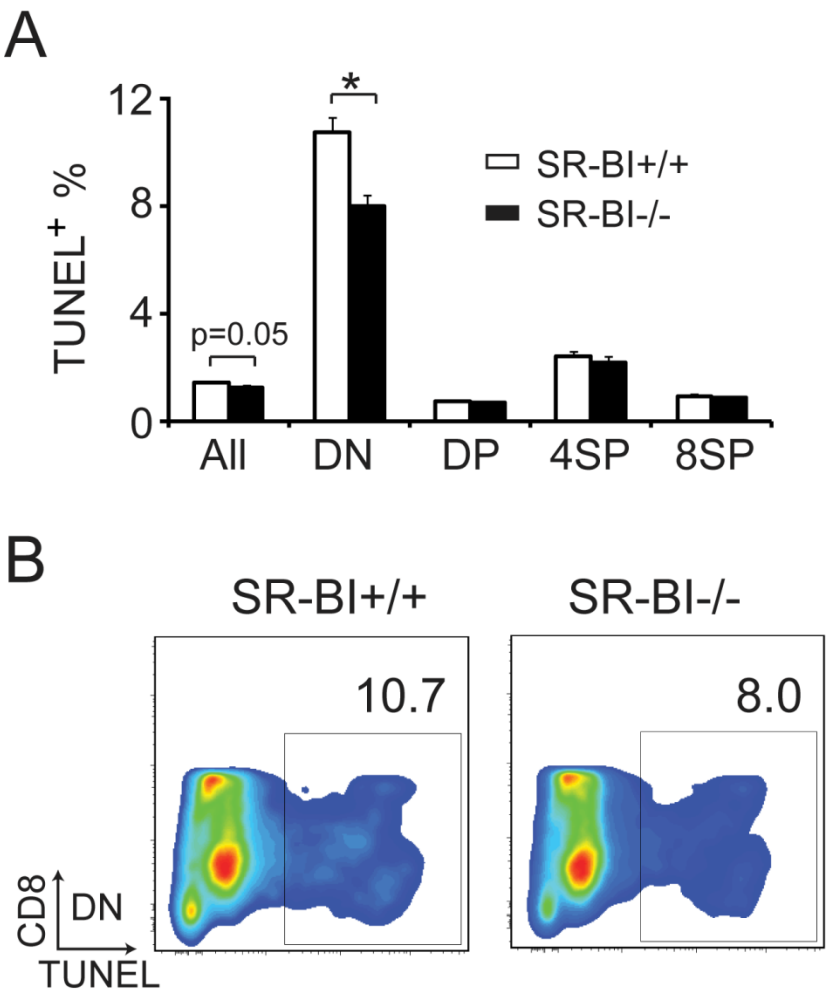

Figure 4.6 SR-BI deficiency causes reduced apoptosis in DN thymocytes. Thymocytes from 5-week-old SR-BI$^{+/+}$ or SR-BI$^{-/-}$ mice were first stained with a panel of fluorescence-labeled antibody. Cells were then fixed and permeabilized, before the DNA strand breaks were detected by TUNEL assay. A) The TUNEL^{+} percentage in all thymocytes and four thymocyte subtypes was statistically analyzed. B) Representative TUNEL^{+} gating plots in DN population are displayed. n=5 per group. *p<0.05.

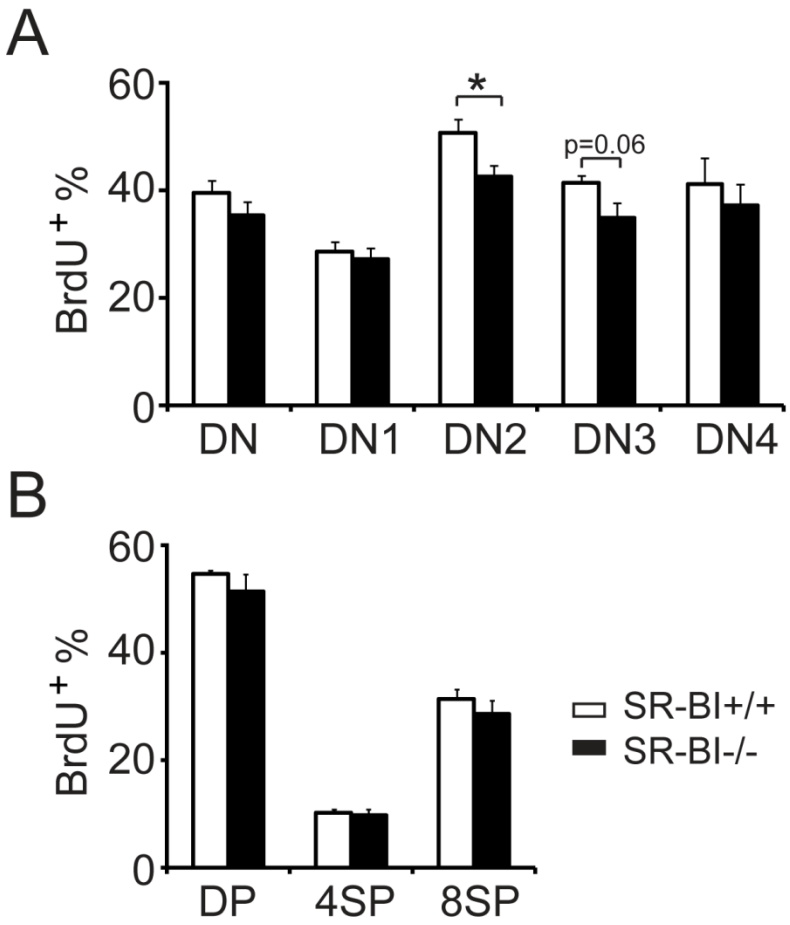

Figure 4.7 SR-BI deficiency causes reduced proliferation in DN2 thymocytes.

Thymocytes isolated from 5-week-old SR-BI$^{+/+}$ or SR-BI$^{-/-}$ mice were first stained with a panel of fluorescence-labeled antibody before the BrdU incorporation in thymocytes was detected with the specific antibody. A) BrdU^{+} percentages in DN thymocytes and four DN thymocyte subtypes were statistically analyzed. B) BrdU^{+} percentage in DP, 4SP and 8SP was statistically analyzed. n=5-7 per group. *p<0.05.

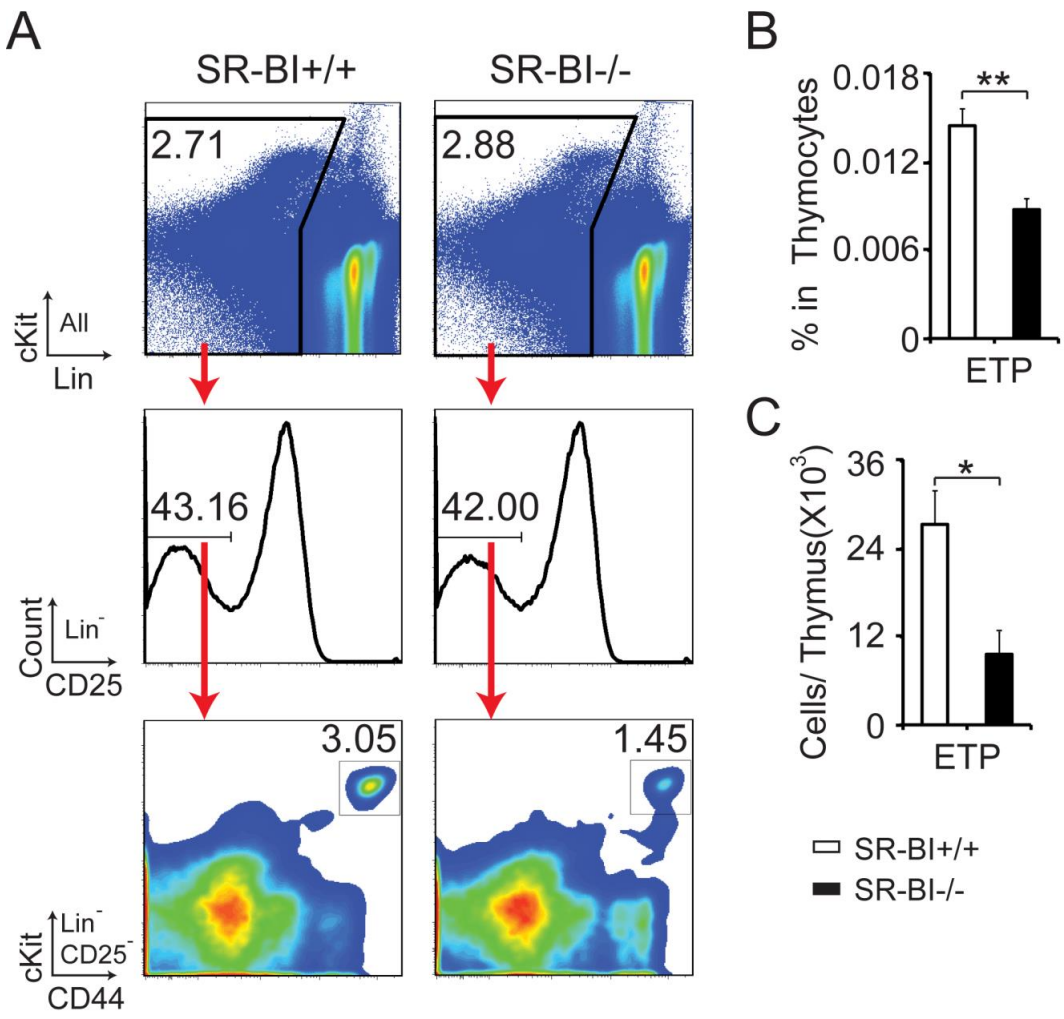

Figure 4.8 SR-BI deficiency decreases the portion of ETPs in thymocytes. Thymocytes isolated from 5-week-old SR-BI$^{+/+}$ or SR-BI$^{-/-}$ mice were stained with a panel of fluorescence-labeled antibodies. A) Gating strategy to distinguish ETPs. The mature thymocytes were first excluded by a panel of lineage markers (anti-CD3ε, CD8α, CD8β, B220, CD19, CD11b, CD11c, GR-1, NK1.1, Ter119, TCR-β and TCR-γ/δ) and then the ETP was defined as the CD25^{-}CD44^{+}cKit^{hi} population in Lin^{-} cells. B) Percentage of ETPs in all thymocytes was statistically analyzed. C) The number of ETPs was calculated by multiplying the percentage

of ETPs in all thymocytes by the number of total thymocytes. n=5-6 per group.*$p<0.05$, **$p<0.01$.

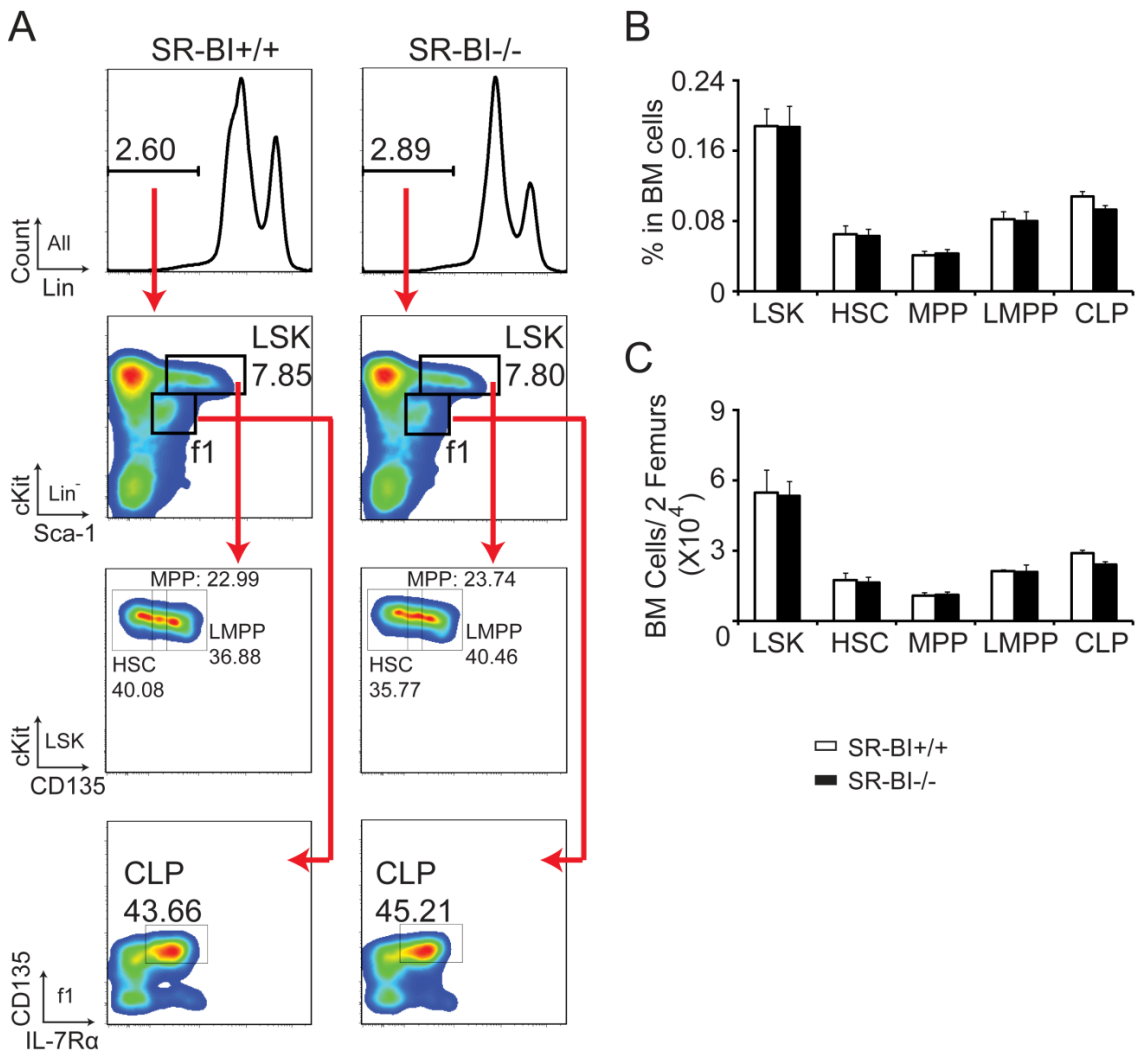

Figure 4.9 SR-BI deficiency does not cause defects in lymphoid progenitor development in bone marrow.

Bone marrow cells from 5-week-old SR-BI$^{+/+}$ or SR-BI$^{+/+}$ mice were stained with a panel of fluorescence-labeled antibodies. A) Gating strategy of bone marrow lymphoid progenitors. Lineage markers to exclude mature bone marrow cells include anti-CD2, CD3ε, CD4, CD8α, B220, CD19, CD11b, GR-1, NK1.1 and Ter119. The HSCs, MPPs and LMPPs were distinguished in LSK population (Lin$^-$ Sca-1$^+$cKit$^+$) based on the expression of CD135, and the CLPs were defined as

IL-7Rα^{+} population in Lin^{-}Sca-1^{int}cKit^{int} cells. B) The percentages of bone marrow progenitor populations were analyzed. C) The number of a given progenitor population was calculated by multiplying its percentage in all bone marrow cells by total bone marrow cell counts. n=5 per group.

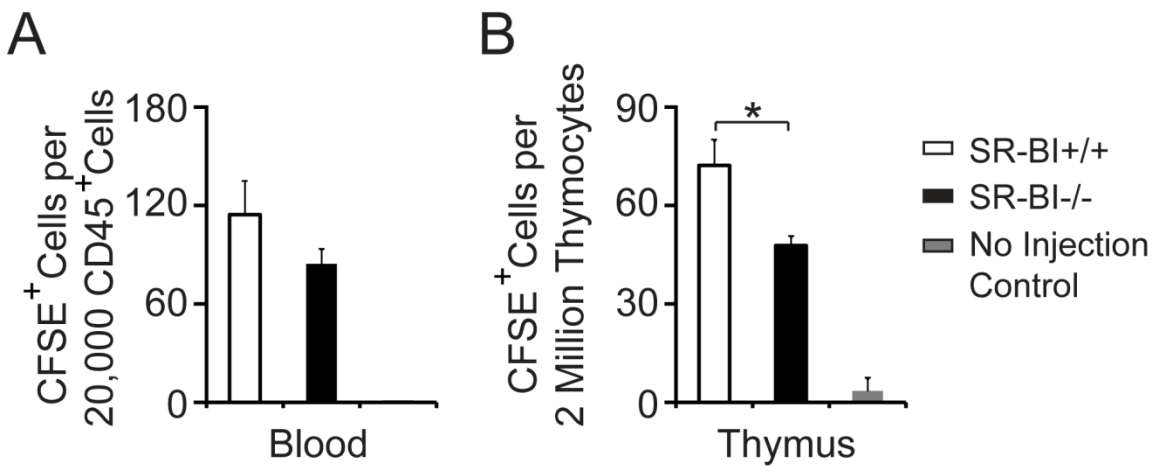

Figure 4.10 SR-BI deficiency causes reduced progenitor cell settlement on thymus.

Twenty million CFSE-labeled bone marrow cells from SR-BI$^{+/+}$ mice were injected into 5-week-old SR-BI$^{+/+}$ or SR-BI$^{-/-}$ mice. Two days later, the CFSE^{+} cells in blood and thymus were analyzed. SR-BI$^{+/+}$ mice without bone marrow cell injection were used as negative controls. A) The percentage of CFSE^{+} cells in blood cells was shown as the number of CFSE^{+} cells per 20,000 CD45^{+} blood cells. B) The percentage of CFSE^{+} cells in thymus was shown as the number of CFSE^{+} cells per 2 million thymocytes. n=7-8 for CFSE^{+} cell injected groups; n=2 for no injection group. *, $p<0.05$.

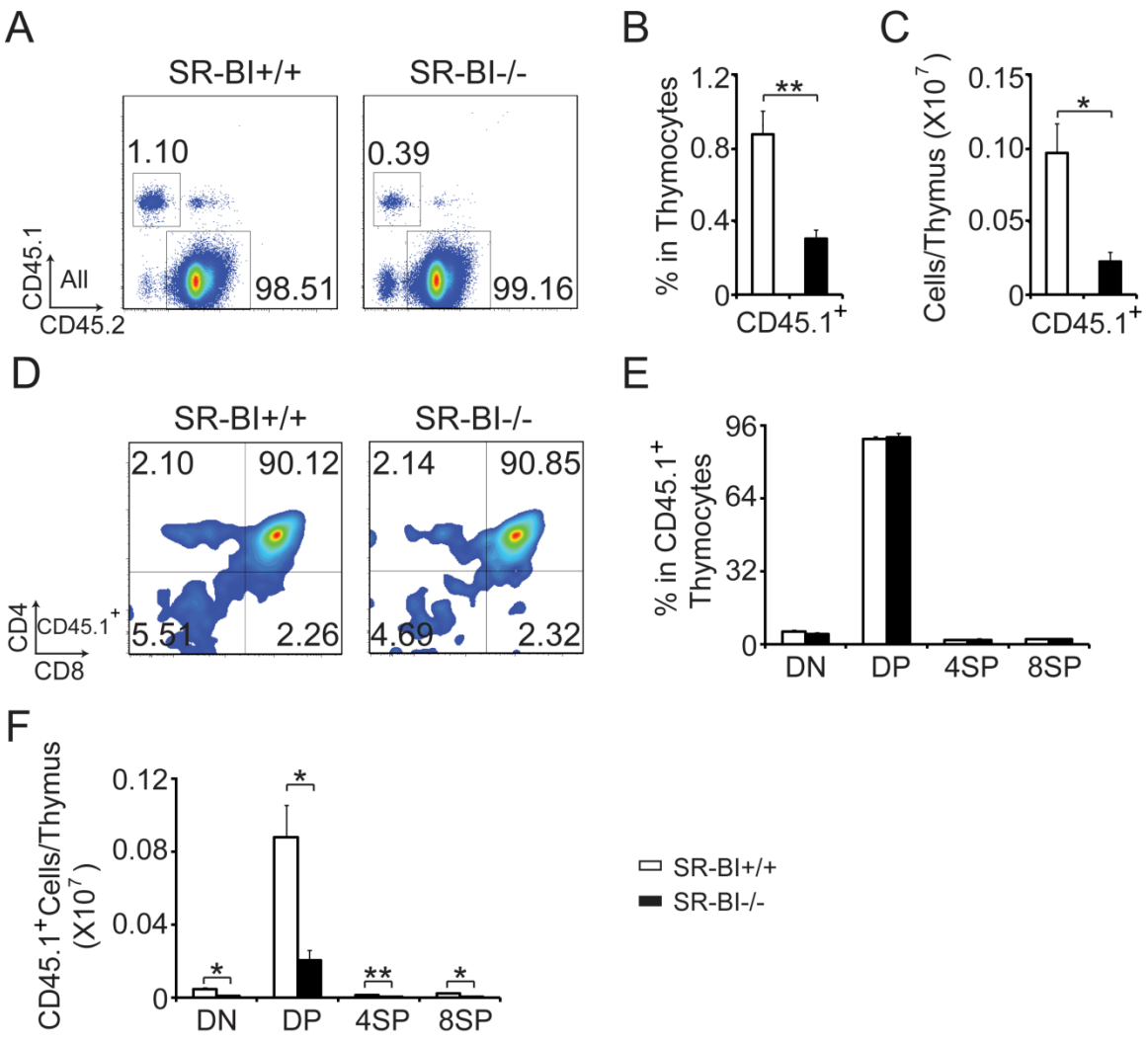

Figure 4.11 SR-BI deficiency reduces the contribution of circulating bone marrow progenitors to thymopoiesis.

Twenty million bone marrow cells from CD45.1 mice were injected into SR-BI$^{+/+}$ or SR-BI$^{-/-}$ mice in C57BL/6J background. Two weeks later, the contribution of CD45.1^{+} bone marrow cells to thymopoiesis was evaluated. A)-B) The percentage of CD45.1^{+} cells in thymi was analyzed. C) The number of CD45.1^{+} population was calculated by multiplying its percentage in thymocytes by total thymocyte numbers. D)-E) The CD4/CD8 profile was analyzed in CD45^{+} cells. E)

The number of a given population in $CD45^+$ cells was calculated by multiplying its percentage in $CD45.1^+$ cells by the number of $CD45.1^+$ cells. n=5-6 per group. *p<0.05; **p<0.01.

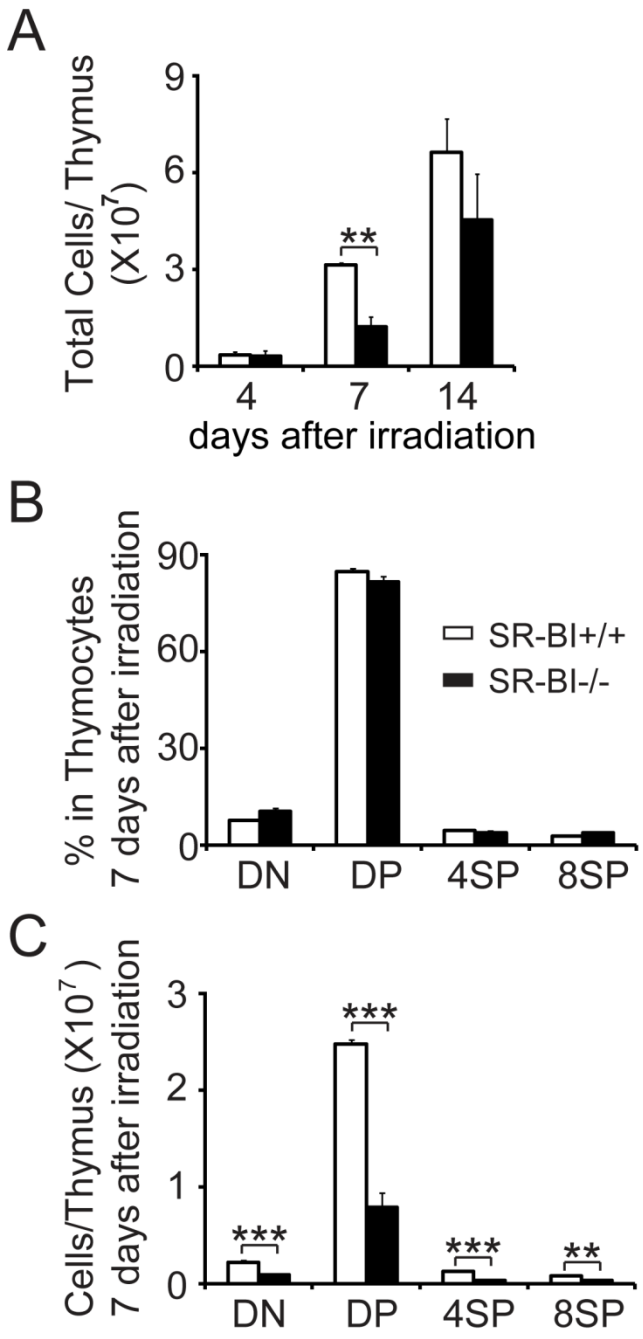

Figure 4.12 SR-BI deficiency impairs thymic recovery after sublethal irradiation.

SR-BI$^{+/+}$ and SR-BI$^{-/-}$ mice were irradiated with a single dose of 450 rads from a cesium source. Thymocytes were analyzed at indicated times after the irradiation. A) Thymocyte numbers of mice were analyzed at indicated times

after irradiation. n=3-5 per group. B) The thymocyte CD4/CD8 profiles were analyzed 7 days after irradiation. C) The number of a given population was calculated by multiplying its percentage in thymocytes by the number of total thymocytes. n=4-5 per group. **p<0.01, ***p<0.001.

Chapter 5 Adrenal SR-BI is required for maintaining normal thymopoiesis and thymic regeneration

5.1 Introduction

SR-BI is a multifunctional receptor expressed in a variety of tissues. SR-BI expressed in different tissues can exert various functions in a number of physiological or pathological processes [135, 159]. For instance, hepatic SR-BI mediates selective uptake from HDL and acts as the key modulator of HDL metabolism [202, 209], adrenal SR-BI controls steroid production under stress [160, 206], and macrophage SR-BI facilitates cholesterol efflux [283] and suppresses inflammatory responses [192]. In chapter 4 we revealed which step of thymopoiesis is affected by SR-BI deficiency. We found that in the absence of SR-BI, mice display impaired progenitor thymic homing, which is responsible for the decreased thymopoiesis. However, how SR-BI deficiency causes these defects in T cell development has not been clear. Therefore, in this chapter, we utilized different mouse models to investigate how the impairments of thymopoiesis are induced by the deficiency of SR-BI.

Given that SR-BI is expressed in T-lineage cells as well as other hematopoietic cells [134], the first question we asked was that how the lack of hematopoietic or non-hematopoietic SR-BI contributes to the thymus defects in SR-BI-null mice. Actually, the progenitor homing assays (Figure 4.10 and Figure 4.11) suggested that the non-hematopoietic SR-BI deficiency is at least partly responsible for the impaired thymopoiesis, as we injected the same labeled cells into SR-BI$^{+/+}$ or SR-BI$^{-/-}$ environment and detected fewer cells homing to the

thymi of SR-BI$^{-/-}$ mice. To determine whether hematopoietic SR-BI deficiency contributes to the impaired thymopoiesis and confirm the contribution of non-hematopoietic SR-BI deficiency, we utilized a series of bone marrow transplantation models. Our data indicate that lacking SR-BI in hematopoietic cells does not lead to any defects in thymopoiesis whereas the non-hematopoietic SR-BI deficiency is responsible for the impaired thymopoiesis in SR-BI-null mice.

The observation that the impaired thymopoiesis of SR-BI-null mice is due to non-hematopoietic SR-BI deficiency raised the possibility that the thymopoiesis defects are induced by the SR-BI deficiency-induced hypercholesterolemia. Indeed, several detects due to SR-BI deficiency have been linked to the hypercholesterolemia [135], such as abnormal erythropoiesis [212, 213], female infertility [210], and impaired lymphocyte homeostasis [134]. Therefore, we hypothesized that non-SR-BI deficiency impairs thymopoiesis by causing hypercholesterolemia. To test this hypothesis, we manipulated plasma cholesterol levels in mice. We found that neither exacerbating nor normalizing hypercholesterolemia affects thymic cellularity of SR-BI-null mice, indicating the impaired thymopoiesis is not due to SR-BI deficiency-induced hypercholesterolemia.

One study reported that cholesterol accumulation in thymic macrophages activates NLRP3 inflammasome, which contributes to the age-related thymic involution in mice [65]. This report led us to hypothesize that SR-BI deficiency impairs thymopoiesis by causing cholesterol accumulation in thymic

macrophages and subsequent NLRP3 activation in mice. However, we did not observe cholesterol accumulation in thymic macrophages of SR-BI-null mice, nor did we detect NLRP3 inflammasome activation, demonstrating that SR-BI deficiency does not cause thymus defects via inducing cholesterol accumulation in thymic macrophages.

Our findings excluded the involvement of the altered cholesterol metabolism in the impaired thymopoiesis of SR-BI-null mice, which led us to consider alternative explanations of how SR-BI deficiency leads to the defects in thymopoiesis. In addition to hypercholesterolemia, another well-studied defect in SR-BI-null mice is the impaired adrenal function. SR-BI-mediated cholesterol uptake is an essential pathway to supply cholesterol to adrenal glands for steroid synthesis [161]. Lack of SR-BI in adrenal causes a deficiency of inducible steroids [206-208], which is responsible for the elevated septic death [206] and the lack of thymocyte apoptosis during sepsis[247]. We utilized adrenal transplantation models to evaluate if the defects in thymopoiesis were a result of the adrenal SR-BI deficiency. Surprisingly, we found that mice with a loss of adrenal SR-BI in mice display defects in T cell development similar with SR-BI-null mice, demonstrating that loss of SR-BI in adrenal gland is the responsible for the impaired thymopoiesis.

In this chapter, we provide data indicating that the adrenal SR-BI is required for maintaining normal T cell development in mice, whereas neither SR-BI deficiency-induced hypercholesterolemia nor a lack of hematopoietic SR-BI is responsible for the impaired thymopoiesis in SR-BI-null mice.

5.2 Results

5.2.1 Hematopoietic SR-BI deficiency does not influence thymopoiesis

To investigate whether hematopoietic SR-BI deficiency contributes to the impaired thymopoiesis, we compared the ability of SR-BI$^{-/-}$ bone marrow cells in competing with CD45.1^{+} bone marrow cells in thymopoiesis with that of SR-BI$^{+/+}$ bone marrow cells in lethally irradiated Rag-1$^{-/-}$ recipients (Figure 5.1A). Notably, the SR-BI$^{-/-}$ mice and their SR-BI$^{+/+}$ littermates used in this assay were all backcrossed more than 10 times to the C57BL/6J background. Rag-1$^{-/-}$ mice were chosen as recipients because they lack T-lineage cells beyond DN3 stage [284] and therefore we can exclude the influence of recipient-derived T-lineage cells on the process of thymocyte repopulation. Six weeks after bone marrow transplantation, Rag-1$^{-/-}$ mice transplanted with SR-BI$^{-/-}$ and SR-BI$^{+/+}$ bone marrow cell mixes show similar CD45.2^{+} percentage in total thymocytes (Figure 5.1B and 5.1C). Meanwhile, the CD45.2^{+} percentage in DN, DP, 4SP and 8SP subsets is all comparable in two groups, indicating that SR-BI$^{-/-}$ bone marrow cells have intact ability to support thymopoiesis. These results reveal that the impaired thymopoiesis in SR-BI$^{-/-}$ mice is not attributed to the hematopoietic SR-BI deficiency.

5.2.2 Non-hematopoietic SR-BI deficiency is responsible for impaired thymopoiesis

We next investigated the contribution of non-hematopoietic SR-BI deficiency to the impaired thymopoiesis. For this purpose, we repopulated lethally irradiated SR-BI$^{-/-}$Rag-1$^{-/-}$ mice and SR-BI$^{+/+}$Rag-1$^{-/-}$ controls with CD45.1^{+}

bone marrow cells (Figure 5.2A). Unexpectedly, before detecting thymopoiesis endpoints six weeks after bone marrow transplantation, we observed a significantly higher mortality in SR-BI$^{-/-}$Rag-1$^{-/-}$ after bone marrow transplantation (Figure 5.2B). Though all the SR-BI$^{+/+}$Rag-1$^{-/-}$ recipients survived after the transplantation, all the male and one in four female SR-BI$^{-/-}$Rag-1$^{-/-}$ recipients died (Figure 5.2C), indicating non-hematopoietic SR-BI deficiency indeed causes a survival disadvantage in bone marrow transplantation.

We then evaluated the development of CD45.1^{+} cells in the thymi of survived recipients 6 weeks after BMT. In both groups of recipients, over 85% thymocytes are CD45.1^{+} cells (Figure 5.3A), indicating the successful thymic repopulation with donor cells. However, SR-BI$^{-/-}$Rag-1$^{-/-}$ recipients display 30% lower CD45.1^{+} thymocytes numbers than SR-BI$^{+/+}$Rag-1$^{-/-}$ recipients (Figure 5.3B). Analysis of CD4/CD8 profile in CD45.1^{+} cells reveals that SR-BI$^{-/-}$ Rag-1$^{-/-}$ recipients do not show significant differences in the percentage of CD45.1^{+} thymocyte subtypes (Figure 5.3C), while only the number of CD45.1^{+} DP cells are significantly reduced in SR-BI$^{-/-}$Rag-1$^{-/-}$ recipients (Figure 5.3D). Interestingly, the donor-derived ETPs are also significantly reduced both in percentage and numbers in SR-BI$^{-/-}$ Rag-1$^{-/-}$ recipients (Figure 5.3E and F). This group of data shows that non-hematopoietic SR-BI deficiency impairs the ability of bone marrow cells to repopulate thymi and thus is responsible for the impaired thymopoiesis in SR-BI$^{-/-}$ mice.

5.2.3 Non-hematopoietic SR-BI deficiency causes decreased T cell pool in the periphery

We also evaluated whether non-hematopoietic SR-BI deficiency affects peripheral T cell repopulation after bone marrow transplantation. Consistent with the observations in the thymus, we found that in lymph nodes of SR-BI$^{-/-}$Rag-1$^{-/-}$ recipients, the numbers of donor-derived CD4^{+} and CD8^{+} cells are reduced by 34% and 44%, respectively, compared with those of SR-BI$^{+/+}$Rag-1$^{-/-}$ recipients (Figure 5.4A). Moreover, SR-BI$^{-/-}$ Rag-1$^{-/-}$ recipients show significantly reduced donor-derived CD4^{+} cells in spleen (Figure 5.4B), and markedly decreased donor-derived CD4^{+} and CD8^{+} cells in blood (Figure 5.4C). These findings indicate that non-hematopoietic SR-BI deficiency impairs not only the regeneration of the thymus but also the repopulation of peripheral T cells after bone marrow transplantation.

5.2.4 Diet-induced hypercholesterolemia does not influence thymic cellularity or ETPs

SR-BI deficiency in mice causes hypercholesterolemia, which further leads to other several defects in mice (discussed in chapter 1.2), we asked if hypercholesterolemia is also responsible for defective thymopoiesis in SR-BI$^{-/-}$ mice. At first, we detected the plasma cholesterol in 5-week-old mice and confirmed that at 5 weeks of age, SR-BI deficiency results in a more than two-fold elevation in plasma cholesterol concentrations (Figure 5.5A). To determine if general hypercholesterolemia has an effect on thymic cellularity in early ages, we fed C57BL/6N mice with high fat diet starting from the age of 3 weeks and

analyzed thymopoiesis two weeks later. As expected, high fat diet-fed C57BL/6N mice display a 4-fold increase in cholesterol concentrations (Figure 5.5B), which notably is even higher than in SR-BI$^{-/-}$ mice. However, compared with mice on control diet, high fat diet-fed mice do not show any difference in thymic cellularity (Figure 5.5C). Meanwhile, the percentages (Figure 5.5D) and numbers of ETPs (Figure 5.5E) are also comparable in high fat diet-fed mice and controls. These data demonstrate that diet-induced hypercholesterolemia does not result in thymic hypocellularity or reduction in ETPs.

5.2.5 SR-BI deficiency-induced hypercholesterolemia is not responsible for impaired thymopoiesis

Because SR-BI deficiency-induced hypercholesterolemia is different from diet-induced hypercholesterolemia as it is characterized by increases in HDL cholesterol [114, 156], we next determined whether or not the hypercholesterolemia due to SR-BI deficiency causes the thymic abnormalities seen in SR-BI$^{-/-}$ mice. For this purpose, we fed SR-BI$^{-/-}$ mice with high fat diet from the age of 3 weeks until analyzing their thymi at the age of 5 weeks. High fat diet exaggerates hypercholesterolemia in SR-BI$^{-/-}$ mice by 3-fold (Figure 5.6A) and slightly decreases their thymocyte numbers (Figure 5.6B). However, compared with control-diet SR-BI$^{-/-}$ mice, high-fat-diet SR-BI$^{-/-}$ mice do not show reductions in either the percentage or the number of ETPs (Figure 5.6C and 5.6D), suggesting the exacerbated thymic cellularity is not due to further decreased ETPs. Given that the high fat diet contains cholic acid that accelerates cholesterol absorption [285, 286] but can cause inflammation [287], we reasoned

that the further decrease in thymocyte number of high fat diet-fed SR-BI$^{-/-}$ mice may result from inflammation-induced thymocyte depletion. To exclude the side effect of the diet and clarify the effect of elevated cholesterol concentration in SR-BI$^{-/-}$ mice on thymus, we compared thymocyte numbers in SR-BI$^{-/-}$ mice with age-matched SR-BI$^{-/-}$LDLR$^{-/-}$ mice, whose cholesterol concentrations are elevated endogenously compared with SR-BI$^{-/-}$ mice [182]. We found that the thymic cellularity is not lower in 5-week-old or 20-week-old SR-BI$^{-/-}$LDLR$^{-/-}$ mice than in age-matched SR-BI$^{-/-}$ mice (Figure 5.6E), demonstrating that the exaggerated hypercholesterolemia does not exacerbate thymic hypocellularity in the SR-BI-deficient animal.

In addition to increasing hypercholesterolemia in SR-BI$^{-/-}$ mice, we also corrected hypercholesterolemia in SR-BI$^{-/-}$ mice by probucol administration and evaluated its effect on thymus. We started to administer 0.2% probucol to SR-BI$^{-/-}$ mice at 3 weeks of age. Two weeks later, the plasma cholesterol concentration of the deficient mice is normalized to levels similar to those in SR-BI$^{+/+}$ mice (Figure 5.7A). However, the thymocyte number of SR-BI$^{-/-}$ mice with probucol administration is not elevated compared to mice without this treatment (Figure 5.7B), indicating that the thymic hypocellularity is not caused by elevated cholesterol levels. To exclude the possibility that the relieved hypercholesterolemia for two weeks is insufficient to influence the thymic cellularity in SR-BI$^{-/-}$ mice, we maintained the deficient mice on the probucol diet for as long as 15 weeks. Similarly, we observed comparable thymic cellularity in SR-BI$^{-/-}$ mice with or without probucol administration (Figure 5.7C). Altogether,

these data indicate that SR-BI deficiency-induced hypercholesterolemia is not the leading cause for impaired thymopoiesis.

5.2.6 SR-BI deficiency does not cause thymic hypocellularity through activating NLRP3 inflammasome

Recently it was reported that age-dependent accumulation of danger signals such as free cholesterol in thymic macrophages induces activation of the NLRP3 inflammasome which contributes to age-related thymic involution [65]. Given the essential role of SR-BI in cholesterol transport, we hypothesized that SR-BI deficiency impairs thymopoiesis by causing increased cholesterol accumulation in thymic macrophages and subsequent activation of the NLRP3 inflammasome at younger ages. To test this hypothesis, we first evaluated cholesterol levels in thymic macrophages ($F4/80^+CD11b^+$ thymocytes) of 5-week-old mice by filipin staining. We found that 5-week-old SR-$BI^{-/-}$ mice do not exhibit elevated cholesterol levels in thymic macrophages in comparison with SR-$BI^{+/+}$ mice (Figure 5.8A and 5.8B), indicating SR-BI deficiency does not cause cholesterol accumulation in thymic macrophages of young mice. To fully rule out the involvement of NLRP3 inflammasome in SR-BI deficiency-impaired thymopoiesis, we evaluated NLPR3 inflammasome activation in the thymi of mice by detecting the cleavage of caspase 1, a hallmark of NLPR3 inflammasome activation [288, 289]. Similarly, we did not detect p20, the cleaved subunits of caspase 1, in either SR-$BI^{+/+}$ or SR-$BI^{-/-}$ mice at the age of 5 weeks or 6 months (Figure 5.8C). These observations indicate that SR-BI deficiency does not impair thymopoiesis via NLRP3 inflammasome activation in mice.

5.2.7 Adrenal SR-BI deficiency reduces thymus size

To determine if adrenal SR-BI plays a role in modulating thymopoiesis, we transplanted adrenal gland from SR-BI$^{+/+}$ or SR-BI$^{-/-}$ mice to adrenalectomized SR-BI$^{+/+}$ mice. Six weeks after surgery, the recipient mice receiving SR-BI$^{-/-}$ adrenal gland (ADR-T SR-BI$^{-/-}$ mice) display significantly reduced thymus weight than those receiving SR-BI$^{+/+}$ one (ADR-T SR-BI$^{+/+}$ mice), indicating that the loss of SR-BI in adrenal gland is responsible for the reduction in thymus weight (Figure 5.9A). Moreover, the thymic cellularity of ADR-T SR-BI$^{-/-}$ mice is ~40% lower than that of ADR-T SR-BI$^{+/+}$ mice, indicating that the absence of adrenal SR-BI leads to thymic hypocellularity (Figure 5.9B). These results reveal that adrenal SR-BI is essential in maintaining normal thymus size.

5.2.8 Adrenal SR-BI deficiency does not affect CD4/CD8 profile or DN1-4 profile in the thymus

We next investigated thymocyte subsets of the adrenal transplanted mice. Similar to SR-BI$^{-/-}$ mice, ADR-T SR-BI$^{-/-}$ mice displayed identical CD4/CD8 profile (Figure 5.10A) and DN1-4 profile (Figure 5.10C) with the ADR-T SR-BI$^{+/+}$ controls. The numbers of DN, DP, 4SP, 8SP (Figure 5.10B) and the DN subtypes (Figure 5.10D) in ADR-T SR-BI$^{-/-}$ were all reduced corresponding with the total thymocyte counts. These observations indicate that the loss of SR-BI in adrenal does not affect thymic CD4/CD8 profile or DN1-4 profile.

5.2.9 Adrenal SR-BI deficiency reduces the percentage of ETPs

We also evaluated if adrenal SR-BI deficiency leads to a reduction in the percentage of ETPs. Compared with ADR-T SR-BI$^{+/+}$ controls, ADR-T SR-BI$^{-/-}$

mice exhibit a 30% decrease in the percentage of ETPs (Figure 5.11A) and a 65% decrease in their numbers (Figure 5.11B), which again mimics the phenotype of SR-BI$^{-/-}$ mice. These data indicate that the adrenal SR-BI deficiency is responsible for the reduction in the percentage of ETPs in SR-BI-null mice.

5.2.10 Adrenal SR-BI deficiency causes impaired thymic recovery after sublethal irradiation

Finally, we sublethally irradiated the adrenal transplanted mice in order to assess if adrenal SR-BI deficiency results in delayed thymic regeneration. Seven days after irradiation, ADR-T SR-BI$^{-/-}$ mice exhibit smaller thymus weight (Figure 5.12A) and 48% lower thymic cellularity (Figure 5.12B) than ADR-T SR-BI$^{+/+}$ mice, indicating the thymic recovery is delayed by adrenal SR-BI deficiency. In line with the observations in SR-BI$^{-/-}$ mice, the percentages of DN, DP, 4SP and 8SP thymocytes in ADR-T SR-BI$^{-/-}$ mice are not significantly different in ADR-T SR-BI$^{+/+}$ mice (Figure 5.12C). The numbers of all these populations in ADR-T SR-BI$^{-/-}$ mice (Figure 5.12D) are all reduced compared with ADR-T SR-BI$^{+/+}$ mice after the irradiation. These results reveal that adrenal SR-BI is required for normal thymic regeneration.

5.3 Summary

In this chapter, we investigated how the SR-BI deficiency causes defects in T cell development. First, using bone marrow transplantation models, we show that hematopoietic SR-BI deficiency does not cause any defect in thymopoiesis as SR-BI$^{-/-}$ bone marrow cells display a comparable ability to give rise to thymocytes with SR-BI$^{+/+}$ controls (Figure 5.1); and non-hematopoietic SR-BI deficiency results in impaired thymopoiesis as in SR-BI$^{-/-}$ recipients, bone marrow cells display reduced ability to support thymopoiesis compared with in SR-BI$^{+/+}$ recipients (Figure 5.3 and 5.4). Next, using cholesterol-manipulating models, we show that non-hematopoietic SR-BI deficiency does not impair thymopoiesis through inducing hypercholesterolemia. In SR-BI$^{+/+}$ mice, diet-induced thymopoiesis fails to induce thymus defects (Figure 5.5); and in SR-BI$^{-/-}$ mice, neither exaggerating nor normalizing hypercholesterolemia alters thymocyte numbers (Figure 5.6 and 5.7). By detecting cholesterol in thymic macrophages and evaluating NLRP3 inflammasome activation in the thymus, we excluded the possibility that non-hematopoietic SR-BI deficiency causes thymus defects by inducing cholesterol accumulation in thymic macrophages in young mice (Figure 5.8). Finally, using adrenal transplantation models, we show that SR-BI deficiency in adrenal gland is responsible for the thymus defects in SR-BI-null mice, since mice with adrenal-specific SR-BI deficiency display reduced thymus size (Figure 5.9), decreased ETP percentage (Figure 5.11) and delayed thymic regeneration (Figure 5.12). Based on these findings, we conclude that adrenal SR-BI is critical in thymopoiesis and thymic recovery in mice.

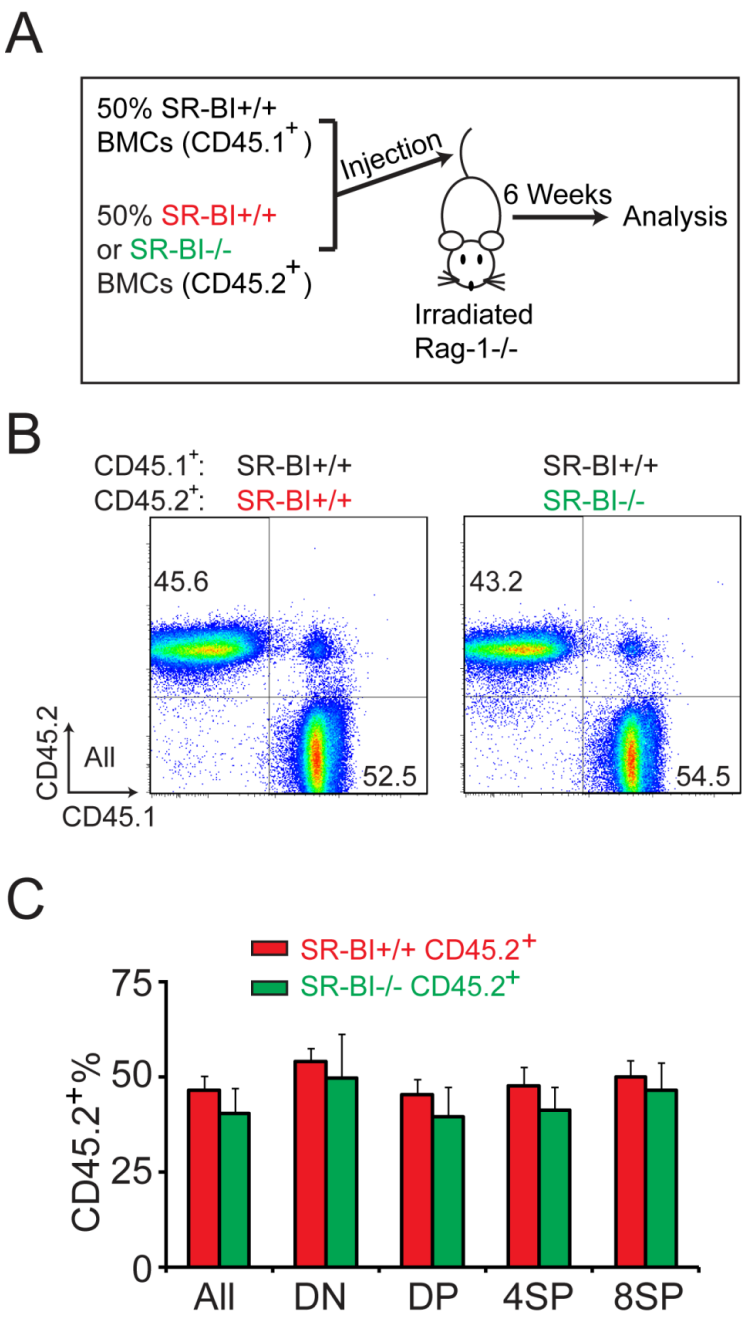

Figure 5.1 Hematopoietic SR-BI deficiency does not cause any defect in thymopoiesis.

A) Design for the bone marrow cell competition experiments. $CD45.1^+$ bone marrow cells were mixed with either $SR\text{-}BI^{+/+}$ bone marrow cells or $SR\text{-}BI^{-/-}$ bone marrow cells (both $CD45.2^+$) with a ratio of 1:1. Five million mixed bone marrow

cells were then injected into lethally irradiated Rag-1$^{-/-}$ mice. Six weeks later, the development of CD45.1^{+} and CD45.2^{+} (either SR-BI$^{+/+}$ or SR-BI$^{-/-}$) cells in the thymi of recipients were evaluated. All the SR-BI$^{+/+}$ and SR-BI$^{-/-}$ mice used as donors in this experiments were in C57BL/6J background. B) Representative CD45.1^{+} and CD45.2^{+} gating plots in total thymocytes are displayed. C) The CD45.2^{+} percentage in all thymocytes and four thymocyte subtypes was statistically analyzed. n=5-6 per group.

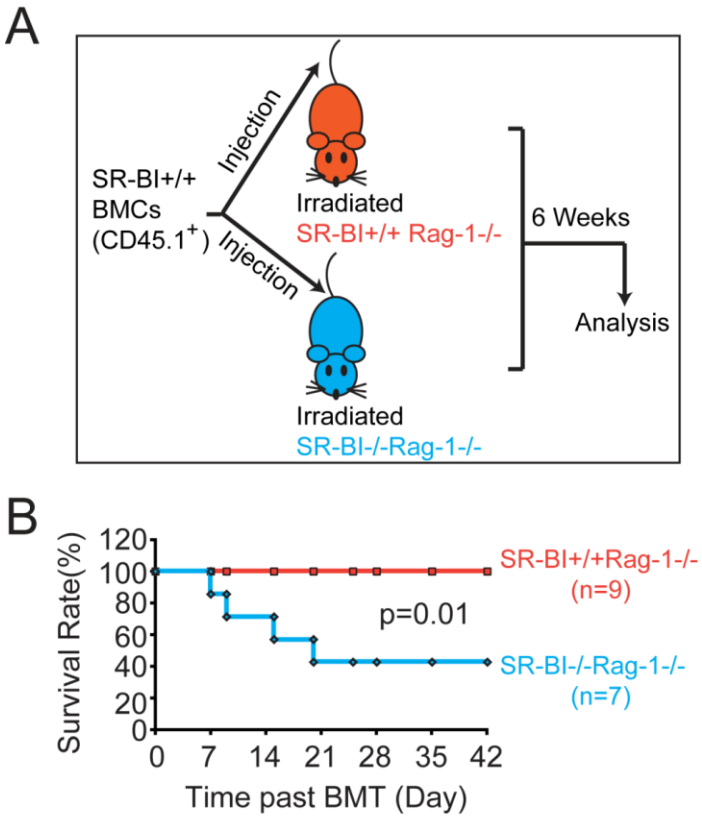

C

Survival Rate of Different Recicients by Gender

Male		Female	
SR-BI+/+ Rag-1-/-	SR-BI-/- Rag-1-/-	SR-BI+/+ Rag-1-/-	SR-BI-/- Rag-1-/-
5/5	0/3	4/4	3/4

Figure 5.2 Non-hematopoietic SR-BI deficiency increases the death rate in bone marrow transplantation.

A) Design for the bone marrow transplantation experiment. Five million CD45.1^{+} bone marrow cells were injected into lethally irradiated SR-BI$^{+/+}$Rag-1$^{-/-}$ or SR-BI$^{-/-}$Rag-1$^{-/-}$ mice. B) Survival curve of SR-BI$^{+/+}$Rag-1$^{-/-}$ or SR-BI$^{-/-}$Rag-1$^{-/-}$ mice after bone marrow transplantation is shown. C) The survival rate of SR-BI$^{+/+}$Rag-1$^{-/-}$ or SR-BI$^{-/-}$Rag-1$^{-/-}$ mice by gender after bone marrow transplantation is displayed.

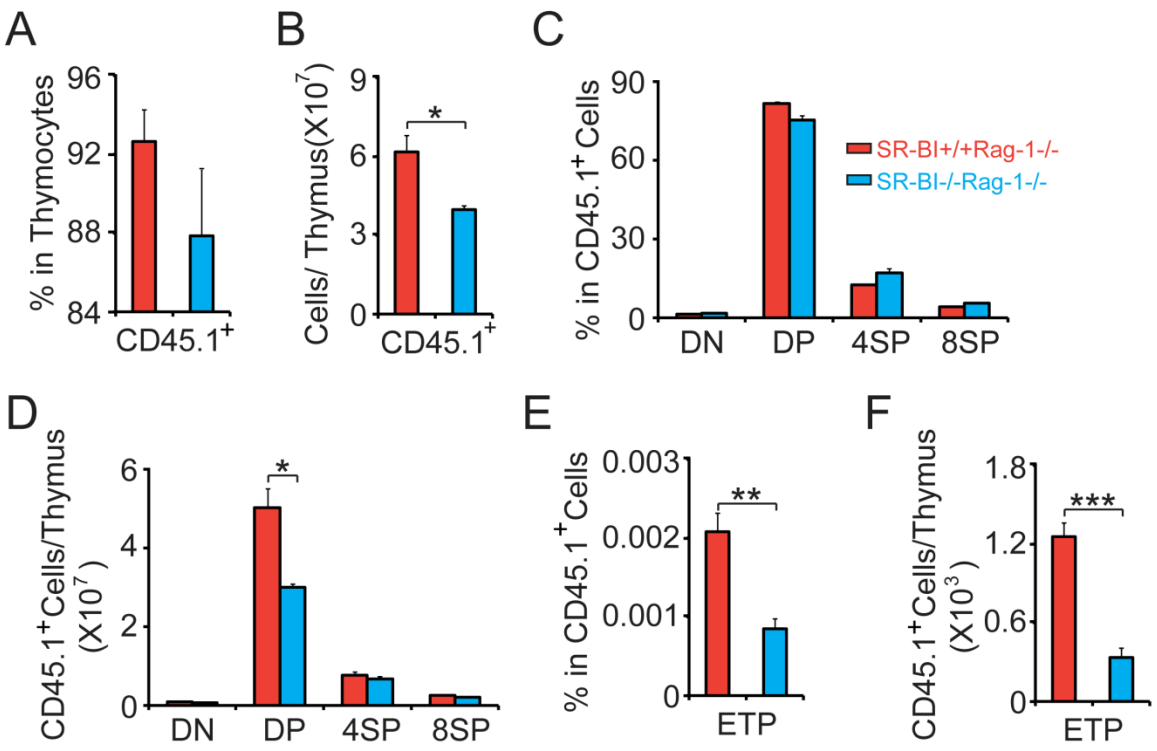

Figure 5.3 Non-hematopoietic SR-BI deficiency is responsible for impaired thymopoiesis.

Five million CD45.1$^+$ bone marrow cells were injected into lethally irradiated SR-BI$^{+/+}$Rag-1$^{-/-}$ or SR-BI$^{-/-}$Rag-1$^{-/-}$ mice. Six weeks later, the development of CD45.1$^+$ cells in the thymi of recipients were evaluated. A) The percentage of CD45.1$^+$ cells in all thymocytes was analyzed. B) The number of CD45.1$^+$ cells was calculated by multiplying the percentage of CD45.1$^+$ cells in all thymocytes by the number of total thymocytes. C) The CD4/CD8 profile was analyzed in CD45.1$^+$ cells. D) The number of a given population in CD45$^+$ cells was calculated by multiplying its percentage in CD45.1$^+$ cells by the number of CD45.1$^+$ cells. E) The ETP percentage was analyzed in CD45$^+$ cells. F) The number of ETPs in CD45$^+$ cells was calculated by multiplying its percentage in

CD45.1$^+$ cells by the number of CD45.1$^+$ cells. n=3-9 per group. *, $p<0.05$; **, $p<0.01$; ***, $p<0.001$.

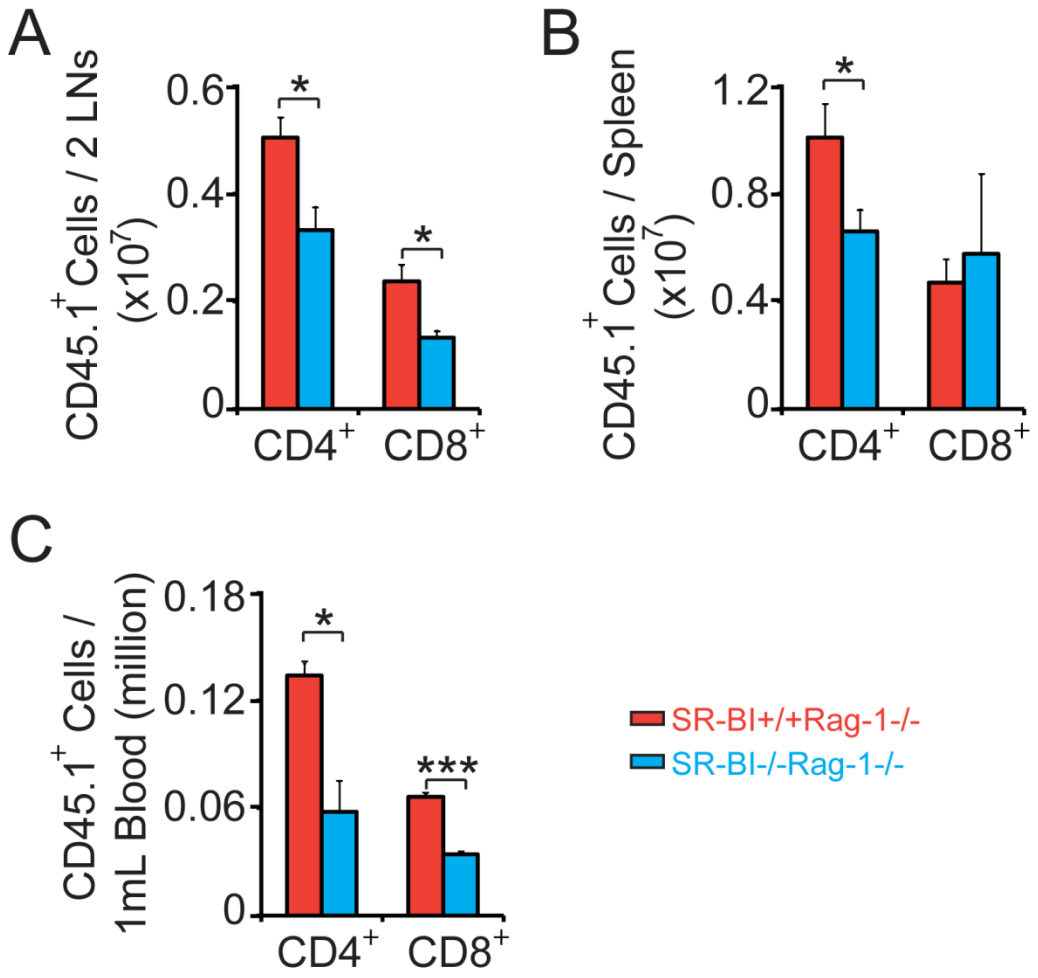

Figure 5.4 Non-hematopoietic SR-BI deficiency impairs peripheral lymphocyte repopulation after bone marrow transplantation.

Five million CD45.1$^+$ bone marrow cells were injected into lethally irradiated SR-BI$^{+/+}$Rag-1$^{-/-}$ or SR-BI$^{-/-}$Rag-1$^{-/-}$ mice. Six weeks later, CD45.1$^+$ T cell numbers in the lymph nodes (A), spleen (B) or blood (C) were evaluated. The number of a given population was calculated by multiplying the its percentage in CD45.1$^+$ cells in lymph nodes, spleen or blood by the CD45.1$^+$ cell numbers in lymph nodes or spleen, or the CD45.1$^+$ cell concentration in blood. n=3-9 per group. *, $p<0.05$; ***, $p<0.001$.

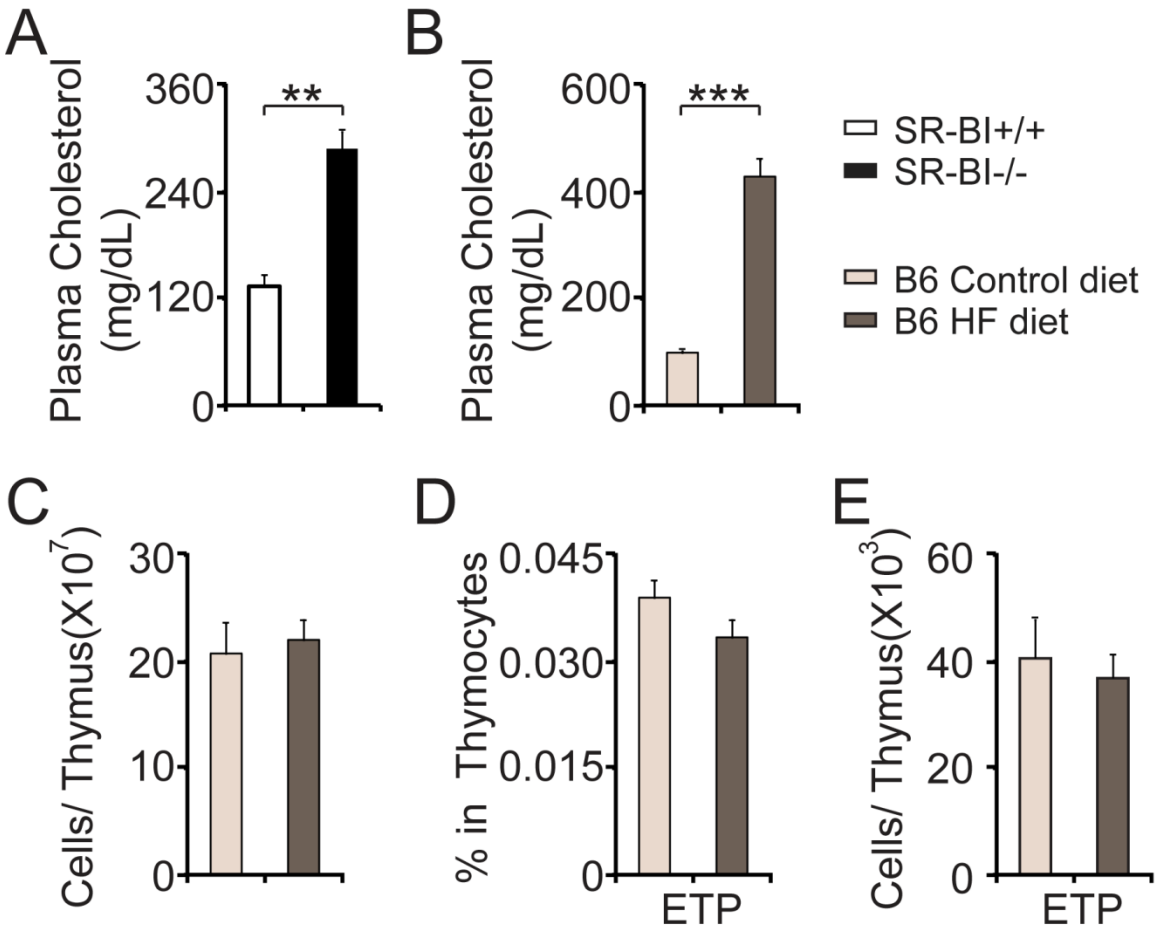

Figure 5.5 Diet-induced hypercholesterolemia does not affect thymopoiesis.

A) Plasma cholesterol concentrations were determined in 5-week-old SR-BI$^{+/+}$ and SR-BI$^{-/-}$ mice. n= 3 per group. B)-E) C57BL/6N mice were fed with high fat diet or control diet starting from the age of 3 weeks. Two weeks later, plasma cholesterol concentrations (B), thymocyte numbers (C), the percentage (D) and numbers (E) of ETP were analyzed. n=5 per group. **, $p<0.01$; ***$p<0.001$.

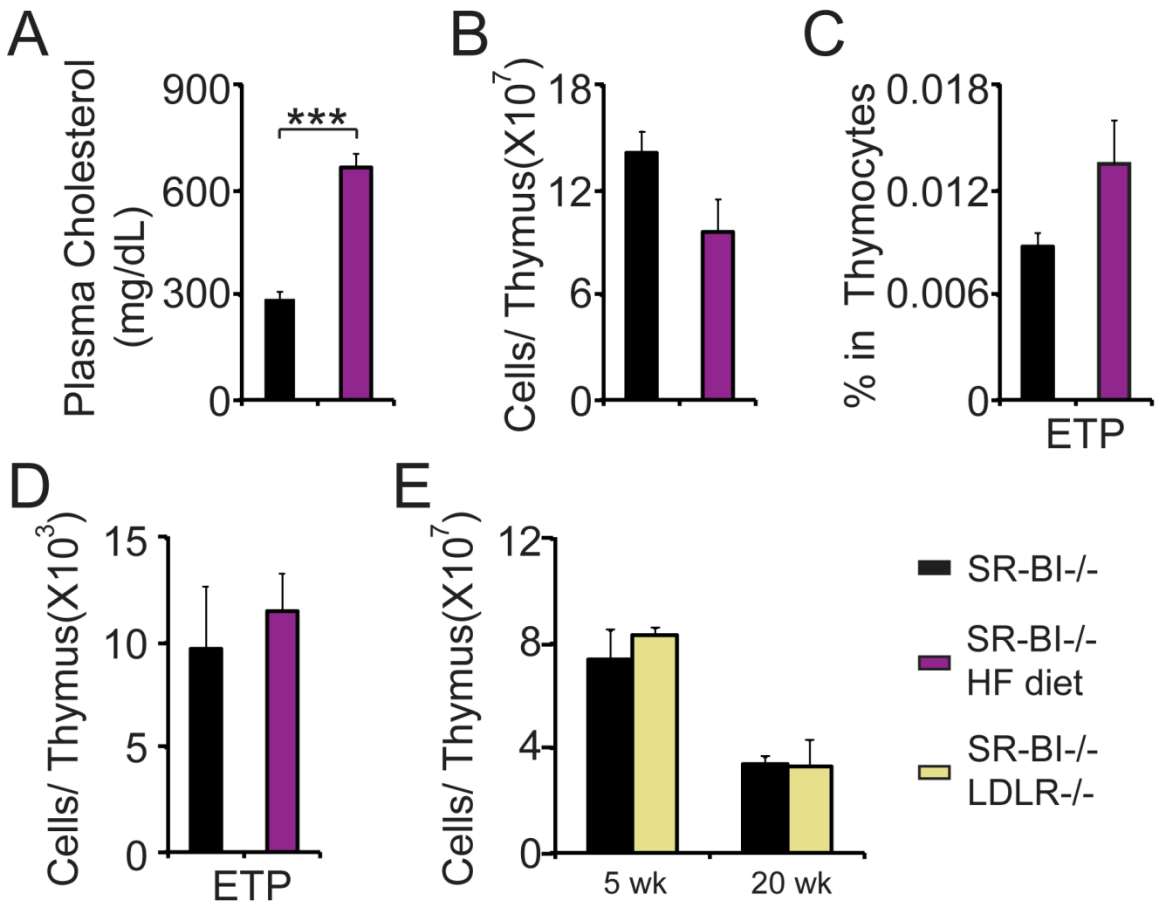

Figure 5.6 Elevating hypercholesterolemia in SR-BI-deficient mice does not further impair thymopoiesis.

A)-D) SR-BI$^{-/-}$ mice were fed with high fat diet or control diet starting from the age of 3 weeks. Two weeks later, plasma cholesterol concentrations (A), thymocyte numbers (B), the percentage (C) and numbers (D) of ETPs were analyzed. n= 4-5 per group. E) Thymocyte numbers of 5-week-old or 20-week-old SR-BI$^{-/-}$ or SR-BI$^{-/-}$LDL$^{-/-}$ mice were analyzed. n=2-4 per group for 5-week-old group; n=9-12 per group for 20-week-old group. ***, $p<0.001$.

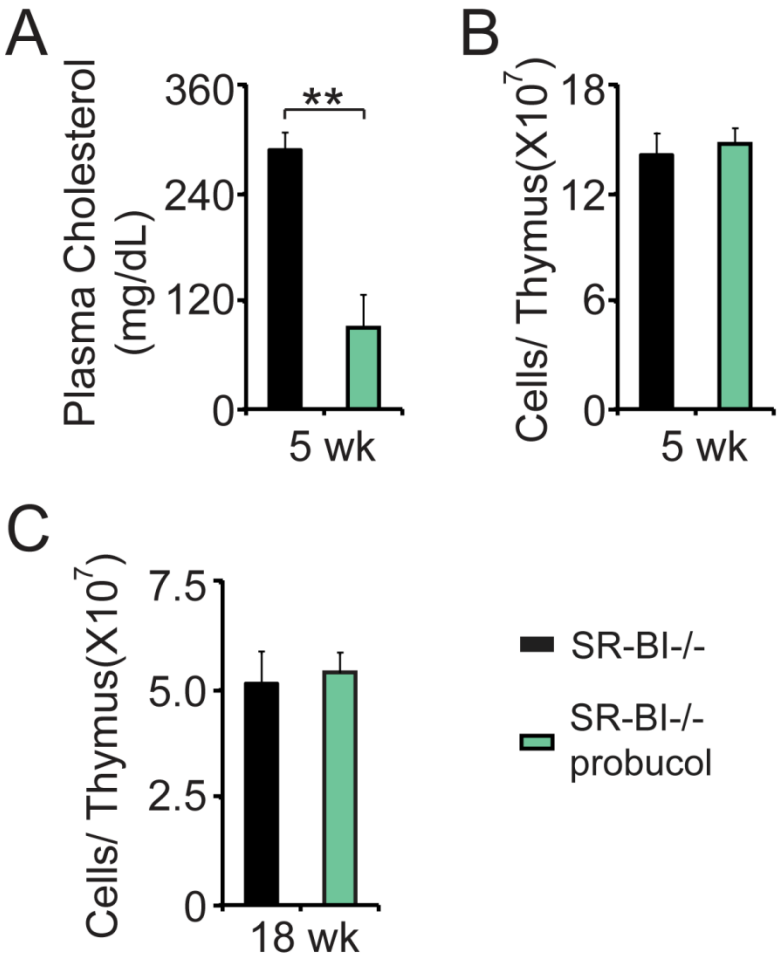

Figure 5.7 Relieving hypercholesterolemia in SR-BI-deficient mice does not correct thymic hypocellularity.

SR-BI$^{-/-}$ mice were fed with a diet containing 0.2% probucol or control diet starting from the age of 3 weeks. A)-B) Two weeks later, plasma cholesterol concentrations (A) and thymocyte numbers (B) were analyzed. n=5-7 per group. C) Fifteen weeks later, thymocyte numbers were analyzed. n=7-9 per group. **, $p<0.01$.

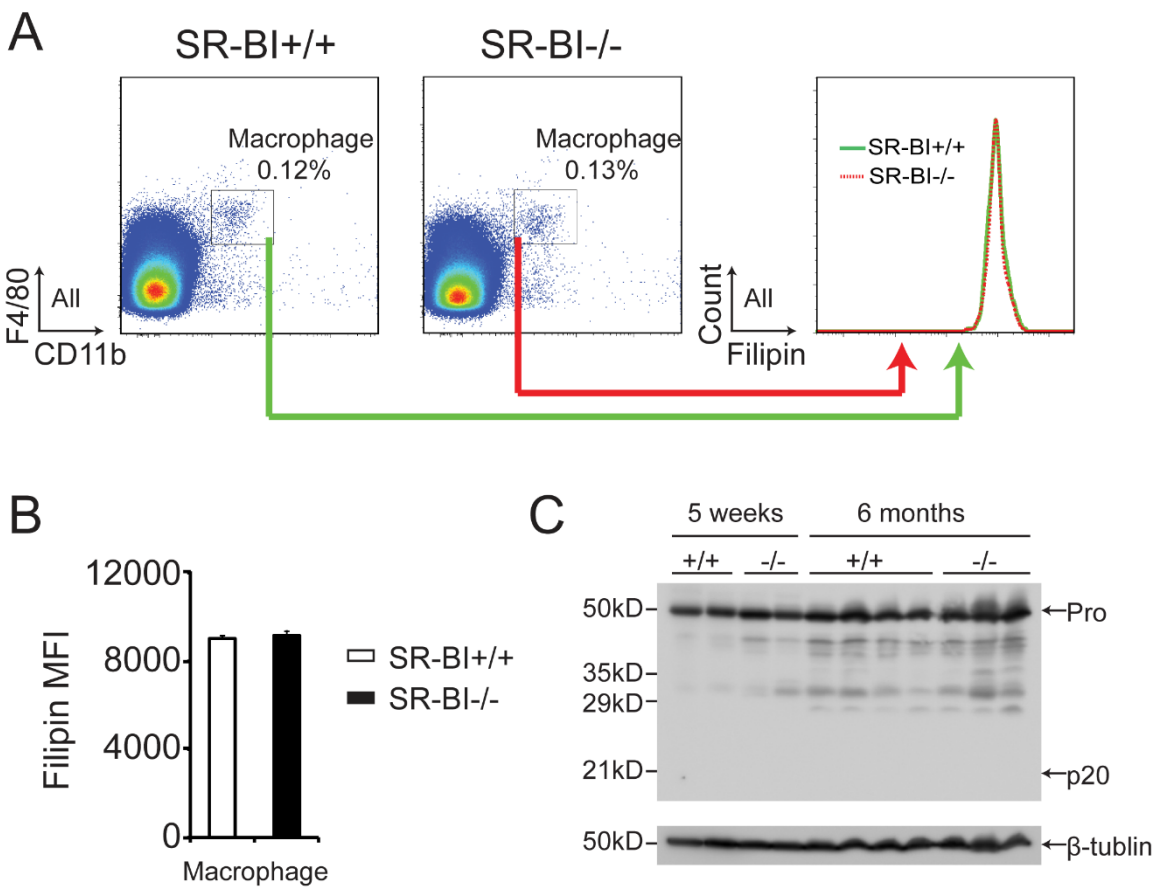

Figure 5.8 SR-BI deficiency does not impair thymopoiesis through activating NLRP3 inflammasome.

A)-B) Thymocytes of 5-week-old SR-BI$^{+/+}$ and SR-BI$^{-/-}$ mice were stained with surface markers and then fixed/ permeabilized, before staining with filipin. A) The thymic macrophage was defined as the F4/80^{+}CD11b^{+} population in thymocytes and the filipin staining in gated thymic macrophage is shown. B) The mean fluorescence density (MFI) of filipin in thymic macrophages was statistically analyzed. n=3 per group. C) Thymi from SR-BI$^{+/+}$ and SR-BI$^{-/-}$ mice were lysed and the whole-thymus lysates were subject to western blot analysis with anti-caspase-1 (4B4) and anti-β-tublin. Representative results from two experiments were showed.

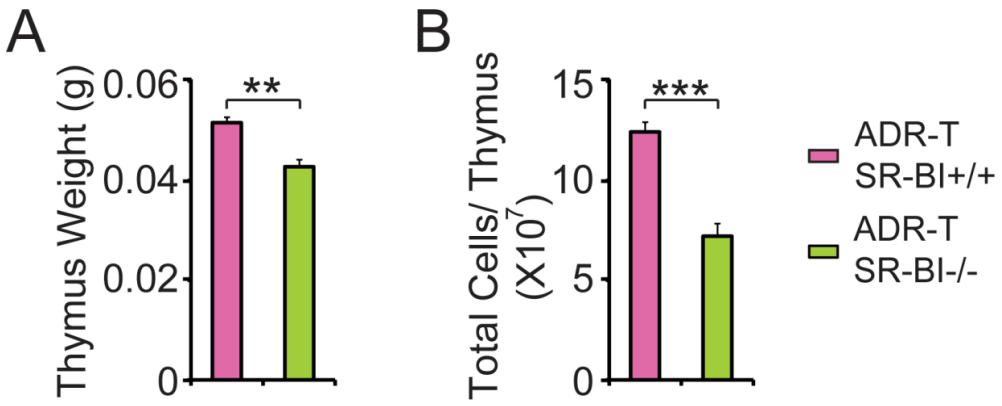

Figure 5.9 Adrenal SR-BI deficiency reduces thymic size.

SR-BI$^{+/+}$ mice (10-12 weeks) were adrenalectomized and transplanted with adrenal gland from either SR-BI$^{+/+}$ or SR-BI$^{-/-}$ donors (9 days) under the right kidney capsule. Six weeks later, thymus weight (A) and thymic cellularity (B) were analyzed. n=4-5 per group. **, $p<0.01$; ***, $p<0.001$.

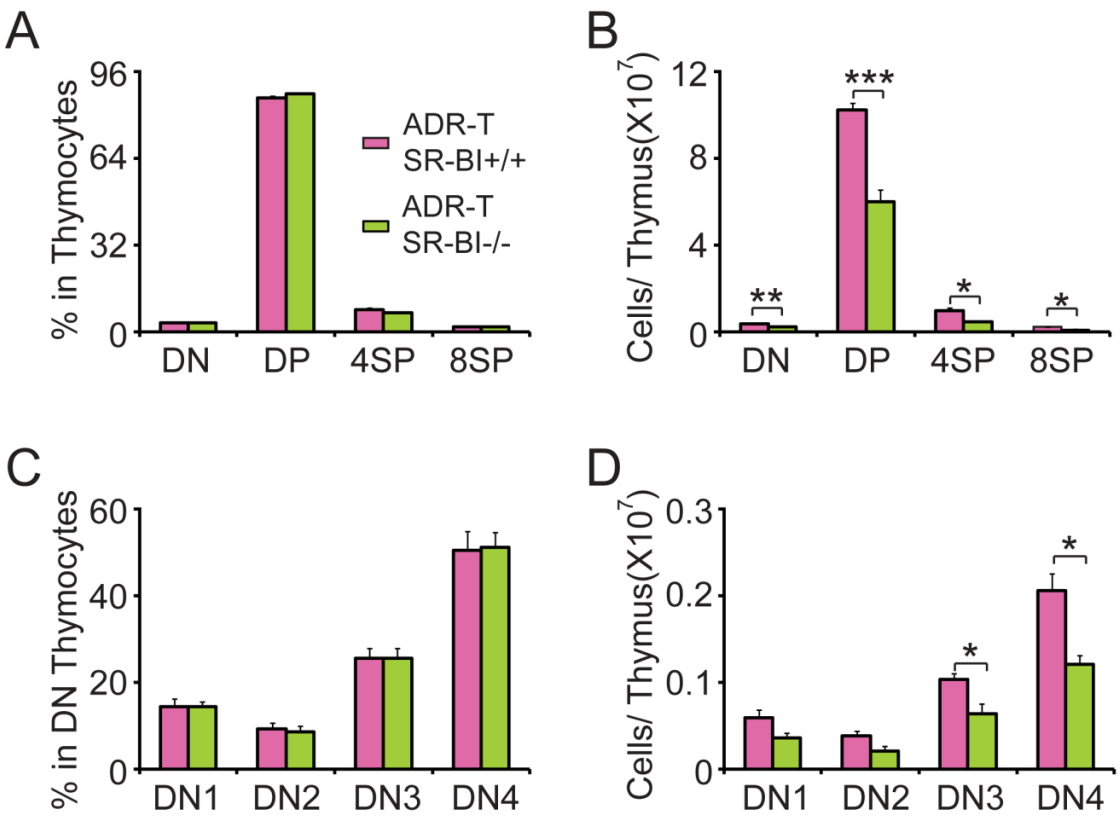

Figure 5.10 Adrenal SR-BI deficiency does not change thymic CD4/CD8 profile or DN1-4 profile.

SR-BI$^{+/+}$ mice (10-12 weeks) were adrenalectomized and transplanted with one adrenal gland from either SR-BI$^{+/+}$ or SR-BI$^{-/-}$ donors (9 days) under the right kidney capsule. Six weeks later, thymocyte subsets of the recipient mice were evaluated. A) The CD4/CD8 profile was analyzed. B) The number of a given population was calculated by multiplying its percentage in thymocytes by the total number of thymocytes. C) The DN1-4 profile was analyzed. D) The number of a given DN population was calculated by multiplying its percentage in DN thymocytes by the number of DN thymocytes. n=4-5 per group. *, $p<0.05$; **, $p<0.01$; ***, $p<0.001$.

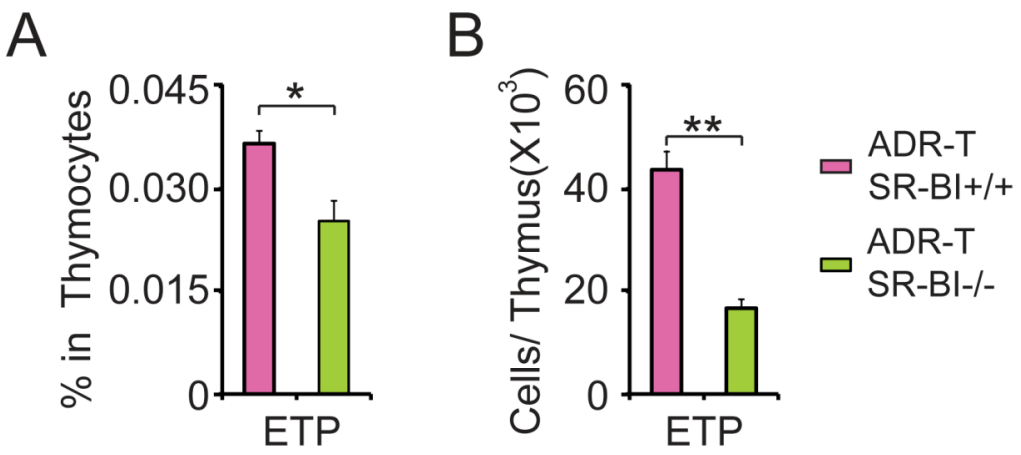

Figure 5.11 Adrenal SR-BI deficiency decreases the portion of ETPs.

SR-BI$^{+/+}$ mice (10-12 weeks) were adrenalectomized and transplanted with one adrenal gland from either SR-BI$^{+/+}$ or SR-BI$^{-/-}$ donors (9 days) under the right kidney capsule. Six weeks later, thymocyte subsets of the recipient mice were evaluated. A) The percentage of ETPs was analyzed. B) The number of ETP was calculated by multiplying its percentage in thymocytes by the total number of thymocytes. n=4-5 per group. *, $p<0.05$; **, $p<0.01$.

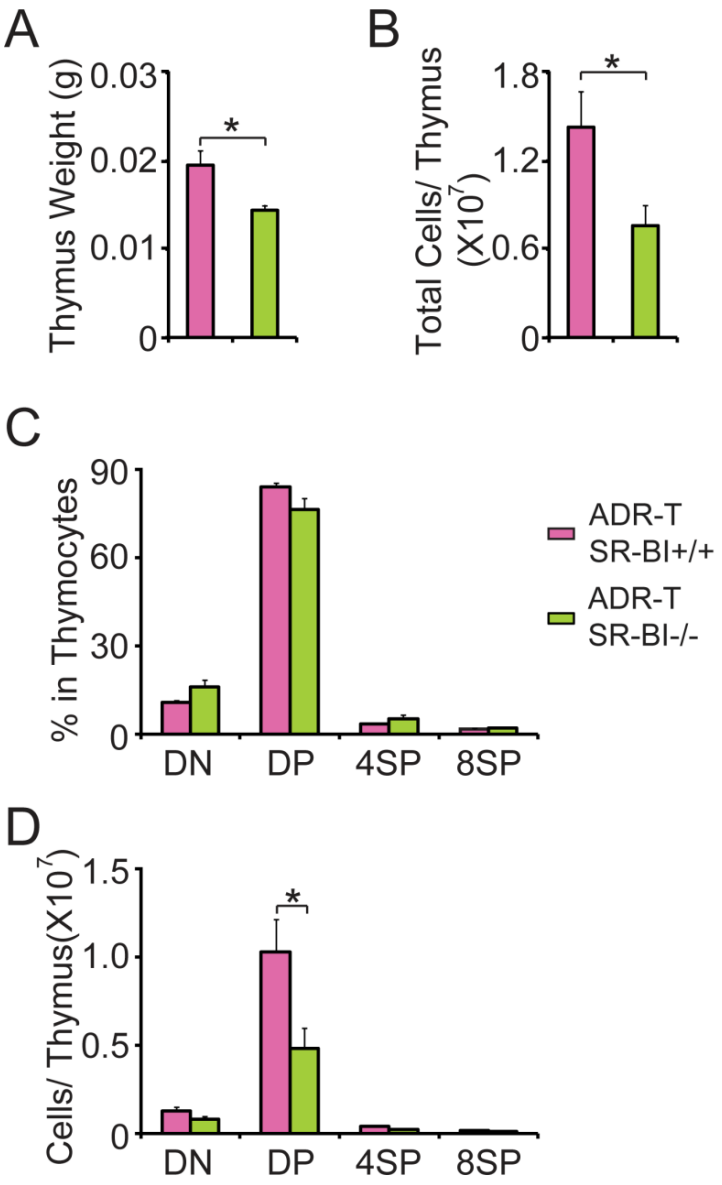

Figure 5.12 Adrenal SR-BI deficiency delays thymic recovery after sublethal irradiation.

SR-BI$^{+/+}$ mice (10-12 weeks) were adrenalectomized and transplanted with one adrenal gland from either SR-BI$^{+/+}$ or SR-BI$^{-/-}$ donors (9 days) under the right kidney capsule. Six weeks later, recipient mice were irradiated with a single dose of 450 rads from a cesium source. Seven days after irradiation, the mice were sacrificed. A) Thymus weight was analyzed. B) Thymocyte numbers of mice

were analyzed. C) The thymocyte CD4/CD8 profile was analyzed. D) The number of a given population was calculated by multiplying its percentage in thymocytes by the number of total thymocytes. n=7-9 per group. *, $p<0.05$.

Chapter 6 Discussion

6.1 Summary of this project

In this project, we identified SR-BI, a well-established HDL receptor that can bind a wide range of ligands, as a novel player in thymopoiesis. Loss of SR-BI in mice leads to a significant reduction in thymus weight (Figure 3.1) and thymic hypocellularity (Figure 3.2) after puberty, which is associated with a marked decrease in T cell production (Figure 3.5). Meanwhile, SR-BI deficiency also induces delayed thymic recovery after sublethal irradiation (Figure 4.12). These findings indicate that SR-BI is required for normal thymopoiesis and thymic regeneration.

In the process of T cell development, SR-BI deficiency impairs the thymic homing process of bone marrow progenitors (Figure 4.10 and 4.11), causing reduced progenitor entry in the thymus and a decreased percentage of ETPs (Figure 4.8). In contrast, SR-BI deficiency does not influence the lymphoid progenitor development in bone marrow (Figure 4.9). T cell developmental processes downstream of ETP are also normal in SR-BI-null mice, as their percentages of thymocyte subsets (Figure 4.1, 4.2 and 4.5) and the expression of TCR-β in thymocytes (Figure 4.3) are all unaltered. In addition, the reduced thymus size of SR-BI-null mice is not due to an increase in thymocyte apoptosis or a decrease in thymocyte proliferation, as we only detected minor changes in apoptosis (Figure 4.6) and proliferation (Figure 4.7) of DN thymocytes, which may be linked to the decrease of ETPs.

Consistent with the reduction in T cell production, SR-BI deficiency leads to a narrowed naïve T cell pool. The naïve $CD4^+$ and naïve $CD8^+$ cell numbers are all decreased in lymph nodes (Figure 3.6 and Figure 3.7), spleen (Figure 3.8) and blood (Figure 3.9) of SR-$BI^{-/-}$ mice at young ages. An increase in proliferation of naïve T cells was also detected in the deficient mice (Figure 3.9). These observations indicate that the reduced T cell production due to SR-BI deficiency impairs T cell homeostasis in the periphery. Moreover, T cells isolated from SR-BI-null mice display reduced responses to TCR stimuli (Figure 3.10 and 3.11), suggesting that the reduction in T cell production also compromises T cell function in these mice.

Using bone marrow transplantation models, we show that the absence of SR-BI in hematopoietic cells does not cause any defect in T cell development whereas the non-hematopoietic SR-BI deficiency is responsible for those defects. The hypercholesterolemia in SR-BI-null mice is not likely the leading cause for the defects in thymus, as neither exaggerating hypercholesterolemia in SR-BI-null mice further decreases their thymic cellularity (Figure 5.6), nor does normalizing hypercholesterolemia relieve their thymic hypocellularity (Figure 5.7). In addition, young SR-BI-null mice do not exhibit cholesterol accumulation in thymic macrophages or activation of NLRP3 inflammasome in the thymus (Figure 5.8), indicating that thymic hypocellularity is not related to thymic macrophage cholesterol accumulation-induced NLRP3 inflammasome activation. Unexpectedly, we observed that the loss of SR-BI in adrenal gland leads to decreased thymus size, reduced ETP percentage and delayed thymic recovery

(Figure 5.9-5.12). With these findings, we demonstrate that the impaired thymopoiesis in SR-BI-null mice is attributed to the adrenal SR-BI deficiency.

6.2 T cell development in the absence of SR-BI

From the HSCs in bone marrow to the mature naïve T cells in the periphery, T cell development can be divided to two major components, lymphoid progenitor development in the bone marrow and the T cell development in the thymus. These two major processes are connected by progenitor thymic homing, in which LMPPs and CLPs migrate from bone marrow to enter thymus via the circulation and then participate in thymopoiesis. Because thymus lacks self-renewal progenitors, long term T cell production requires continuous progenitor entry into thymus [68].

In the absence of SR-BI, the progenitor thymic homing processes in mice are impaired, leading to reduced thymus size and decreased thymic cellularity. The impaired progenitor thymic homing due to SR-BI deficiency is directly elucidated with progenitor homing assays. In these assays, we show that when comparable concentrations of bone marrow cells are present in the circulation, fewer bone marrow cells settle into thymi in SR-BI$^{-/-}$ mice than in SR-BI$^{+/+}$ mice (Figure 4.10). Moreover, the reduced amount of seeded progenitors gives rise to fewer downstream thymocytes in the deficient mice, indicating that the contribution of circulating bone marrow progenitors to generating developing thymocyte is also impaired (Figure 4.11). Meanwhile, in the bone marrow transplantation models, the decreased repopulation of donor-derived thymocytes (Figure 5.3) and reduced numbers of donor-derived peripheral T cells (Figure

5.4) in SR-BI$^{-/-}$Rag-1$^{-/-}$ recipients can also be explained by the impaired progenitor homing, as they are transplanted with the same numbers of donor bone marrow cells via the circulation with SR-BI$^{+/+}$Rag-1$^{-/-}$ recipients. These three models together reveal the fact that due to the impaired thymic homing, fewer bone marrow progenitors enter thymus in the absence of SR-BI, which leads to the thymic hypocellularity and the reduced T cell generation.

A direct consequence of the impaired thymic homing is a decrease in the percentage of ETPs. For example, CCR7/CCR9 double knockout mice and P-selectin glycoprotein ligand 1 (PSGL-1) knockout mice, in whom the progenitor thymic homing is blocked, display significant reduction in the percentage of ETPs in thymocytes [83, 84]. SR-BI-null mice also show a dramatic reduction in the percentage of ETPs (Figure 4.8). In addition, SR-BI-null mice exhibit unchanged percentage of DN1-4 profile (Figure 4.2) and reduced thymic cellularity (Figure 3.2), which is similar to the other two mouse strains whose progenitor thymic homing is reduced [83, 84]. Interestingly, we detected a significant decrease in the proliferation of DN2 population in SR-BI-null mice (Figure 4.7). Because DN2 cells are direct descendants of ETPs, the reduced proliferation is probably due to the reductions in ETPs. The decreased apoptosis of DN cells (Figure 4.6) may be a consequence of the reduced proliferation of DN2 cells, which we speculate causes fewer DN cells to enter β-selection.

The other steps of T cell development in SR-BI-null mice appear normal. For the lymphoid progenitor development in bone marrow, we did not observe any change in the percentage or the number of bone marrow progenitors in SR-

BI-null mice, indicating there is not any significant blockage in the lymphoid progenitor development. The thymopoiesis events downstream of ETPs are also intact in SR-BI-null mice. First, SR-BI-null mice display normal a CD4/CD8 profile (Figure 4.1) and DN1-4 profile (Figure 4.2), indicating that there is not a significant blockage between thymocyte subtypes. Second, SR-BI-null mice exhibit identical TCR-β expression in thymocytes (Figure 4.3), indicating that the selection processes are not altered by SR-BI deficiency. Third, SR-BI-null mice display unchanged percentage of immature and mature SP cells (Figure 4.5), indicating intact SP cell maturation in these mice. Finally, SR-BI-null mice do not show reduced proliferation or elevated apoptosis in most thymocyte subtypes, excluding the possibility that SR-BI deficiency impairs thymopoiesis by decelerating the proliferation or increasing apoptosis of thymocytes. More importantly, in the long-term homing assay, although fewer numbers of donor-derived thymocytes were detected in SR-BI$^{-/-}$ mice, the CD4/CD8 profile of donor-derived thymocytes is identical in SR-BI$^{-/-}$ mice and SR-BI$^{+/+}$ controls (Figure 4.11). This observation indicates that the settled progenitors in SR-BI-null thymi, despite lower numbers, are following a normal developmental program to generate downstream thymocytes, strongly supporting that SR-BI deficiency does not affect T cell development downstream of ETPs. In addition, in bone marrow transplanted SR-BI$^{-/-}$ mice (Figure 5.3) and sublethal irradiated SR-BI$^{-/-}$ mice (Figure 4.12), the CD4/CD8 profiles of thymocytes are also not significantly changed, further indicating the intact T cell development downstream of ETPs.

The impairment in progenitor thymic homing and the reduction of ETPs in SR-BI-null mice lead to reduced thymus size, which is characterized by the decrease in thymus weight (Figure 3.1) and the thymic hypocellularity (Figure 3.2). Notably, the reduction in thymus size was not observed in 1-week-old SR-BI-null mice (Figure 3.4), indicating SR-BI does not impair thymus development before birth.

6.3 SR-BI deficiency-impaired thymopoiesis contributes to the lymphocyte imbalance

Our data reveal that the T cell production is decreased by the SR-BI deficiency, since both the frequency and the number of TRECs, which are correlated with RTEs, are reduced in the T cells of SR-BI-null mice (Figure 3.5). As a consequence of the reduction in T cell production, young SR-BI-null mice display impaired T cell homeostasis in the periphery, characterized by reduced naïve T cell portion (Figure 3.6-3.8) and increased naïve T cell (Figure 3.9) proliferation.

Interestingly, 5-week-old and 20-week-old SR-BI-null mice display marked differences in lymphocytes. Formerly, our group reported that 20-week-old SR-BI$^{-/-}$ mice have T cell expansion and hyperactivation in spleen. Though the reduced naïve T cell percentage was also observed in 20-week-old SR-BI$^{-/-}$ mice, we thought it was due to the heightened T cell activation, because their naïve T cell numbers are not decreased, whereas the memory T cell numbers are significantly increased [134]. Results from current project show that the reduced thymopoiesis actually has a contribution to the decrease in the portion of naïve T

cells. Five-week-old SR-BI-null mice exhibit a remarkable reduction in naïve T cell pool in lymph nodes, spleen and blood. Nevertheless, memory T cells are not increased in any of these sites (Figure 3.6 and 3.6), indicating that at young age, SR-BI deficiency does not induce T cell hyperactivation, but the reduction in thymopoiesis has started to affect the T cell homeostasis. The number of T cells is not higher in 5-week-old SR-BI-null mice than wild-type mice (Figure 3.6E), indicating that T cell expansion also has not been induced by SR-BI deficiency in 5-week-old mice. The T cell homeostasis in lymph nodes of 13-week-old SR-BI-null mice is similar with 5-week-old SR-BI-null mice (Figure 3.7), but the T cells in spleen have shown a slight expansion (data not shown), indicating that between 5 weeks and 20 weeks of age, the dysfunctional HDL begins to take over, increasing T cell numbers and inducing the T cell hyperactivation.

Consistent with former reports showing that the reduced T cell production causes compromised T cell functions [62-64], we found that T cells from SR-BI-null mice display impaired responsiveness to stimuli (Figure 3.10 and 3.11). We speculate the impaired T cell function in SR-BI-null mice is linked with the reduced refreshment of T cell pool by RTEs, which is known to be responsible for increased longevity of naïve T cells and accumulation of anergic T cells [54]. However, as dysfunctional HDL from SR-BI-null mice can also modulate T cells, we cannot exclude its contribution to the impaired T cell functions. Further investigation is warranted to further understand how the reduction in T cell function is induced by SR-BI deficiency.

We also reported that aged SR-BI-null mice suffer from an autoimmune problem, as shown by increased autoantibody concentration in the circulation, and elevated lymphocyte infiltration and the presence of immunocomplexes in the kidney [134]. The lymphocyte hyperactivation due to the dysfunctional HDL in SR-BI-null mice was thought to be the leading cause of the autoimmune problems. Our current findings raise the possibility that the autoimmune disease due to SR-BI deficiency is influenced by the impaired thymopoiesis, as thymopoiesis can remove the self-reactive T cells in the periphery [54] and reduced T cell production is known to cause autoimmune problems [57]. The underlying mechanisms by which SR-BI deficiency leads to the autoimmune problem will be an interesting subject for future study.

6.4 Impaired thymopoiesis in SR-BI-null mice is not due to hematopoietic SR-BI deficiency or abnormal cholesterol metabolism

In addition to investigating how T cell development is changed in SR-BI-null mice, we studied how SR-BI deficiency causes these changes. Because SR-BI is expressed in hematopoietic cells such as T cells, B cells [134], and macrophages [290], it is possible that absence of SR-BI in hematopoietic cells is responsible for the T cell development defects. Hematopoietic SR-BI deficiency has been shown to induce elevated susceptibility to atherosclerosis [178, 182, 188-190], increased inflammation [192], and the red blood cell abnormalities (unpublished data). However, Our data indicate that hematopoietic SR-BI deficiency is not responsible for the thymic defects, as bone marrow cells from SR-BI-null mice do not show any disadvantage in supporting thymopoiesis

compared with those from wild-type mice in bone marrow transplantation experiments (Figure 5.1).

If hematopoietic SR-BI deficiency does not lead to impaired thymopoiesis, it follows that non-hematopoietic SR-BI deficiency causes the thymic defects in SR-BI-null mice. Using another group of bone marrow transplantation assay, we confirmed the contribution of non-hematopoietic SR-BI deficiency to the thymic defects. SR-BI-deficient recipients display reduced donor-derived cells in the thymus (Figure 5.3) and decreased peripheral donor-derived T cells (Figure 5.4), indicating that the non-hematopoietic SR-BI deficiency environment is the major cause of impaired thymopoiesis. Moreover, in the progenitor homing assays, labeled bone marrow cells show lower ability to settle in the thymus (Figure 4.10) and give rise to downstream thymocytes in SR-BI$^{-/-}$ recipients (Figure 4.11), further suggesting that the non-hematopoietic SR-BI deficiency causes impaired progenitor thymic homing in mice.

The fact that the non-hematopoietic SR-BI deficiency causes impaired thymopoiesis led us to ask if the impaired thymopoiesis is induced by the SR-BI deficiency-induced hypercholesterolemia. Actually, several defects due to SR-BI deficiency has been shown to be secondary to the defective cholesterol metabolism [135]. For example, SR-BI deficiency causes erythrocyte defects through inducing cholesterol accumulation in erythrocyte [212, 213]; and SR-BI deficiency-induced female infertility is caused by the abnormal HDL particles [210]. Abnormalities that are caused by defective cholesterol metabolism in SR-BI-deficient mice can be relieved by normalizing the cholesterol metabolism. For

instance, treatment with probucol, a cholesterol lowering drug, in SR-BI$^{-/-}$ mice is able to correct some defects, including increased susceptibility to cardiovascular disease [262], female infertility [210], and abnormalities in red blood cells [262]. More importantly, the lymphocyte expansion and hyperactivation is correlated with the level of hypercholesterolemia in mice, as in SR-BI-null mice, lymphocyte expansion is exaggerated by elevated hypercholesterolemia; and furthermore it can be corrected by normalization of hypercholesterolemia (unpublished data). However, we did not obtain the same results with T cell development in SR-BI-null mice. We found that neither elevating hypercholesterolemia nor correcting hypercholesterolemia in SR-BI-null mice has any effect on their thymic cellularity (Figure 5.6 and 5.7), indicating the impaired T cell development is apparently not likely linked with impaired cholesterol metabolism.

Our findings are not inconsistent with current knowledge on how cholesterol metabolism is linked with T cell development. It was reported that deficiency of ABCG1, a key transporter mediating cholesterol efflux in RCT [244, 245], causes increased cholesterol accumulation in thymocytes, which induces increased thymocyte proliferation [241]. We find that SR-BI-null mice do not show increased cholesterol accumulation in thymocytes (data not shown) or elevated proliferation rate, indicating SR-BI is not an essential player in regulating cholesterol homeostasis in thymocytes. Also it was reported that free cholesterol accumulation in thymic macrophages induces activation of NLRP3 inflammasome, which contributes to age-related thymic involution [65]. We observed that young SR-BI-null mice do not have cholesterol accumulation in

thymic macrophages, nor do they show the activation of NLRP3 inflammasome in thymus (Figure 5.8), indicating that SR-BI deficiency also does not affect cholesterol homeostasis in thymic macrophages.

Taken together, our data indicate that the impaired thymopoiesis in SR-BI-null mice is caused by the non-hematopoietic SR-BI deficiency but it is not due to the impaired cholesterol homeostasis. SR-BI deficiency should cause the defects in T cell development via an alternative mechanism.

6.5 Adrenal SR-BI deficiency is responsible for impaired thymopoiesis

To figure out the mechanism by which SR-BI deficiency leads to the impaired thymopoiesis, we evaluated the contribution of adrenal SR-BI deficiency to the impaired thymopoiesis. SR-BI expressed in adrenal gland is essential in mediating the uptake of cholesterol from HDL, which provides cholesterol as resources for steroid synthesis [161]. Using adrenal transplantation models, Hoekstra M et al. showed that the absence of SR-BI in adrenal gland causes glucocorticoid insufficiency during fasting, highlighting the essential role of adrenal SR-BI *in vivo* [171]. The glucocorticoid insufficiency in SR-BI-null mice has been shown to be responsible for elevated inflammation, decreased thymocyte apoptosis and increased death rate in sepsis [135, 206, 247].

In this study, we also utilized adrenal transplantation technique to generate mice with SR-BI deficiency in adrenal gland. We found that the ADR-T SR-BI$^{-/-}$ mice display identical thymic phenotypes with SR-BI$^{-/-}$ mice. Compared with ADR-T SR-BI$^{+/+}$ mice, ADR-T SR-BI$^{-/-}$ mice show significantly reduced thymus weight and thymic cellularity (Figure 5.9), unaltered CD4/CD8 profile

(Figure 5.10) and decreased portion of ETPs (Figure 5.11). Notably, it was six weeks after adrenal transplantation that we observed changes in the thymus. Given that all the thymocytes can be fully replaced by bone marrow progenitor-derived cells in four weeks [54], at the time point we evaluated the thymi, the thymocytes of the adrenal transplanted mice should all be originated from bone marrow cells that enter thymi after surgery. Thus, the thymic defects in ADR-T SR-BI$^{-/-}$ mice are likely due to the impaired thymic homing. These findings indicate that the impaired thymopoiesis of SR-BI-null mice is induced by its abnormal adrenal functions.

These results are surprising for two major reasons. First, although adrenal SR-BI deficiency causes impaired adrenal functions, previous data indicated that it only causes an insufficiency of inducible glucocorticoid. Under normal conditions, the adrenal function is considered normal, as no significant decrease in the concentration of circulating glucocorticoid was detected in SR-BI-null mice [206, 207]. However, the impaired thymopoiesis is seen in young SR-BI-null mice under normal conditions. The linkage between the SR-BI deficiency in adrenal gland and the impaired thymopoiesis indicates that the adrenal functions of SR-BI-null mice are not intact as was thought previously. Absence of adrenal SR-BI leads to changes in adrenal steroid production under normal conditions, which subsequently causes the defects in T cell development. How adrenal function is affected by SR-BI deficiency under normal condtions warrant further study.

Second, our findings appear contradictory to current concepts on the effect of steroids on thymopoiesis. Prior to our study, the effect of glucocorticoid

on T cell development has been intensively investigated. It is well known that during inflammatory process such as sepsis, a high level of glucocorticoid is induced that causes thymocyte apoptosis [291, 292]. Under normal conditions, glucocorticoid is also predicted to suppress T cell development as evidenced by the findings that overexpression of GC receptor in thymocytes leads to decreased thymic cellularity in mice [293] and adrenalectomy is well-known to cause an increase in thymocyte numbers [294, 295]. The discovery of the intrathymic glucocorticoid synthesis [296-298] indicated the effect of glucocorticoid is more complicated than originally thought. The intrathymic glucocorticoid seems to be regulated differently from its adrenal production [299], and it has been shown to play a role in regulating thymus size [293, 299] and selection processes in thymopoiesis [300, 301]. Given that adrenal SR-BI causes impaired adrenal function and reduced inducible glucocorticoid production, one may predict that adrenal deficiency of SR-BI should contribute to increasing thymus size. But interestingly we got an opposite observation.

How impaired adrenal function causes impaired thymopoiesis is a puzzle that remains to be solved. However, for the first time, we demonstrate that the progenitor homing process is the link between them. It is worth noting that SR-BI controls the synthesis of not only glucocorticoids but also several other steroids [135]. The decrease in the production of other steroids may be responsible for the impaired thymopoiesis in the adrenal SR-BI-deficient mice, as the physiological concentrations of glucocorticoids are not changed. Further investigation is warranted to identify how the adrenal SR-BI deficiency changes T

cell development, which may lead to novel findings on the roles of steroids in thymopoiesis.

6.6 SR-BI is required for normal thymic regeneration

Another major finding in this project is that SR-BI deficiency causes impaired thymic regeneration. Using the sublethal irradiation model, which mimics the whole body irradiation in humans, we found that SR-BI-null mice show a slower recovery after the thymocyte depletion (Figure 4.12). The irradiation causes thymocyte depletion and reduces thymocytes of SR-BI$^{+/+}$ and SR-BI$^{-/-}$ mice to comparably low levels in 4 days. After the lowest point, thymocytes are increased by 8.4-fold in SR-BI$^{+/+}$ mice 7 days after irradiation. In contrast, in SR-BI$^{-/-}$ mice these cells are only elevated by 3.1-fold. As long as 14 days after irradiation, the thymocyte numbers of SR-BI$^{-/-}$ mice are still 40% lower than that of SR-BI$^{+/+}$ mice, clearly indicating impaired thymic recovery after irradiation. Similarly, during the recovery from CLP-induced sepsis, the thymocyte numbers of SR-BI-null mice are also much smaller than those of wild-type controls 7 days after the surgery (data not shown), which probably also results from the delayed thymic recovery due to SR-BI deficiency.

Both the irradiation resistant T cell progenitors such as ETP and the circulating bone marrow progenitors have been shown to be essential for the thymic recovery [68, 277]. In the sublethal irradiation model, the thymic recovery is mainly dependent on the intrathymic T cell progenitors, as it usually takes around 2 weeks for circulating progenitors to develop to double positive stage [77, 277]. In our long term homing assay, two weeks after the injection of bone

marrow cells into the non-irradiated mice, the donor-derived cells are only ~1% in total thymocytes (Figure 4.11A and B), also indicating a slow contribution of circulating bone marrow cells to thymopoiesis. Thus, in the sublethally irradiated SR-BI-null mice, the delayed thymic recovery is mainly attributed to the decrease in the percentage of ETPs. Actually, our bone marrow transplantation experiments in which we tested the contribution of non-hematopoietic SR-BI deficient to the impaired thymopoiesis (Figure 5.3), can be seen as a model to evaluate the contribution of circulating progenitors to thymic recovery in SR-BI-null mice. In this model, most intrathymic progenitors are deleted by lethal irradiation and thus the thymic regeneration is mainly dependent on circulating progenitors [277]. The reduced donor-derived thymocyte numbers and ETPs in SR-BI$^{-/-}$Rag-1$^{-/-}$ recipients after bone marrow transplantation indicate that the impaired thymic homing is also responsible for the compromised thymic recovery in SR-BI-null mice.

More importantly, we show that adrenal SR-BI deficiency induces the impaired thymic recovery after sublethal irradiation (Figure 5.12), providing a formerly unseen link between adrenal function and thymic regeneration. As thymocyte depletion increases the risks to infection and is extremely slow to recover [109, 110, 113], understanding how adrenal function plays a role in regulating thymic regeneration may lead to novel methods to accelerate thymic recovery in patients.

6.7 Prospective

In this project, we discovered that adrenal SR-BI is required to maintain normal thymopoiesis and T cell homeostasis. Several key questions still remain to be solved. The most important of these is how SR-BI deficiency impairs adrenal function under normal conditions and how impaired adrenal function induces the defects in T cell development. Answering this question could be challenging, because SR-BI controls synthesis of multiple steroids in adrenal, and each steroid (such as glucocorticoids) may play complex roles in T cell development. However, understanding how the adrenal-generated steroid affects thymopoiesis will be of great significance, as it may lead to new strategies to increase thymic functions in the elderly or patients with thymocyte depletion.

Another interesting question will be how progenitor thymic homing is affected by adrenal SR-BI deficiency. The thymic homing process is mediated by several adhesion molecules. It is possible the adhesion molecules on thymic endothelial cells or bone marrow progenitors are down-regulated in SR-BI-null mice. Or, SR-BI deficiency may cause more bone marrow progenitor cell death in the circulating. Elucidating how SR-BI deficiency affects thymic homing will deepen our understanding of the regulation of progenitor thymic homing, a process that has not been well-understood.

In addition, many detailed questions regarding the adaptive immune system of SR-BI-null mice remain to be solved. For example, how the impaired thymopoiesis and dysfunctional HDL-induced T cell expansion contribute to the impaired lymphocyte homeostasis and the autoimmune problem; how the TCR

repertories and the primary immune responses are affected by SR-BI deficiency; and how SR-BI deficiency affects the non T-lineage cells in thymus. Understanding the role of SR-BI in immunity may generate novel findings that link HDL metabolism or adrenal functions to the immune system.

In summary, in this project, we identified a formerly unseen function of SR-BI in thymopoiesis. SR-BI deficiency causes reduced thymic size, decreased T cell production and delayed thymic recovery in mice by causing impaired progenitor thymic homing. Adrenal SR-BI deficiency is responsible for the defects in T cell development.

REFERENCES

[1] Janeway CA, Jr. Approaching the asymptote? Evolution and revolution in immunology. Cold Spring Harbor symposia on quantitative biology 1989; 54 Pt 1:1-13.

[2] Dempsey PW, Vaidya SA, Cheng G. The art of war: Innate and adaptive immune responses. Cell Mol Life Sci 2003; 60:2604-2621.

[3] Myers CD. Role of B cell antigen processing and presentation in the humoral immune response. FASEB J 1991; 5:2547-2553.

[4] Coffman RL, Seymour BW, Lebman DA *et al.* The role of helper T cell products in mouse B cell differentiation and isotype regulation. Immunol Rev 1988; 102:5-28.

[5] Abraham E. T- and B-cell function and their roles in resistance to infection. New horizons 1993; 1:28-36.

[6] Davis MM, Bjorkman PJ. T-cell antigen receptor genes and T-cell recognition. Nature 1988; 334:395-402.

[7] Holtmeier W, Kabelitz D. gammadelta T cells link innate and adaptive immune responses. Chemical immunology and allergy 2005; 86:151-183.

[8] Born WK, Reardon CL, O'Brien RL. The function of gammadelta T cells in innate immunity. Current opinion in immunology 2006; 18:31-38.

[9] Fleury SG, Croteau G, Sekaly RP. CD4 and CD8 recognition of class II and class I molecules of the major histocompatibility complex. Seminars in immunology 1991; 3:177-185.

[10] Zamoyska R. CD4 and CD8: modulators of T-cell receptor recognition of antigen and of immune responses? Current opinion in immunology 1998; 10:82-87.

[11] Swain SL, Bradley LM, Croft M *et al.* Helper T-cell subsets: phenotype, function and the role of lymphokines in regulating their development. Immunol Rev 1991; 123:115-144.

[12] Farrar JD, Asnagli H, Murphy KM. T helper subset development: roles of instruction, selection, and transcription. J Clin Invest 2002; 109:431-435.

[13] Sprent J, Surh CD. Normal T cell homeostasis: the conversion of naive cells into memory-phenotype cells. Nat Immunol 2011; 12:478-484.
[14] Picker LJ, Butcher EC. Physiological and molecular mechanisms of lymphocyte homing. Annu Rev Immunol 1992; 10:561-591.
[15] Budd RC, Cerottini JC, Horvath C *et al.* Distinction of virgin and memory T lymphocytes. Stable acquisition of the Pgp-1 glycoprotein concomitant with antigenic stimulation. J Immunol 1987; 138:3120-3129.
[16] Stout RD, Suttles J. T cells bearing the CD44hi "memory" phenotype display characteristics of activated cells in G1 stage of cell cycle. Cell Immunol 1992; 141:433-443.
[17] Surh CD, Sprent J. Homeostasis of naive and memory T cells. Immunity 2008; 29:848-862.
[18] Sallusto F, Geginat J, Lanzavecchia A. Central memory and effector memory T cell subsets: function, generation, and maintenance. Annu Rev Immunol 2004; 22:745-763.
[19] Sallusto F, Lenig D, Forster R *et al.* Two subsets of memory T lymphocytes with distinct homing potentials and effector functions. Nature 1999; 401:708-712.
[20] Bruno L, von Boehmer H, Kirberg J. Cell division in the compartment of naive and memory T lymphocytes. European journal of immunology 1996; 26:3179-3184.
[21] Tanchot C, Lemonnier FA, Perarnau B *et al.* Differential requirements for survival and proliferation of CD8 naive or memory T cells. Science 1997; 276:2057-2062.
[22] Kirberg J, Berns A, von Boehmer H. Peripheral T cell survival requires continual ligation of the T cell receptor to major histocompatibility complex-encoded molecules. J Exp Med 1997; 186:1269-1275.
[23] Rathmell JC, Farkash EA, Gao W, Thompson CB. IL-7 enhances the survival and maintains the size of naive T cells. J Immunol 2001; 167:6869-6876.
[24] Tan JT, Dudl E, LeRoy E *et al.* IL-7 is critical for homeostatic proliferation and survival of naive T cells. Proceedings of the National Academy of Sciences of the United States of America 2001; 98:8732-8737.

[25] Takada K, Jameson SC. Naive T cell homeostasis: from awareness of space to a sense of place. Nature reviews. Immunology 2009; 9:823-832.
[26] Boyman O, Letourneau S, Krieg C, Sprent J. Homeostatic proliferation and survival of naive and memory T cells. European journal of immunology 2009; 39:2088-2094.
[27] Bradley LM, Haynes L, Swain SL. IL-7: maintaining T-cell memory and achieving homeostasis. Trends in immunology 2005; 26:172-176.
[28] Burkett PR, Koka R, Chien M *et al.* IL-15R alpha expression on CD8+ T cells is dispensable for T cell memory. Proc Natl Acad Sci U S A 2003; 100:4724-4729.
[29] Sakaguchi S, Sakaguchi N, Shimizu J *et al.* Immunologic tolerance maintained by CD25+ CD4+ regulatory T cells: their common role in controlling autoimmunity, tumor immunity, and transplantation tolerance. Immunol Rev 2001; 182:18-32.
[30] Flynn KJ, Belz GT, Altman JD *et al.* Virus-specific CD8+ T cells in primary and secondary influenza pneumonia. Immunity 1998; 8:683-691.
[31] Blattman JN, Antia R, Sourdive DJ *et al.* Estimating the precursor frequency of naive antigen-specific CD8 T cells. J Exp Med 2002; 195:657-664.
[32] Jenkins MK, Khoruts A, Ingulli E *et al.* In vivo activation of antigen-specific CD4 T cells. Annu Rev Immunol 2001; 19:23-45.
[33] Takahama Y. Journey through the thymus: stromal guides for T-cell development and selection. Nature reviews. Immunology 2006; 6:127-135.
[34] Love PE, Bhandoola A. Signal integration and crosstalk during thymocyte migration and emigration. Nature reviews. Immunology 2011; 11:469-477.
[35] Shortman K, Wu L. Early T lymphocyte progenitors. Annual review of immunology 1996; 14:29-47.
[36] Allman D, Sambandam A, Kim S *et al.* Thymopoiesis independent of common lymphoid progenitors. Nature immunology 2003; 4:168-174.
[37] Sprent J, Kishimoto H, Cai Z *et al.* The thymus and T cell death. Advances in experimental medicine and biology 1996; 406:191-198.

[38] Boyman O, Purton JF, Surh CD, Sprent J. Cytokines and T-cell homeostasis. Current opinion in immunology 2007; 19:320-326.
[39] Michie AM, Zuniga-Pflucker JC. Regulation of thymocyte differentiation: pre-TCR signals and beta-selection. Seminars in immunology 2002; 14:311-323.
[40] Starr TK, Jameson SC, Hogquist KA. Positive and negative selection of T cells. Annual review of immunology 2003; 21:139-176.
[41] Carlson CM, Endrizzi BT, Wu J *et al.* Kruppel-like factor 2 regulates thymocyte and T-cell migration. Nature 2006; 442:299-302.
[42] Cyster JG, Schwab SR. Sphingosine-1-phosphate and lymphocyte egress from lymphoid organs. Annual review of immunology 2012; 30:69-94.
[43] den Braber I, Mugwagwa T, Vrisekoop N *et al.* Maintenance of peripheral naive T cells is sustained by thymus output in mice but not humans. Immunity 2012; 36:288-297.
[44] Bourgeois C, Hao Z, Rajewsky K *et al.* Ablation of thymic export causes accelerated decay of naive CD4 T cells in the periphery because of activation by environmental antigen. Proc Natl Acad Sci U S A 2008; 105:8691-8696.
[45] Mancebo E, Clemente J, Sanchez J *et al.* Longitudinal analysis of immune function in the first 3 years of life in thymectomized neonates during cardiac surgery. Clinical and experimental immunology 2008; 154:375-383.
[46] Sauce D, Larsen M, Fastenackels S *et al.* Evidence of premature immune aging in patients thymectomized during early childhood. J Clin Invest 2009; 119:3070-3078.
[47] Kovaiou RD, Weiskirchner I, Keller M *et al.* Age-related differences in phenotype and function of CD4+ T cells are due to a phenotypic shift from naive to memory effector CD4+ T cells. International immunology 2005; 17:1359-1366.
[48] Messaoudi I, Guevara Patino JA, Dyall R *et al.* Direct link between mhc polymorphism, T cell avidity, and diversity in immune defense. Science 2002; 298:1797-1800.
[49] Nikolich-Zugich J, Slifka MK, Messaoudi I. The many important facets of T-cell repertoire diversity. Nature reviews. Immunology 2004; 4:123-132.

[50] Rocha B, von Boehmer H. Peripheral selection of the T cell repertoire. Science 1991; 251:1225-1228.
[51] Mackall CL, Hakim FT, Gress RE. T-cell regeneration: all repertoires are not created equal. Immunology today 1997; 18:245-251.
[52] Ge Q, Rao VP, Cho BK *et al.* Dependence of lymphopenia-induced T cell proliferation on the abundance of peptide/ MHC epitopes and strength of their interaction with T cell receptors. Proc Natl Acad Sci U S A 2001; 98:1728-1733.
[53] Moses CT, Thorstenson KM, Jameson SC, Khoruts A. Competition for self ligands restrains homeostatic proliferation of naive CD4 T cells. Proc Natl Acad Sci U S A 2003; 100:1185-1190.
[54] Berzins SP, Boyd RL, Miller JF. The role of the thymus and recent thymic migrants in the maintenance of the adult peripheral lymphocyte pool. The Journal of experimental medicine 1998; 187:1839-1848.
[55] Tanchot C, Rocha B. Peripheral selection of T cell repertoires: the role of continuous thymus output. J Exp Med 1997; 186:1099-1106.
[56] Ahmed M, Lanzer KG, Yager EJ *et al.* Clonal expansions and loss of receptor diversity in the naive CD8 T cell repertoire of aged mice. J Immunol 2009; 182:784-792.
[57] Sakaguchi S, Sakaguchi N. Thymus and autoimmunity: capacity of the normal thymus to produce pathogenic self-reactive T cells and conditions required for their induction of autoimmune disease. J Exp Med 1990; 172:537-545.
[58] Smith H, Chen IM, Kubo R, Tung KS. Neonatal thymectomy results in a repertoire enriched in T cells deleted in adult thymus. Science 1989; 245:749-752.
[59] Lazuardi L, Jenewein B, Wolf AM *et al.* Age-related loss of naive T cells and dysregulation of T-cell/B-cell interactions in human lymph nodes. Immunology 2005; 114:37-43.
[60] Tough DF, Sprent J. Turnover of naive- and memory-phenotype T cells. J Exp Med 1994; 179:1127-1135.

[61] Tanchot C, Rocha B. The peripheral T cell repertoire: independent homeostatic regulation of virgin and activated CD8+ T cell pools. European journal of immunology 1995; 25:2127-2136.
[62] Tatari-Calderone Z, Stojakovic M, Dewan R *et al.* Age-related accumulation of T cells with markers of relatively stronger autoreactivity leads to functional erosion of T cells. BMC immunology 2012; 13:8.
[63] Patel HR, Miller RA. Age-associated changes in mitogen-induced protein phosphorylation in murine T lymphocytes. European journal of immunology 1992; 22:253-260.
[64] Saini A, Sei Y. Age-related impairment of early and late events of signal transduction in mouse immune cells. Life Sci 1993; 52:1759-1765.
[65] Youm YH, Kanneganti TD, Vandanmagsar B *et al.* The Nlrp3 inflammasome promotes age-related thymic demise and immunosenescence. Cell Rep 2012; 1:56-68.
[66] Vallejo AN, Michel JJ, Bale LK *et al.* Resistance to age-dependent thymic atrophy in long-lived mice that are deficient in pregnancy-associated plasma protein A. Proceedings of the National Academy of Sciences of the United States of America 2009; 106:11252-11257.
[67] Zhou T, Edwards CK, 3rd, Mountz JD. Prevention of age-related T cell apoptosis defect in CD2-fas-transgenic mice. The Journal of experimental medicine 1995; 182:129-137.
[68] Zlotoff DA, Bhandoola A. Hematopoietic progenitor migration to the adult thymus. Annals of the New York Academy of Sciences 2011; 1217:122-138.
[69] Donskoy E, Goldschneider I. Thymocytopoiesis is maintained by blood-borne precursors throughout postnatal life. A study in parabiotic mice. J Immunol 1992; 148:1604-1612.
[70] Osawa M, Hanada K, Hamada H, Nakauchi H. Long-term lymphohematopoietic reconstitution by a single CD34-low/negative hematopoietic stem cell. Science 1996; 273:242-245.
[71] Spangrude GJ, Heimfeld S, Weissman IL. Purification and characterization of mouse hematopoietic stem cells. Science 1988; 241:58-62.

[72] Adolfsson J, Borge OJ, Bryder D *et al.* Upregulation of Flt3 expression within the bone marrow Lin(-)Sca1(+)c-kit(+) stem cell compartment is accompanied by loss of self-renewal capacity. Immunity 2001; 15:659-669.
[73] Morrison SJ, Wandycz AM, Hemmati HD *et al.* Identification of a lineage of multipotent hematopoietic progenitors. Development 1997; 124:1929-1939.
[74] Adolfsson J, Mansson R, Buza-Vidas N *et al.* Identification of Flt3+ lympho-myeloid stem cells lacking erythro-megakaryocytic potential a revised road map for adult blood lineage commitment. Cell 2005; 121:295-306.
[75] Kondo M, Weissman IL, Akashi K. Identification of clonogenic common lymphoid progenitors in mouse bone marrow. Cell 1997; 91:661-672.
[76] Mansson R, Zandi S, Welinder E *et al.* Single-cell analysis of the common lymphoid progenitor compartment reveals functional and molecular heterogeneity. Blood 2010; 115:2601-2609.
[77] Zlotoff DA, Schwarz BA, Bhandoola A. The long road to the thymus: the generation, mobilization, and circulation of T-cell progenitors in mouse and man. Seminars in immunopathology 2008; 30:371-382.
[78] Luc S, Luis TC, Boukarabila H *et al.* The earliest thymic T cell progenitors sustain B cell and myeloid lineage potential. Nature immunology 2012; 13:412-419.
[79] Schwarz BA, Sambandam A, Maillard I *et al.* Selective thymus settling regulated by cytokine and chemokine receptors. J Immunol 2007; 178:2008-2017.
[80] Sumen C, Mempel TR, Mazo IB, von Andrian UH. Intravital microscopy: visualizing immunity in context. Immunity 2004; 21:315-329.
[81] Ceredig R, Bosco N, Rolink AG. The B lineage potential of thymus settling progenitors is critically dependent on mouse age. European journal of immunology 2007; 37:830-837.
[82] Scimone ML, Aifantis I, Apostolou I *et al.* A multistep adhesion cascade for lymphoid progenitor cell homing to the thymus. Proceedings of the National Academy of Sciences of the United States of America 2006; 103:7006-7011.

[83] Rossi FM, Corbel SY, Merzaban JS *et al.* Recruitment of adult thymic progenitors is regulated by P-selectin and its ligand PSGL-1. Nature immunology 2005; 6:626-634.
[84] Zlotoff DA, Sambandam A, Logan TD *et al.* CCR7 and CCR9 together recruit hematopoietic progenitors to the adult thymus. Blood 2010; 115:1897-1905.
[85] Miller JF. Immunological function of the thymus. Lancet 1961; 2:748-749.
[86] Steinmann GG. Changes in the human thymus during aging. Current topics in pathology. Ergebnisse der Pathologie 1986; 75:43-88.
[87] Linton PJ, Dorshkind K. Age-related changes in lymphocyte development and function. Nature immunology 2004; 5:133-139.
[88] Torroba M, Zapata AG. Aging of the vertebrate immune system. Microscopy research and technique 2003; 62:477-481.
[89] Dooley J, Liston A. Molecular control over thymic involution: from cytokines and microRNA to aging and adipose tissue. European journal of immunology 2012; 42:1073-1079.
[90] Sempowski GD, Gooding ME, Liao HX *et al.* T cell receptor excision circle assessment of thymopoiesis in aging mice. Molecular immunology 2002; 38:841-848.
[91] Douek DC, McFarland RD, Keiser PH *et al.* Changes in thymic function with age and during the treatment of HIV infection. Nature 1998; 396:690-695.
[92] Naylor K, Li G, Vallejo AN *et al.* The influence of age on T cell generation and TCR diversity. J Immunol 2005; 174:7446-7452.
[93] Goronzy JJ, Lee WW, Weyand CM. Aging and T-cell diversity. Experimental gerontology 2007; 42:400-406.
[94] Zediak VP, Maillard I, Bhandoola A. Multiple prethymic defects underlie age-related loss of T progenitor competence. Blood 2007; 110:1161-1167.
[95] Min H, Montecino-Rodriguez E, Dorshkind K. Reduction in the developmental potential of intrathymic T cell progenitors with age. J Immunol 2004; 173:245-250.

[96] Aw D, Taylor-Brown F, Cooper K, Palmer DB. Phenotypical and morphological changes in the thymic microenvironment from ageing mice. Biogerontology 2009; 10:311-322.
[97] Aw D, Silva AB, Maddick M *et al.* Architectural changes in the thymus of aging mice. Aging cell 2008; 7:158-167.
[98] Takeoka Y, Chen SY, Yago H *et al.* The murine thymic microenvironment: changes with age. International archives of allergy and immunology 1996; 111:5-12.
[99] Youm YH, Yang H, Sun Y *et al.* Deficient ghrelin receptor-mediated signaling compromises thymic stromal cell microenvironment by accelerating thymic adiposity. The Journal of biological chemistry 2009; 284:7068-7077.
[100] Gruver AL, Hudson LL, Sempowski GD. Immunosenescence of ageing. The Journal of pathology 2007; 211:144-156.
[101] Shanley DP, Aw D, Manley NR, Palmer DB. An evolutionary perspective on the mechanisms of immunosenescence. Trends in immunology 2009; 30:374-381.
[102] Gruver AL, Sempowski GD. Cytokines, leptin, and stress-induced thymic atrophy. Journal of leukocyte biology 2008; 84:915-923.
[103] Wang SD, Huang KJ, Lin YS, Lei HY. Sepsis-induced apoptosis of the thymocytes in mice. J Immunol 1994; 152:5014-5021.
[104] Savino W. The thymus is a common target organ in infectious diseases. PLoS pathogens 2006; 2:e62.
[105] Howard JK, Lord GM, Matarese G *et al.* Leptin protects mice from starvation-induced lymphoid atrophy and increases thymic cellularity in ob/ob mice. The Journal of clinical investigation 1999; 104:1051-1059.
[106] Kendall MD, Clarke AG. The thymus in the mouse changes its activity during pregnancy: a study of the microenvironment. Journal of anatomy 2000; 197 Pt 3:393-411.
[107] van den Brink MR, Alpdogan O, Boyd RL. Strategies to enhance T-cell reconstitution in immunocompromised patients. Nature reviews. Immunology 2004; 4:856-867.

[108] Storek J, Geddes M, Khan F *et al.* Reconstitution of the immune system after hematopoietic stem cell transplantation in humans. Seminars in immunopathology 2008; 30:425-437.
[109] Berger M, Figari O, Bruno B *et al.* Lymphocyte subsets recovery following allogeneic bone marrow transplantation (BMT): CD4+ cell count and transplant-related mortality. Bone marrow transplantation 2008; 41:55-62.
[110] Small TN, Papadopoulos EB, Boulad F *et al.* Comparison of immune reconstitution after unrelated and related T-cell-depleted bone marrow transplantation: effect of patient age and donor leukocyte infusions. Blood 1999; 93:467-480.
[111] Dudakov JA, Hanash AM, Jenq RR *et al.* Interleukin-22 drives endogenous thymic regeneration in mice. Science 2012; 336:91-95.
[112] Berzins SP, Uldrich AP, Sutherland JS *et al.* Thymic regeneration: teaching an old immune system new tricks. Trends in molecular medicine 2002; 8:469-476.
[113] Storek J, Zhao Z, Lin E *et al.* Recovery from and consequences of severe iatrogenic lymphopenia (induced to treat autoimmune diseases). Clinical immunology 2004; 113:285-298.
[114] Krieger M. Scavenger receptor class B type I is a multiligand HDL receptor that influences diverse physiologic systems. The Journal of clinical investigation 2001; 108:793-797.
[115] Mineo C, Shaul PW. Functions of scavenger receptor class B, type I in atherosclerosis. Current opinion in lipidology 2012; 23:487-493.
[116] Neculai D, Schwake M, Ravichandran M *et al.* Structure of LIMP-2 provides functional insights with implications for SR-BI and CD36. Nature 2013; 504:172-176.
[117] Webb NR, Connell PM, Graf GA *et al.* SR-BII, an isoform of the scavenger receptor BI containing an alternate cytoplasmic tail, mediates lipid transfer between high density lipoprotein and cells. The Journal of biological chemistry 1998; 273:15241-15248.

[118] Greaves DR, Gordon S. The macrophage scavenger receptor at 30 years of age: current knowledge and future challenges. Journal of lipid research 2009; 50 Suppl:S282-286.
[119] Stephen SL, Freestone K, Dunn S *et al.* Scavenger receptors and their potential as therapeutic targets in the treatment of cardiovascular disease. International journal of hypertension 2010; 2010:646929.
[120] Canton J, Neculai D, Grinstein S. Scavenger receptors in homeostasis and immunity. Nature reviews. Immunology 2013; 13:621-634.
[121] Areschoug T, Gordon S. Scavenger receptors: role in innate immunity and microbial pathogenesis. Cellular microbiology 2009; 11:1160-1169.
[122] Acton SL, Scherer PE, Lodish HF, Krieger M. Expression cloning of SR-BI, a CD36-related class B scavenger receptor. The Journal of biological chemistry 1994; 269:21003-21009.
[123] Rigotti A, Acton SL, Krieger M. The class B scavenger receptors SR-BI and CD36 are receptors for anionic phospholipids. The Journal of biological chemistry 1995; 270:16221-16224.
[124] Murao K, Terpstra V, Green SR *et al.* Characterization of CLA-1, a human homologue of rodent scavenger receptor BI, as a receptor for high density lipoprotein and apoptotic thymocytes. The Journal of biological chemistry 1997; 272:17551-17557.
[125] Acton S, Rigotti A, Landschulz KT *et al.* Identification of scavenger receptor SR-BI as a high density lipoprotein receptor. Science 1996; 271:518-520.
[126] Vishnyakova TG, Bocharov AV, Baranova IN *et al.* Binding and internalization of lipopolysaccharide by Cla-1, a human orthologue of rodent scavenger receptor B1. The Journal of biological chemistry 2003; 278:22771-22780.
[127] Vishnyakova TG, Kurlander R, Bocharov AV *et al.* CLA-1 and its splicing variant CLA-2 mediate bacterial adhesion and cytosolic bacterial invasion in mammalian cells. Proceedings of the National Academy of Sciences of the United States of America 2006; 103:16888-16893.

[128] Scarselli E, Ansuini H, Cerino R *et al.* The human scavenger receptor class B type I is a novel candidate receptor for the hepatitis C virus. The EMBO journal 2002; 21:5017-5025.
[129] Landschulz KT, Pathak RK, Rigotti A *et al.* Regulation of scavenger receptor, class B, type I, a high density lipoprotein receptor, in liver and steroidogenic tissues of the rat. The Journal of clinical investigation 1996; 98:984-995.
[130] Cao G, Garcia CK, Wyne KL *et al.* Structure and localization of the human gene encoding SR-BI/CLA-1. Evidence for transcriptional control by steroidogenic factor 1. The Journal of biological chemistry 1997; 272:33068-33076.
[131] Uittenbogaard A, Shaul PW, Yuhanna IS *et al.* High density lipoprotein prevents oxidized low density lipoprotein-induced inhibition of endothelial nitric-oxide synthase localization and activation in caveolae. The Journal of biological chemistry 2000; 275:11278-11283.
[132] Duncan KG, Bailey KR, Kane JP, Schwartz DM. Human retinal pigment epithelial cells express scavenger receptors BI and BII. Biochemical and biophysical research communications 2002; 292:1017-1022.
[133] Buechler C, Ritter M, Quoc CD *et al.* Lipopolysaccharide inhibits the expression of the scavenger receptor Cla-1 in human monocytes and macrophages. Biochemical and biophysical research communications 1999; 262:251-254.
[134] Feng H, Guo L, Wang D *et al.* Deficiency of scavenger receptor BI leads to impaired lymphocyte homeostasis and autoimmune disorders in mice. Arteriosclerosis, thrombosis, and vascular biology 2011; 31:2543-2551.
[135] Zheng Z, Ai J, Li XA. Scavenger receptor class B type I and immune dysfunctions. Current opinion in endocrinology, diabetes, and obesity 2014; 21:121-128.
[136] Eisenberg S. High density lipoprotein metabolism. Journal of lipid research 1984; 25:1017-1058.

[137] Schaefer EJ, Foster DM, Jenkins LL *et al.* The composition and metabolism of high density lipoprotein subfractions. Lipids 1979; 14:511-522.
[138] Feng H, Li XA. Dysfunctional high-density lipoprotein. Current opinion in endocrinology, diabetes, and obesity 2009; 16:156-162.
[139] Zhu X, Parks JS. New roles of HDL in inflammation and hematopoiesis. Annual review of nutrition 2012; 32:161-182.
[140] Gordon T, Castelli WP, Hjortland MC *et al.* High density lipoprotein as a protective factor against coronary heart disease. The Framingham Study. The American journal of medicine 1977; 62:707-714.
[141] Castelli WP, Doyle JT, Gordon T *et al.* HDL cholesterol and other lipids in coronary heart disease. The cooperative lipoprotein phenotyping study. Circulation 1977; 55:767-772.
[142] Spady DK. Reverse cholesterol transport and atherosclerosis regression. Circulation 1999; 100:576-578.
[143] Fisher EA, Feig JE, Hewing B *et al.* High-density lipoprotein function, dysfunction, and reverse cholesterol transport. Arteriosclerosis, thrombosis, and vascular biology 2012; 32:2813-2820.
[144] De Nardo D, Labzin LI, Kono H *et al.* High-density lipoprotein mediates anti-inflammatory reprogramming of macrophages via the transcriptional regulator ATF3. Nature immunology 2014; 15:152-160.
[145] Poston RN, Haskard DO, Coucher JR *et al.* Expression of intercellular adhesion molecule-1 in atherosclerotic plaques. The American journal of pathology 1992; 140:665-673.
[146] Ansell BJ, Navab M, Hama S *et al.* Inflammatory/antiinflammatory properties of high-density lipoprotein distinguish patients from control subjects better than high-density lipoprotein cholesterol levels and are favorably affected by simvastatin treatment. Circulation 2003; 108:2751-2756.
[147] Parthasarathy S, Barnett J, Fong LG. High-density lipoprotein inhibits the oxidative modification of low-density lipoprotein. Biochimica et biophysica acta 1990; 1044:275-283.

[148] Barter PJ, Nicholls S, Rye KA *et al.* Antiinflammatory properties of HDL. Circulation research 2004; 95:764-772.
[149] Silver DL, Jiang XC, Arai T *et al.* Receptors and lipid transfer proteins in HDL metabolism. Annals of the New York Academy of Sciences 2000; 902:103-111; discussion 111-102.
[150] Fielding CJ, Fielding PE. Molecular physiology of reverse cholesterol transport. Journal of lipid research 1995; 36:211-228.
[151] von Eckardstein A, Nofer JR, Assmann G. High density lipoproteins and arteriosclerosis. Role of cholesterol efflux and reverse cholesterol transport. Arteriosclerosis, thrombosis, and vascular biology 2001; 21:13-27.
[152] Yaguchi H, Tsutsumi K, Shimono K *et al.* Involvement of high density lipoprotein as substrate cholesterol for steroidogenesis by bovine adrenal fasciculo-reticularis cells. Life sciences 1998; 62:1387-1395.
[153] Azhar S, Tsai L, Medicherla S *et al.* Human granulosa cells use high density lipoprotein cholesterol for steroidogenesis. The Journal of clinical endocrinology and metabolism 1998; 83:983-991.
[154] Bochem AE, Holleboom AG, Romijn JA *et al.* High density lipoprotein as a source of cholesterol for adrenal steroidogenesis: a study in individuals with low plasma HDL-C. Journal of lipid research 2013; 54:1698-1704.
[155] Kozarsky KF, Donahee MH, Rigotti A *et al.* Overexpression of the HDL receptor SR-BI alters plasma HDL and bile cholesterol levels. Nature 1997; 387:414-417.
[156] Rigotti A, Trigatti BL, Penman M *et al.* A targeted mutation in the murine gene encoding the high density lipoprotein (HDL) receptor scavenger receptor class B type I reveals its key role in HDL metabolism. Proceedings of the National Academy of Sciences of the United States of America 1997; 94:12610-12615.
[157] Vergeer M, Korporaal SJ, Franssen R *et al.* Genetic variant of the scavenger receptor BI in humans. N Engl J Med 2011; 364:136-145.

[158] Brunham LR, Tietjen I, Bochem AE *et al.* Novel mutations in scavenger receptor BI associated with high HDL cholesterol in humans. Clinical genetics 2011; 79:575-581.
[159] Rhainds D, Brissette L. The role of scavenger receptor class B type I (SR-BI) in lipid trafficking. defining the rules for lipid traders. The international journal of biochemistry & cell biology 2004; 36:39-77.
[160] Hoekstra M, Van Berkel TJ, Van Eck M. Scavenger receptor BI: a multi-purpose player in cholesterol and steroid metabolism. World J Gastroenterol 2010; 16:5916-5924.
[161] Temel RE, Trigatti B, DeMattos RB *et al.* Scavenger receptor class B, type I (SR-BI) is the major route for the delivery of high density lipoprotein cholesterol to the steroidogenic pathway in cultured mouse adrenocortical cells. Proc Natl Acad Sci U S A 1997; 94:13600-13605.
[162] Out R, Hoekstra M, Spijkers JA *et al.* Scavenger receptor class B type I is solely responsible for the selective uptake of cholesteryl esters from HDL by the liver and the adrenals in mice. Journal of lipid research 2004; 45:2088-2095.
[163] Brundert M, Ewert A, Heeren J *et al.* Scavenger receptor class B type I mediates the selective uptake of high-density lipoprotein-associated cholesteryl ester by the liver in mice. Arteriosclerosis, thrombosis, and vascular biology 2005; 25:143-148.
[164] Trigatti BL, Krieger M, Rigotti A. Influence of the HDL receptor SR-BI on lipoprotein metabolism and atherosclerosis. Arteriosclerosis, thrombosis, and vascular biology 2003; 23:1732-1738.
[165] Meyer JM, Graf GA, van der Westhuyzen DR. New developments in selective cholesteryl ester uptake. Current opinion in lipidology 2013.
[166] Wang N, Arai T, Ji Y *et al.* Liver-specific overexpression of scavenger receptor BI decreases levels of very low density lipoprotein ApoB, low density lipoprotein ApoB, and high density lipoprotein in transgenic mice. The Journal of biological chemistry 1998; 273:32920-32926.
[167] Zhang Y, Da Silva JR, Reilly M *et al.* Hepatic expression of scavenger receptor class B type I (SR-BI) is a positive regulator of macrophage reverse

cholesterol transport in vivo. The Journal of clinical investigation 2005; 115:2870-2874.
[168] Stylianou IM, Svenson KL, VanOrman SK *et al.* Novel ENU-induced point mutation in scavenger receptor class B, member 1, results in liver specific loss of SCARB1 protein. PloS one 2009; 4:e6521.
[169] Huby T, Doucet C, Dachet C *et al.* Knockdown expression and hepatic deficiency reveal an atheroprotective role for SR-BI in liver and peripheral tissues. The Journal of clinical investigation 2006; 116:2767-2776.
[170] Varban ML, Rinninger F, Wang N *et al.* Targeted mutation reveals a central role for SR-BI in hepatic selective uptake of high density lipoprotein cholesterol. Proc Natl Acad Sci U S A 1998; 95:4619-4624.
[171] Hoekstra M, van der Sluis RJ, Van Eck M, Van Berkel TJ. Adrenal-specific scavenger receptor BI deficiency induces glucocorticoid insufficiency and lowers plasma very-low-density and low-density lipoprotein levels in mice. Arteriosclerosis, thrombosis, and vascular biology 2013; 33:e39-46.
[172] Rohrer L, Cavelier C, Fuchs S *et al.* Binding, internalization and transport of apolipoprotein A-I by vascular endothelial cells. Biochimica et biophysica acta 2006; 1761:186-194.
[173] Rohrer L, Ohnsorg PM, Lehner M *et al.* High-density lipoprotein transport through aortic endothelial cells involves scavenger receptor BI and ATP-binding cassette transporter G1. Circulation research 2009; 104:1142-1150.
[174] Lim HY, Thiam CH, Yeo KP *et al.* Lymphatic vessels are essential for the removal of cholesterol from peripheral tissues by SR-BI-mediated transport of HDL. Cell metabolism 2013; 17:671-684.
[175] Martel C, Li W, Fulp B *et al.* Lymphatic vasculature mediates macrophage reverse cholesterol transport in mice. The Journal of clinical investigation 2013; 123:1571-1579.
[176] Ji Y, Jian B, Wang N *et al.* Scavenger receptor BI promotes high density lipoprotein-mediated cellular cholesterol efflux. The Journal of biological chemistry 1997; 272:20982-20985.

[177] Jian B, de la Llera-Moya M, Ji Y *et al.* Scavenger receptor class B type I as a mediator of cellular cholesterol efflux to lipoproteins and phospholipid acceptors. The Journal of biological chemistry 1998; 273:5599-5606.
[178] Van Eck M, Bos IS, Hildebrand RB *et al.* Dual role for scavenger receptor class B, type I on bone marrow-derived cells in atherosclerotic lesion development. Am J Pathol 2004; 165:785-794.
[179] Wang X, Collins HL, Ranalletta M *et al.* Macrophage ABCA1 and ABCG1, but not SR-BI, promote macrophage reverse cholesterol transport in vivo. The Journal of clinical investigation 2007; 117:2216-2224.
[180] Ueda Y, Gong E, Royer L *et al.* Relationship between expression levels and atherogenesis in scavenger receptor class B, type I transgenics. The Journal of biological chemistry 2000; 275:20368-20373.
[181] Huszar D, Varban ML, Rinninger F *et al.* Increased LDL cholesterol and atherosclerosis in LDL receptor-deficient mice with attenuated expression of scavenger receptor B1. Arteriosclerosis, thrombosis, and vascular biology 2000; 20:1068-1073.
[182] Covey SD, Krieger M, Wang W *et al.* Scavenger receptor class B type I-mediated protection against atherosclerosis in LDL receptor-negative mice involves its expression in bone marrow-derived cells. Arteriosclerosis, thrombosis, and vascular biology 2003; 23:1589-1594.
[183] Braun A, Trigatti BL, Post MJ *et al.* Loss of SR-BI expression leads to the early onset of occlusive atherosclerotic coronary artery disease, spontaneous myocardial infarctions, severe cardiac dysfunction, and premature death in apolipoprotein E-deficient mice. Circulation research 2002; 90:270-276.
[184] Kozarsky KF, Donahee MH, Glick JM *et al.* Gene transfer and hepatic overexpression of the HDL receptor SR-BI reduces atherosclerosis in the cholesterol-fed LDL receptor-deficient mouse. Arteriosclerosis, thrombosis, and vascular biology 2000; 20:721-727.
[185] Arai T, Wang N, Bezouevski M *et al.* Decreased atherosclerosis in heterozygous low density lipoprotein receptor-deficient mice expressing the

scavenger receptor BI transgene. The Journal of biological chemistry 1999; 274:2366-2371.
[186] El Bouhassani M, Gilibert S, Moreau M *et al.* Cholesteryl ester transfer protein expression partially attenuates the adverse effects of SR-BI receptor deficiency on cholesterol metabolism and atherosclerosis. The Journal of biological chemistry 2011; 286:17227-17238.
[187] Picataggi A, Lim GF, Kent AP *et al.* A coding variant in SR-BI (I179N) significantly increases atherosclerosis in mice. Mammalian genome : official journal of the International Mammalian Genome Society 2013.
[188] Zhang W, Yancey PG, Su YR *et al.* Inactivation of macrophage scavenger receptor class B type I promotes atherosclerotic lesion development in apolipoprotein E-deficient mice. Circulation 2003; 108:2258-2263.
[189] Pei Y, Chen X, Aboutouk D *et al.* SR-BI in Bone Marrow Derived Cells Protects Mice from Diet Induced Coronary Artery Atherosclerosis and Myocardial Infarction. PLoS One 2013; 8:e72492.
[190] Zhao Y, Pennings M, Hildebrand RB *et al.* Enhanced foam cell formation, atherosclerotic lesion development, and inflammation by combined deletion of ABCA1 and SR-BI in Bone marrow-derived cells in LDL receptor knockout mice on western-type diet. Circ Res 2010; 107:e20-31.
[191] Yancey PG, Jerome WG, Yu H *et al.* Severely altered cholesterol homeostasis in macrophages lacking apoE and SR-BI. Journal of lipid research 2007; 48:1140-1149.
[192] Cai L, Wang Z, Meyer JM *et al.* Macrophage SR-BI regulates LPS-induced pro-inflammatory signaling in mice and isolated macrophages. J Lipid Res 2012; 53:1472-1481.
[193] Zhao Y, Pennings M, Vrins CL *et al.* Hypocholesterolemia, foam cell accumulation, but no atherosclerosis in mice lacking ABC-transporter A1 and scavenger receptor BI. Atherosclerosis 2011; 218:314-322.
[194] Van Eck M, Hoekstra M, Hildebrand RB *et al.* Increased oxidative stress in scavenger receptor BI knockout mice with dysfunctional HDL. Arterioscler Thromb Vasc Biol 2007; 27:2413-2419.

[195] Aharoni S, Aviram M, Fuhrman B. Paraoxonase 1 (PON1) reduces macrophage inflammatory responses. Atherosclerosis 2013; 228:353-361.
[196] Seetharam D, Mineo C, Gormley AK *et al.* High-density lipoprotein promotes endothelial cell migration and reendothelialization via scavenger receptor-B type I. Circulation research 2006; 98:63-72.
[197] Yuhanna IS, Zhu Y, Cox BE *et al.* High-density lipoprotein binding to scavenger receptor-BI activates endothelial nitric oxide synthase. Nature medicine 2001; 7:853-857.
[198] Li XA, Titlow WB, Jackson BA *et al.* High density lipoprotein binding to scavenger receptor, Class B, type I activates endothelial nitric-oxide synthase in a ceramide-dependent manner. The Journal of biological chemistry 2002; 277:11058-11063.
[199] Azhar S, Stewart D, Reaven E. Utilization of cholesterol-rich lipoproteins by perfused rat adrenals. J Lipid Res 1989; 30:1799-1810.
[200] Azhar S, Leers-Sucheta S, Reaven E. Cholesterol uptake in adrenal and gonadal tissues: the SR-BI and 'selective' pathway connection. Front Biosci 2003; 8:s998-1029.
[201] Connelly MA, Kellner-Weibel G, Rothblat GH, Williams DL. SR-BI-directed HDL-cholesteryl ester hydrolysis. J Lipid Res 2003; 44:331-341.
[202] Connelly MA, Williams DL. SR-BI and HDL cholesteryl ester metabolism. Endocr Res 2004; 30:697-703.
[203] Borkowski AJ, Levin S, Delcroix C *et al.* Blood cholesterol and hydrocortisone production in man: quantitative aspects of the utilization of circulating cholesterol by the adrenals at rest and under adrenocorticotropin stimulation. J Clin Invest 1967; 46:797-811.
[204] Brown MS, Goldstein JL. A receptor-mediated pathway for cholesterol homeostasis. Science 1986; 232:34-47.
[205] Rigotti A, Miettinen HE, Krieger M. The role of the high-density lipoprotein receptor SR-BI in the lipid metabolism of endocrine and other tissues. Endocrine reviews 2003; 24:357-387.

[206] Cai L, Ji A, de Beer FC *et al.* SR-BI protects against endotoxemia in mice through its roles in glucocorticoid production and hepatic clearance. The Journal of clinical investigation 2008; 118:364-375.
[207] Guo L, Song Z, Li M *et al.* Scavenger Receptor BI Protects against Septic Death through Its Role in Modulating Inflammatory Response. The Journal of biological chemistry 2009; 284:19826-19834.
[208] Hoekstra M, Meurs I, Koenders M *et al.* Absence of HDL cholesteryl ester uptake in mice via SR-BI impairs an adequate adrenal glucocorticoid-mediated stress response to fasting. J Lipid Res 2008; 49:738-745.
[209] Trigatti B, Rayburn H, Vinals M *et al.* Influence of the high density lipoprotein receptor SR-BI on reproductive and cardiovascular pathophysiology. Proceedings of the National Academy of Sciences of the United States of America 1999; 96:9322-9327.
[210] Miettinen HE, Rayburn H, Krieger M. Abnormal lipoprotein metabolism and reversible female infertility in HDL receptor (SR-BI)-deficient mice. J Clin Invest 2001; 108:1717-1722.
[211] Yesilaltay A, Morales MG, Amigo L *et al.* Effects of hepatic expression of the high-density lipoprotein receptor SR-BI on lipoprotein metabolism and female fertility. Endocrinology 2006; 147:1577-1588.
[212] Holm TM, Braun A, Trigatti BL *et al.* Failure of red blood cell maturation in mice with defects in the high-density lipoprotein receptor SR-BI. Blood 2002; 99:1817-1824.
[213] Meurs I, Hoekstra M, van Wanrooij EJ *et al.* HDL cholesterol levels are an important factor for determining the lifespan of erythrocytes. Exp Hematol 2005; 33:1309-1319.
[214] Dole VS, Matuskova J, Vasile E *et al.* Thrombocytopenia and platelet abnormalities in high-density lipoprotein receptor-deficient mice. Arteriosclerosis, thrombosis, and vascular biology 2008; 28:1111-1116.
[215] Valiyaveettil M, Kar N, Ashraf MZ *et al.* Oxidized high-density lipoprotein inhibits platelet activation and aggregation via scavenger receptor BI. Blood 2008; 111:1962-1971.

[216] Korporaal SJ, Meurs I, Hauer AD *et al.* Deletion of the high-density lipoprotein receptor scavenger receptor BI in mice modulates thrombosis susceptibility and indirectly affects platelet function by elevation of plasma free cholesterol. Arterioscler Thromb Vasc Biol 2011; 31:34-42.
[217] Korporaal SJA, Meurs I, Hauer AD *et al.* Deletion of the High-Density Lipoprotein Receptor Scavenger Receptor BI in Mice Modulates Thrombosis Susceptibility and Indirectly Affects Platelet Function by Elevation of Plasma Free Cholesterol. Arterioscl Throm Vas 2011; 31:34-+.
[218] Li XA, Guo L, Asmis R *et al.* Scavenger receptor BI prevents nitric oxide-induced cytotoxicity and endotoxin-induced death. Circulation research 2006; 98:e60-65.
[219] Azhar S, Reaven E. Scavenger receptor class BI and selective cholesteryl ester uptake: partners in the regulation of steroidogenesis. Molecular and cellular endocrinology 2002; 195:1-26.
[220] Guo L, Chen M, Song Z *et al.* C323 of SR-BI is required for SR-BI-mediated HDL binding and cholesteryl ester uptake. Journal of lipid research 2011; 52:2272-2278.
[221] Guo L, Zheng Z, Ai J *et al.* Hepatic scavenger receptor BI protects against polymicrobial-induced sepsis through promoting LPS clearance in mice. The Journal of biological chemistry 2014.
[222] Burlone ME, Budkowska A. Hepatitis C virus cell entry: role of lipoproteins and cellular receptors. The Journal of general virology 2009; 90:1055-1070.
[223] Bartosch B, Vitelli A, Granier C *et al.* Cell entry of hepatitis C virus requires a set of co-receptors that include the CD81 tetraspanin and the SR-B1 scavenger receptor. The Journal of biological chemistry 2003; 278:41624-41630.
[224] Zeisel MB, Koutsoudakis G, Schnober EK *et al.* Scavenger receptor class B type I is a key host factor for hepatitis C virus infection required for an entry step closely linked to CD81. Hepatology 2007; 46:1722-1731.
[225] Catanese MT, Graziani R, von Hahn T *et al.* High-avidity monoclonal antibodies against the human scavenger class B type I receptor efficiently block

hepatitis C virus infection in the presence of high-density lipoprotein. Journal of virology 2007; 81:8063-8071.
[226] Grove J, Huby T, Stamataki Z *et al.* Scavenger receptor BI and BII expression levels modulate hepatitis C virus infectivity. Journal of virology 2007; 81:3162-3169.
[227] Lavillette D, Tarr AW, Voisset C *et al.* Characterization of host-range and cell entry properties of the major genotypes and subtypes of hepatitis C virus. Hepatology 2005; 41:265-274.
[228] Dorner M, Horwitz JA, Robbins JB *et al.* A genetically humanized mouse model for hepatitis C virus infection. Nature 2011; 474:208-211.
[229] Lacek K, Vercauteren K, Grzyb K *et al.* Novel human SR-BI antibodies prevent infection and dissemination of HCV in vitro and in humanized mice. Journal of hepatology 2012.
[230] Meuleman P, Catanese MT, Verhoye L *et al.* A human monoclonal antibody targeting scavenger receptor class B type I precludes hepatitis C virus infection and viral spread in vitro and in vivo. Hepatology 2012; 55:364-372.
[231] Rice CM. New insights into HCV replication: potential antiviral targets. Topics in antiviral medicine 2011; 19:117-120.
[232] Dreux M, Pietschmann T, Granier C *et al.* High density lipoprotein inhibits hepatitis C virus-neutralizing antibodies by stimulating cell entry via activation of the scavenger receptor BI. The Journal of biological chemistry 2006; 281:18285-18295.
[233] Voisset C, Callens N, Blanchard E *et al.* High density lipoproteins facilitate hepatitis C virus entry through the scavenger receptor class B type I. The Journal of biological chemistry 2005; 280:7793-7799.
[234] von Hahn T, Lindenbach BD, Boullier A *et al.* Oxidized low-density lipoprotein inhibits hepatitis C virus cell entry in human hepatoma cells. Hepatology 2006; 43:932-942.
[235] Maillard P, Huby T, Andreo U *et al.* The interaction of natural hepatitis C virus with human scavenger receptor SR-BI/Cla1 is mediated by ApoB-containing

lipoproteins. FASEB journal : official publication of the Federation of American Societies for Experimental Biology 2006; 20:735-737.
[236] Catanese MT, Ansuini H, Graziani R *et al.* Role of scavenger receptor class B type I in hepatitis C virus entry: kinetics and molecular determinants. Journal of virology 2010; 84:34-43.
[237] Barth H, Schnober EK, Neumann-Haefelin C *et al.* Scavenger receptor class B is required for hepatitis C virus uptake and cross-presentation by human dendritic cells. Journal of virology 2008; 82:3466-3479.
[238] Sorci-Thomas MG, Thomas MJ. High density lipoprotein biogenesis, cholesterol efflux, and immune cell function. Arteriosclerosis, thrombosis, and vascular biology 2012; 32:2561-2565.
[239] Wilhelm AJ, Zabalawi M, Grayson JM *et al.* Apolipoprotein A-I and its role in lymphocyte cholesterol homeostasis and autoimmunity. Arteriosclerosis, thrombosis, and vascular biology 2009; 29:843-849.
[240] Wilhelm AJ, Zabalawi M, Owen JS *et al.* Apolipoprotein A-I modulates regulatory T cells in autoimmune LDLr-/-, ApoA-I-/- mice. The Journal of biological chemistry 2010; 285:36158-36169.
[241] Armstrong AJ, Gebre AK, Parks JS, Hedrick CC. ATP-binding cassette transporter G1 negatively regulates thymocyte and peripheral lymphocyte proliferation. J Immunol 2010; 184:173-183.
[242] Bensinger SJ, Bradley MN, Joseph SB *et al.* LXR signaling couples sterol metabolism to proliferation in the acquired immune response. Cell 2008; 134:97-111.
[243] Plump AS, Azrolan N, Odaka H *et al.* ApoA-I knockout mice: characterization of HDL metabolism in homozygotes and identification of a post-RNA mechanism of apoA-I up-regulation in heterozygotes. J Lipid Res 1997; 38:1033-1047.
[244] Wang N, Lan D, Chen W *et al.* ATP-binding cassette transporters G1 and G4 mediate cellular cholesterol efflux to high-density lipoproteins. Proceedings of the National Academy of Sciences of the United States of America 2004; 101:9774-9779.

[245] Kennedy MA, Barrera GC, Nakamura K *et al.* ABCG1 has a critical role in mediating cholesterol efflux to HDL and preventing cellular lipid accumulation. Cell metabolism 2005; 1:121-131.
[246] Brundert M, Heeren J, Bahar-Bayansar M *et al.* Selective uptake of HDL cholesteryl esters and cholesterol efflux from mouse peritoneal macrophages independent of SR-BI. Journal of lipid research 2006; 47:2408-2421.
[247] Guo L, Zheng Z, Ai J *et al.* Scavenger Receptor BI and High-Density Lipoprotein Regulate Thymocyte Apoptosis in Sepsis. Arterioscler Thromb Vasc Biol 2014.
[248] Yvan-Charvet L, Pagler T, Gautier EL *et al.* ATP-binding cassette transporters and HDL suppress hematopoietic stem cell proliferation. Science 2010; 328:1689-1693.
[249] Van Eck M, Twisk J, Hoekstra M *et al.* Differential effects of scavenger receptor BI deficiency on lipid metabolism in cells of the arterial wall and in the liver. The Journal of biological chemistry 2003; 278:23699-23705.
[250] Gratzner HG, Leif RC. An immunofluorescence method for monitoring DNA synthesis by flow cytometry. Cytometry 1981; 1:385-393.
[251] Mehta BA, Maino VC. Simultaneous detection of DNA synthesis and cytokine production in staphylococcal enterotoxin B activated CD4+ T lymphocytes by flow cytometry. Journal of immunological methods 1997; 208:49-59.
[252] von Boehmer H, Hafen K. The life span of naive alpha/beta T cells in secondary lymphoid organs. J Exp Med 1993; 177:891-896.
[253] Whitman SC, Rateri DL, Szilvassy SJ *et al.* Depletion of natural killer cell function decreases atherosclerosis in low-density lipoprotein receptor null mice. Arterioscler Thromb Vasc Biol 2004; 24:1049-1054.
[254] Cassis LA, Rateri DL, Lu H, Daugherty A. Bone marrow transplantation reveals that recipient AT1a receptors are required to initiate angiotensin II-induced atherosclerosis and aneurysms. Arteriosclerosis, thrombosis, and vascular biology 2007; 27:380-386.

[255] Gossens K, Naus S, Corbel SY *et al.* Thymic progenitor homing and lymphocyte homeostasis are linked via S1P-controlled expression of thymic P-selectin/CCL25. The Journal of experimental medicine 2009; 206:761-778.
[256] Kenins L, Gill JW, Boyd RL *et al.* Intrathymic expression of Flt3 ligand enhances thymic recovery after irradiation. The Journal of experimental medicine 2008; 205:523-531.
[257] Alpdogan O, Hubbard VM, Smith OM *et al.* Keratinocyte growth factor (KGF) is required for postnatal thymic regeneration. Blood 2006; 107:2453-2460.
[258] Escola-Gil JC, Marzal-Casacuberta A, Julve-Gil J *et al.* Human apolipoprotein A-II is a pro-atherogenic molecule when it is expressed in transgenic mice at a level similar to that in humans: evidence of a potentially relevant species-specific interaction with diet. J Lipid Res 1998; 39:457-462.
[259] Nong Z, Gonzalez-Navarro H, Amar M *et al.* Hepatic lipase expression in macrophages contributes to atherosclerosis in apoE-deficient and LCAT-transgenic mice. J Clin Invest 2003; 112:367-378.
[260] Franceschini G, Sirtori M, Vaccarino V *et al.* Mechanisms of HDL reduction after probucol. Changes in HDL subfractions and increased reverse cholesteryl ester transfer. Arteriosclerosis 1989; 9:462-469.
[261] Yamashita S, Matsuzawa Y. Where are we with probucol: a new life for an old drug? Atherosclerosis 2009; 207:16-23.
[262] Braun A, Zhang S, Miettinen HE *et al.* Probucol prevents early coronary heart disease and death in the high-density lipoprotein receptor SR-BI/apolipoprotein E double knockout mouse. Proceedings of the National Academy of Sciences of the United States of America 2003; 100:7283-7288.
[263] Karpac J, Ostwald D, Bui S *et al.* Development, maintenance, and function of the adrenal gland in early postnatal proopiomelanocortin-null mutant mice. Endocrinology 2005; 146:2555-2562.
[264] Negoescu A, Lorimier P, Labat-Moleur F *et al.* In situ apoptotic cell labeling by the TUNEL method: improvement and evaluation on cell preparations. J Histochem Cytochem 1996; 44:959-968.

[265] Grasl-Kraupp B, Ruttkay-Nedecky B, Koudelka H *et al.* In situ detection of fragmented DNA (TUNEL assay) fails to discriminate among apoptosis, necrosis, and autolytic cell death: a cautionary note. Hepatology 1995; 21:1465-1468.
[266] Muller CP, Stephany DA, Winkler DF *et al.* Filipin as a flow microfluorometry probe for cellular cholesterol. Cytometry 1984; 5:42-54.
[267] Hassall DG, Graham A. Changes in free cholesterol content, measured by filipin fluorescence and flow cytometry, correlate with changes in cholesterol biosynthesis in THP-1 macrophages. Cytometry 1995; 21:352-362.
[268] Hazenberg MD, Verschuren MC, Hamann D *et al.* T cell receptor excision circles as markers for recent thymic emigrants: basic aspects, technical approach, and guidelines for interpretation. J Mol Med (Berl) 2001; 79:631-640.
[269] Broers AE, Meijerink JP, van Dongen JJ *et al.* Quantification of newly developed T cells in mice by real-time quantitative PCR of T-cell receptor rearrangement excision circles. Experimental hematology 2002; 30:745-750.
[270] Weston SA, Parish CR. New fluorescent dyes for lymphocyte migration studies. Analysis by flow cytometry and fluorescence microscopy. Journal of immunological methods 1990; 133:87-97.
[271] Lowry OH, Rosebrough NJ, Farr AL, Randall RJ. Protein measurement with the Folin phenol reagent. The Journal of biological chemistry 1951; 193:265-275.
[272] Gui J, Mustachio LM, Su DM, Craig RW. Thymus Size and Age-related Thymic Involution: Early Programming, Sexual Dimorphism, Progenitors and Stroma. Aging and disease 2012; 3:280-290.
[273] Ackman JB, Kovacina B, Carter BW *et al.* Sex difference in normal thymic appearance in adults 20-30 years of age. Radiology 2013; 268:245-253.
[274] Hale JS, Boursalian TE, Turk GL, Fink PJ. Thymic output in aged mice. Proc Natl Acad Sci U S A 2006; 103:8447-8452.
[275] Mackall CL, Gress RE. Thymic aging and T-cell regeneration. Immunol Rev 1997; 160:91-102.
[276] Bosco N, Swee LK, Benard A *et al.* Auto-reconstitution of the T-cell compartment by radioresistant hematopoietic cells following lethal irradiation and bone marrow transplantation. Experimental hematology 2010; 38:222-232 e222.

[277] Zlotoff DA, Zhang SL, De Obaldia ME *et al.* Delivery of progenitors to the thymus limits T-lineage reconstitution after bone marrow transplantation. Blood 2011; 118:1962-1970.
[278] Xing Y, Jameson SC, Hogquist KA. Thymoproteasome subunit-beta5T generates peptide-MHC complexes specialized for positive selection. Proceedings of the National Academy of Sciences of the United States of America 2013; 110:6979-6984.
[279] Bell JJ, Bhandoola A. The earliest thymic progenitors for T cells possess myeloid lineage potential. Nature 2008; 452:764-767.
[280] Germar K, Dose M, Konstantinou T *et al.* T-cell factor 1 is a gatekeeper for T-cell specification in response to Notch signaling. Proceedings of the National Academy of Sciences of the United States of America 2011; 108:20060-20065.
[281] Smith-Berdan S, Nguyen A, Hassanein D *et al.* Robo4 cooperates with CXCR4 to specify hematopoietic stem cell localization to bone marrow niches. Cell stem cell 2011; 8:72-83.
[282] Hiramatsu M, Hotchkiss RS, Karl IE, Buchman TG. Cecal ligation and puncture (CLP) induces apoptosis in thymus, spleen, lung, and gut by an endotoxin and TNF-independent pathway. Shock 1997; 7:247-253.
[283] Ji A, Meyer JM, Cai L *et al.* Scavenger receptor SR-BI in macrophage lipid metabolism. Atherosclerosis 2011; 217:106-112.
[284] Mombaerts P, Iacomini J, Johnson RS *et al.* RAG-1-deficient mice have no mature B and T lymphocytes. Cell 1992; 68:869-877.
[285] Woollett LA, Buckley DD, Yao L *et al.* Cholic acid supplementation enhances cholesterol absorption in humans. Gastroenterology 2004; 126:724-731.
[286] Vahouny GV, Gregorian HM, Treadwell CR. Comparative effects of bile acids on intestinal absorption of cholesterol. Proceedings of the Society for Experimental Biology and Medicine. Society for Experimental Biology and Medicine 1959; 101:538-540.

[287] Vergnes L, Phan J, Strauss M *et al.* Cholesterol and cholate components of an atherogenic diet induce distinct stages of hepatic inflammatory gene expression. The Journal of biological chemistry 2003; 278:42774-42784.
[288] Mariathasan S, Weiss DS, Newton K *et al.* Cryopyrin activates the inflammasome in response to toxins and ATP. Nature 2006; 440:228-232.
[289] Marina-Garcia N, Franchi L, Kim YG *et al.* Pannexin-1-mediated intracellular delivery of muramyl dipeptide induces caspase-1 activation via cryopyrin/NLRP3 independently of Nod2. J Immunol 2008; 180:4050-4057.
[290] Chinetti G, Gbaguidi FG, Griglio S *et al.* CLA-1/SR-BI is expressed in atherosclerotic lesion macrophages and regulated by activators of peroxisome proliferator-activated receptors. Circulation 2000; 101:2411-2417.
[291] Hotchkiss RS, Swanson PE, Cobb JP *et al.* Apoptosis in lymphoid and parenchymal cells during sepsis: findings in normal and T- and B-cell-deficient mice. Critical care medicine 1997; 25:1298-1307.
[292] Ayala A, Herdon CD, Lehman DL *et al.* The induction of accelerated thymic programmed cell death during polymicrobial sepsis: control by corticosteroids but not tumor necrosis factor. Shock 1995; 3:259-267.
[293] Pazirandeh A, Jondal M, Okret S. Conditional expression of a glucocorticoid receptor transgene in thymocytes reveals a role for thymic-derived glucocorticoids in thymopoiesis in vivo. Endocrinology 2005; 146:2501-2507.
[294] Padgett EL, Sibley DA, Jerrells TR. Effect of adrenalectomy on ethanol-associated changes in lymphocyte cell numbers and subpopulations in thymus, spleen, and gut-associated lymphoid tissues. International journal of immunopharmacology 2000; 22:285-298.
[295] Kawiak J, Hoser G, Malendowicz LK *et al.* Thymocyte and splenocyte subpopulations in normal and leukemia-bearing mice after adrenalectomy. Folia histochemica et cytobiologica / Polish Academy of Sciences, Polish Histochemical and Cytochemical Society 1996; 34:75-78.
[296] Vacchio MS, Papadopoulos V, Ashwell JD. Steroid production in the thymus: implications for thymocyte selection. The Journal of experimental medicine 1994; 179:1835-1846.

[297] Lechner O, Wiegers GJ, Oliveira-Dos-Santos AJ *et al.* Glucocorticoid production in the murine thymus. European journal of immunology 2000; 30:337-346.
[298] Qiao S, Chen L, Okret S, Jondal M. Age-related synthesis of glucocorticoids in thymocytes. Experimental cell research 2008; 314:3027-3035.
[299] Qiao S, Okret S, Jondal M. Thymocyte-synthesized glucocorticoids play a role in thymocyte homeostasis and are down-regulated by adrenocorticotropic hormone. Endocrinology 2009; 150:4163-4169.
[300] Vacchio MS, Lee JY, Ashwell JD. Thymus-derived glucocorticoids set the thresholds for thymocyte selection by inhibiting TCR-mediated thymocyte activation. J Immunol 1999; 163:1327-1333.
[301] Mittelstadt PR, Monteiro JP, Ashwell JD. Thymocyte responsiveness to endogenous glucocorticoids is required for immunological fitness. J Clin Invest 2012; 122:2384-2394.

VITA

Zhong Zheng

Place of Birth

Pingyin County, Shandong Province, China

Educational History

08/2010-PRESENT

Ph.D. candidate in Nutrional Sciences,

Department of Pharmacology and Nutritional Sciences, College of Medicine,

University of Kentucky, Lexington, Kentucky, USA

09/2006-06/2010

B.S. in Life Science,

School of Life Science,

Shandong University, Jinan, Shandong Province, China

Rearch Experimence

08/2010-PRESENT

Research Assistant,

Department of Pharmacology and Nutritional Sciences, College of Medicine,

University of Kentucky, Lexington, Kentucky, USA

10/2009-06/2010

Volunteer,

School of Life Science,

Shandong University, Jinan, Shandong Province, China

07/2009-09/2009

Summer Internship,

Shanghai Institute of Biochemistry and Cell Biology,

Chinese Academy of Science, Shanghai, China

07/2008-07/2009

Volunteer,

State Key Laboratory of Microbial Technology, School of Life Science,

Shandong University, Jinan, Shandong Province, China

Honors and Awards

2012-2013 Kentucky Opportunity Fellowship

06/2008 Shandong University First-class Scholarship

06/2008 Shandong University Merit Student

06/2007 Shandong University Third-class Scholarship

06/2007 Shandong University Scholarship for Overseas Experience

Publications

1. Feng H, Guo L, Wang D, Gao H, Hou G, **Zheng Z**, Ai J, Foreman O, Daugherty A, Li XA. Deficiency of scavenger receptor BI leads to impaired lymphocyte homeostasis and autoimmune disorders in mice. 2011. Arterioscler Thromb Vasc Biol. 2011 Nov;31(11):2543-51.
2. Guo L, **Zheng Z**, Ai J, Huang B, Li XA. Comment on "Class B scavenger receptor types I and II and CD36 targeting improves sepsis survival and acute outcomes in mice". J Immunol. 2012 Jul 15;189(2):501.
3. Guo L, Ai J, **Zheng Z**, Howatt DA, Daugherty A, Huang B, Li XA. High density lipoprotein protects against polymicrobe-induced sepsis in mice. J Biol Chem. 2013 Jun 21;288(25):17947-53.
4. **Zheng Z**, Ai J, Li XA. SR-BI and immune dysfunctions. Curr Opin Endocrinol Diabetes Obes. 2014 Apr; 21(2):121-8.
5. Guo L, **Zheng Z**, Ai J, Howatt DA, Mittelstadt PR, Thacker S, Daugherty A, Ashwell JD, Remaley AT, Li XA. Scavenger receptor BI and high-density lipoprotein regulate thymocyte apoptosis in sepsis. Arterioscler Thromb Vasc Biol. 2014 May;34(5):966-75.
6. Guo L, **Zheng Z**, Ai J, Huang B, Li XA. Hepatic scavenger receptor BI protects against polymicrobial-induced sepsis through promoting LPS clearance in mice. J Biol Chem. 2014 Apr 9. Epub ahead of print.

Abstracts

1. Ai J, **Zheng Z**, Feng H, Guo L, Li Z, Li XA. SR-BI deficiency and hypercholesterolemia synergistically lead to impaired erythropoiesis. 14th Annual Gill Heart Institute Research Day, October 21, 2011; Lexington, KY.
2. **Zheng Z**, Feng H, Guo L, Ai J, Li XA. Dysfunctional HDL due to SR-BI deficiency disrupts lymphocyte homeostasis in mice. 2nd Barnstable Brown Obesity and Diabetes Research Day, May 14, 2012; Lexington, KY.
3. **Zheng Z**, Ai J, Guo L, Howatt DA, Daugherty A, Bondada S, Li XA. Scavenger receptor BI-deficiency-induced hypercholesterolemia impairs lymphocyte homeostasis. Arteriosclerosis, Thrombosis and Vascular Biology 2013 Scientific Sessions. Lake Buena Vista, Florida.
4. **Zheng Z**, Ai J, Guo L, Howatt DA, Daugherty A, Bondada S, Li XA. Scavenger receptor BI deficiency impairs thymopoiesis and peripheral T cell homeostasis in mice.3rd Barnstable Brown Obesity and Diabetes Research Day, May 13, 2013; Lexington, KY.